Title
Endogenous Functions and Genetic Variation in SLC22 Family Transporters

Author
Shima, James

Publication Date
2011

Peer reviewed|Thesis/dissertation

Endogenous Functions and Genetic Variation in SLC22 Family Transporters

by

James E. Shima

DISSERTATION

Submitted in partial satisfaction of the requirements for the degree of

DOCTOR OF PHILOSOPHY

in

Pharmaceutical Sciences and Pharmacogenomics

in the

GRADUATE DIVISION

of the

UNIVERSITY OF CALIFORNIA, SAN FRANCISCO

Endogenous Functions and Genetic Variation in SLC22 Family Transporters

James E. Shima

Members of the Solute Carrier (SLC) 22 family of transporters have been studied extensively due to their well-known role in drug excretion and disposition. However, numerous lines of evidence suggest that these transporters are likely to possess previously unrecognized roles in basal physiological processes. These studies were undertaken to better delineate the potential physiological importance of 2 organic anion transporters (OATs) expressed on the apical membrane of the apical membrane of renal tubule cells, *SLC22A11* (OAT4) and *SLC22A12* (URAT1), the impact of genetic variants of these two transporters, and to create a humanized mouse model suitable for an additional physiological and drug disposition studies of another SLC22 transporter, *SLC22A1* (OCT1).

Of the 9 OAT4 nonsynonymous variants studied, the L29P, R48Stop, and H469R variants all displayed negligible uptake of 3 canonical, endogenous substrates (estrone sulfate, ochratoxin A, and uric acid) likely due to the absence of plasma membrane protein localization. Extending this research to URAT1, 4 nonsynonymous variants, G65W, I131V, W277R, and R342H, as well as a C-terminal frameshift variant T542LysfX13, all displayed some reduction in uptake of uric acid, with the T542LysfX13 reduction likely due to the loss of a protein-binding motif and resultant plasma membrane localization. Collectively, the presence of these variants provides mechanistic reasons for variability in reabsorption of solutes from the urine in the human population, potentially affecting metabolite homeostasis as well as drug pharmacokinetics.

Comparisons of the evolutionary, genetic, and molecular features of OAT4 and URAT1 demonstrated that both are under general purifying selection and that their evolution has diverged considerably within the mammalian lineage, with numerous species lacking clear orthologs for either transporter. Likewise, expression of OAT4 was also found in the epididymis, an embryonically related tissue to the kidney but involved in the maturation of spermatozoa. In addition, profiling of substrate preferences for these two transporters showed considerably divergent sets of interacting molecules, including the uptake of AMP and ADP by URAT1 and an apparent binding site size restriction difference. These results suggest that these transporters, while evolutionarily related, have diverged to accommodate specialized physiological roles in a subset of mammalian lineage.

Finally, a mouse model expressing human OCT1 in the liver was created using the mouse albumin core promoter and distal enhancer to drive liver-specific expression. Absolute OCT1 transgene expression levels were 4 times higher in the transgenic line compared to the normal human liver and 20 times higher than any other mouse tissue. While expression was not restricted to the liver as anticipated, this model can aid in the assessment of drug substrates of OCT1 and provide a flexible model to evaluate the physiological repercussions of human OCT1 in an intact animal model.

This work demonstrates that while these transporters are important from a drug development standpoint, they also may be involved in specialized physiological processes, which may be modulated by naturally occurring genetic variants. Additional studies are required to better understand the full impact of these transporters on human physiology and the resultant impact on human health.

Table of Contents

Chapter 3

Genetic Variants of Human Organic Anion Transporter 4 Demonstrate Altered Transport of Endogenous Substrates

Chapter 4

Molecular Effects of Nonsynonymous Polymorphisms in URAT1

Chapter 5

Genetic and functional divergence between the apical renal organic anion transporters OAT4 and URAT1

Chapter 6

Generation and Validation of a Transgenic Mouse Model Expressing Human Organic Cation Transporter 1 in the Liver

Chapter 7

Summary and Future Considerations

List of Tables

Chapter 2

Chapter 3

Chapter 4

Chapter 5

Chapter 6

List of Figures

Chapter 1

Chapter 2

Chapter 3

Chapter 4

Chapter 5

Chapter 6

Chapter 1

Physiological Roles of Organic Anion Transporters (OATs)

Introduction

Maintenance of physiological levels of metabolites and micronutrients is of critical importance in human health. Disruption of physiological acceptable levels of these small molecules are known to result in numerous diseases ranging from gout (the accumulation of excess uric acid) to goiters (iodine deficiency) to a general failure to thrive (carnitine deficiency). Membrane transporters act as the gatekeepers for entrance into and exit from the cellular cytoplasmic compartment for small molecules that cannot easily permeate the plasma membrane. While the chemical milieu inside and outside of a cell is considerably complex, an equally complex system of transporters has evolved to handle a variety of tasks related to the movement these small molecules across membranes. One of the most diverse and functionally varied sets of transporters belong to the Solute Carrier (SLC) family, which are known to transport a wide assortment of endogenous small molecules including neurotransmitters, micronutrients, amino acids, sulfates, phosphates, and heavy metals, in addition to well-studied roles in the uptake and excretion of a variety of xenobiotics.

One branch of this transporter family encompasses the SLC22 transporters which are commonly cited as one of the major determinants of xenobiotic uptake and excretion in the kidney, liver, brain, placenta, and other excretory/barrier tissues. There are approximately 19 members of this family in humans and are

further separated into 4 general classes based on substrate preference: organic cation transporters (OCTs), novel organic cation transporters (OCTNs), organic anion transporters (OATs), and orphan transporters whose primary substrates are currently unknown. These transporters are commonly identified molecularly through overall protein similarity and the presence of 12 transmembrane domains, a major facilitator superfamily (MFS) functional domain, and a large extracellular domain between the first and second transmembrane domains[1]. Functionally, these transporters share common characteristics, namely the transport of compounds with a net negative charge at physiological pH into a cell coupled with an outwardly directed carboxylate gradient. The delineation of these subgroups based on their molecular evolutionary history is depicted in Figure 1.1. Considerable effort has been put toward determining how these "xenobiotic transporters" impact the response to and toxicities resulting from the treatment with pharmaceutical agents. However, mounting evidence suggests that many of these transporters are involved in a multitude of physiological processes.

The OATs are one of the more well-studied groups of transporters in the SLC22 family. This group of transporters is believed to have been derived from a single common ancestor and have undergone a number of lineage- and species-specific gene duplication and deletion events[2, 3] and there are currently 9 established OATs in humans which display a wide array of molecular and physiological features. These proteins are known to facilitate the transport of numerous endogenous substrates including uric acid, steroid sulfates,

prostaglandins, and a multitude of small carboxylate molecules[4] with each member of the OAT family sharing common substrates and functionalities as well as their own preferential set of distinct substrates and transport mechanisms. Additionally, while many of the OATs are restricted in their expression to major excretory or metabolic tissues such as the kidney and liver, some members of the OAT family are also expressed in unique tissues such as the olfactory epithelium, brain, testis, and epididymis.

The relatively recent divergence and promulgation of the OATs has provided a rich realm to investigate the role of transporters in basal physiological processes. In particular, the large number of OATs and their overlapping yet unique substrate specificities and tissue expression are indicative of transporter specialization. While the reasons behind this expansion and specialization of OATs are not readily forthcoming, it could be due to the need for functional redundancy to ensure the physiological status quo or an adaptation to the increasingly complex physiological states present as the evolution of mammals proceeded. The work presented herein focused on two different OATs, OAT4 and URAT1, but was undertaken with the overriding idea that while important, OAT-mediated effects on drug disposition are likely only a small component of the full, and presently vastly understudied, functional roles of these transporters, mediated largely by the expansion of the OAT family, the tissue-specific regulation of OATs, and the genetic variability that occurs within the OAT family of transporters.

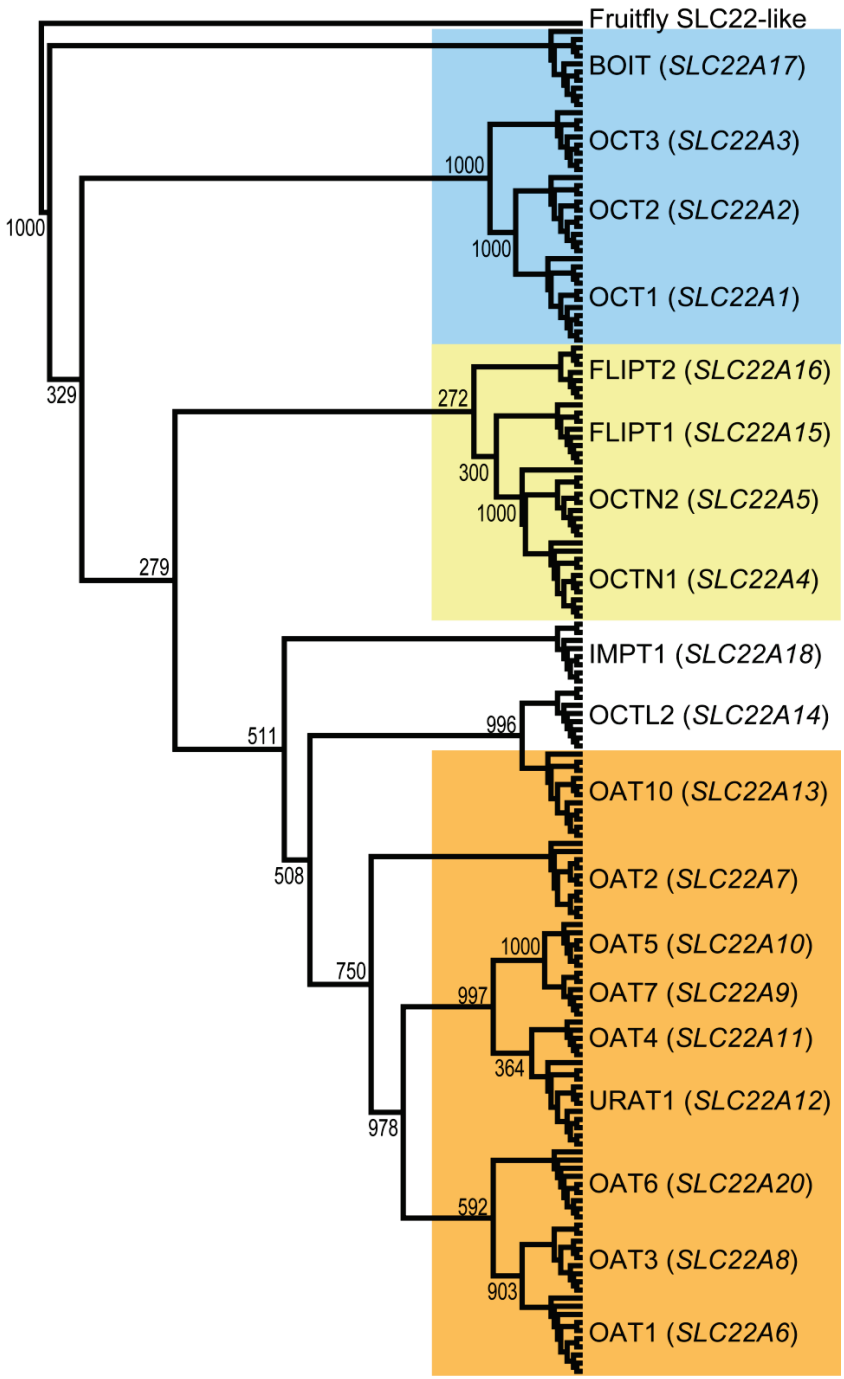

Figure 1.1: Phylogram of known SL22 transporters in mammals. Bootstrapped phylogram of 167 complete protein sequences of known SLC22 transporters from 11 mammalian species. Numbers represent bootstrap values as determined using PHYLIP[5]. Colors represent functional groupings: blue for cation transporters, yellow for cation/carnitine transporters, orange for anion transporters, and white for transporters with indeterminate substrate specificities (orphan transporters).

Physiological functions of OATs

Renal elimination of anionic small molecules

The kidney plays a significant role in both maintaining homeostasis of critical metabolites and in the elimination of potentially harmful xenobiotics and excess toxic metabolites via excretion in the urine. Since the discovery of organic anion transporter expression in the kidney, significant work has been undertaken to better understand the role of these transporters at both of the critical junctures in the excretory process: across the basolateral membrane from the blood and into the urine after transport across the apical membrane. A number of OATs are expressed in the kidney, including OAT1, OAT2, and OAT3 on the basolateral membrane and OAT4, OAT10, and URAT1 on the apical membrane. These sets of transporters provide a simple route of elimination of anionic toxins, metabolites, and drugs; in particular, a number of studies have determined that OAT1 and OAT3 are responsible for the initial uptake of these compounds from the blood and are requisite for the renal excretion of a number of small molecules.

Organic anion transporter 1 (OAT1) is a 550 amino acid protein that was initially identified through expression cloning from rat kidney in 1997[6, 7]. OAT1 functions as a Na^+-independent organic anion-dicarboxylate exchanger as described by the groups responsible for its initial cloning[6, 7]. This initial discovery provided the first evidence of a specific protein responsible for the movement of organic anions against their electrochemical gradient and their eventual excretion in the

urine. OAT1 was localized to the basolateral membrane of renal proximal tubule cells[8] and was recently found to be the highest expressed xenobiotic transporter (out of 36 examined) in the kidney[9]. Similar to OAT1, organic anion transporter 3 (OAT3) is a 542 amino acid protein originally cloned from rat brain in 1999[10] with the human ortholog cloned shortly thereafter[11]. OAT3 is expressed at its highest level in the kidney[12], with some expression in the brain, liver, and adrenal glands[12, 13], and also functions in a similar fashion to OAT1 with its primary mode of transport being the exchange of organic anions for dicarboxylates following an indirectly coupled Na^+ gradient[14]. OAT3 was also determined to have renal expression levels only somewhat below that of OAT1, likely making significant contributions to renal function as a result[9].

Investigations into the physiological role of OAT1 and OAT3 have largely been limited to renal function but have uncovered a number of unique physiological features, albeit none that may directly lead to human disease. The primary role of OAT1 and OAT3, as mentioned previously, is thus far believed to be the effective elimination of anionic metabolites and toxins by facilitating the initial transport step moving organic anions from the blood, across the basolateral membrane of renal tubular cells and into the urine. This process is important for the effective protection of organs from accumulation of toxic endogenous metabolites as well as preventing exogenous toxins from reaching dangerous levels in critical organs. Knockout mouse models of both Oat1 and Oat3 have substantiated this role; knockout mice lacking Oat1 expression were found to be viable, fertile, and grossly normal at both the whole body and renal level with the

only appreciable phenotype being the significant loss of *in vitro* renal uptake of p-aminohippurate (PAH), a model anionic substrate for OATs, and the altered *in vivo* plasma and/or urine levels of PAH[15]. Additionally, Oat1 knockout mice displayed significantly altered blood and/or urine levels of a number of endogenous metabolites including 4-hydroxyphenylpyruvate, benzoate, 4-hydroxyphenyllactate, N-acetylaspartate, and 3-hydroxybutyrate. Subsequent uptake experiments confirmed these interactions experimentally and provided strong evidence of both the breadth of Oat1 substrate interaction and the potential for modulation of levels of endogenous metabolites. To fully discern the impact of OATs on renal function, an Oat3 knockout mouse model was also developed by the same research group[16]. These mice, much like Oat1 knockout mice, were unremarkable and the only observable phenotype was a distinct lack of estrone sulfate and PAH uptake in renal tissue slices. A lack of fluorescein transport in isolated choroid plexus samples was also observed suggestive of an additional role in protecting the central nervous system from toxic molecules present in the cerebrospinal fluid[16]. In spite of these two models, organic anion excretion was not completely ablated in either. It is believed that the substrate specificities of these two transporters overlap enough to compensate for the loss of a single transporter, thereby acting as redundant mechanism for renal excretion of small organic anions.Oat1 and OatT3 double knockout mice have been proposed[17, 18] in order to more precisely investigate the potential physiological changes related to OAT1 but no reports of successfully produced Oat1/Oat3 double knockout mice have currently been published.

It is worth noting that in addition to renal excretion, the localization of OAT1 and OAT3 to the apical membrane in cells comprising the choroid plexus suggests alternative protective measures in other tissues. This reversal of localization compared to the kidney is believed to function by necessity so that toxins and waste products flow away from the cerebrospinal fluid and into the blood for eventual excretion[19]. Thus the OAT1/OAT3 pair may act, likely in concert with other transporters, in a protective fashion whereby potentially harmful metabolites or exogenous toxins are ultimately shuttled into the blood (and eventually excretion in the kidney) thus preventing accumulation of harmful substances in sensitive tissues.

Genetic variants of these two transporters may also impact their normal function in the kidney. Fujita, et al. found a number of variants in OAT1 in normal subjects and among these, one variant (R454Q) showed a dramatic loss of function in the transport of PAH, methotrexate, and ochratoxin B, suggestive of a possible source of inherent difference in renal clearance of anionic substrates. However, a subsequent clinical study examining the effect of this same variant on the renal clearance of adefovir failed to identify a substantial genotype-phenotype link[20]. Erdman, et al. also found three loss-of-function variants in OAT3 that failed to transport estrone sulfate or cimetidine[21]. Like OAT1, the variants identified in OAT3 also occurred at a low frequency in healthy volunteers. While this doesn't preclude a genetic component in renal excretion based on OAT1 and OAT3, it does suggest that both of these genes are under

substantial selective pressure, likely a result of an important physiological activity that does not readily tolerate altered functionality.

While it remains to be seen whether disruption of OAT1 and OAT3 function results in any significant physiological perturbation in humans, this may be due to built-in redundancies in the renal excretion of organic anions that are necessary to ensure that excess metabolic waste products and toxins are effectively eliminated.

Uric acid homeostasis

Uric acid is the end-product of purine degradation in most high-order primates, including humans, due to the genetic silencing of the Uricase gene. Most commonly known for comprising the concretions responsible for gout, uric acid is also linked to a number of disease states including multiple sclerosis[22], metabolic syndrome[23], and cardiovascular events[24], among others, when the blood levels of uric acid are dysregulated. Normally, uric acid levels are high in the blood (between 200 and 500 μM) although until recently it was assumed that these high levels were the result of high rates of purine turnover. Consequently, the discovery in 2002 of a high affinity transporter for uric acid changed this perception; the transporter URAT1 was cloned from human kidney and found to be a 555 amino acid long protein localized to the apical membrane of the renal proximal tubule[25]. URAT1 functionality is similar to many other OATs, namely in that it is Na^+-independent and appears to function predominantly as an exchanger with other small organic anions, namely nicotinate and lactate[25, 26].

However, it was also observed that URAT1 transport activity is coupled with Cl^- concentrations providing a distinct mechanism of transport for uric acid, possibly in cases where the normal physiological state of the kidney is perturbed.

Other OATs are also known to transport uric acid, namely OAT1, OAT2, OAT3, OAT4, and OAT10. While measurable and reproducible uptake has been identified in all of these transporters in regards to uric acid, both the rate of transport and the measured affinities for uric acid suggest that these transporters are unlikely to mediate drastic changes in uric acid levels, especially in comparison to URAT1. Expression of OAT1 and OAT3 on the basolateral membrane of renal tubule cells implicated them in the transport of uric acid initially; however, their relatively modest rates of transport indicate they are likely involved in the excretory step of uric acid transport in the kidney[11, 27, 28]. Analysis of knockout models for these two transporters also found that uric acid levels were altered (exemplified by an approximately 30% reduction in uric acid levels in the urine) when either protein was absent in the kidney[29] and confirmed that these two transporters mediate the flow of uric acid into the urine rather than its reabsorption. On the apical membrane of renal proximal tubule cells, OAT4 is capable of transporting uric acid at appreciable levels, albeit substantially lower than URAT1. Its pairing with URAT1 on the apical membrane of renal proximal tubule cells is suggestive of a redundant mechanism to allow for continued uric acid reabsorption in the face of altered physiologic conditions. In particular, the use of differing sets of anionic molecules during substrate transport and the coupling to slightly different ion gradients may allow for basal levels of uric acid

absorption to occur or for normal levels when physiological conditions are perturbed. In consideration of the great degree of variability in the concentration of metabolites in the urine, alternative mechanisms of uric acid reabsorption in the kidney would be beneficial.

High levels of uric acid are maintained through its continuous reabsorption from the urine via URAT1. While the ultimate reason that humans and other primates evolved this mechanism for reclamation of uric acid remains unresolved, a number of possibilities can be put forth. It is well accepted that uric acid has anti-oxidant properties and can act as a free radical scavenger. Proctor, et al. and others have proposed that elevated levels of uric acid act as a protective mechanism against neurodegeneration in the case of ischemic stroke[30], something newly requisite with high order primates possessing more evolved brain functions. Similarly, high levels of uric acid in the blood may also have evolved from the need to protect against free radicals encountered from the environment or in disease states. It has been reported that uric acid improves endothelial cell function in patients with type 2 diabetes or who are chronic smokers thus underlining the potential for the beneficial effect of high uric acid levels[31]. Conversely, high uric acid levels have also been associated with increased risk of death from cardiovascular events and adverse outcomes in cases of metabolic syndrome or when other risk factors are involved[32]. Ultimately the impact of URAT1 in these diseases is not known but as it is a key regulator or uric acid levels and thus may influence the development of states conducive or protective towards specific diseases.

Variation of transporters known to interact with uric acid also provide a distinct mechanism for the wide range of uric acid levels in the human population and in the risk of developing a number of disease states linked to uric acid levels. A small number of variants identified in normal volunteers in URAT1 (Chapter 4), OAT4 (Chapter 3), and OAT10 (unpublished results) were found to transport uric acid with decreased efficiency. However, the frequency of these variants in the general population is exceedingly low with the majority occurring as singletons in a single ethnic group. In spite of this, numerous variants have been reported that occur with higher frequency in patients presenting with idiopathic renal hypouricemia[25, 33-36]. These non-functional genetic variants of URAT1 were provide a definitive link between URAT1 and regulation of uric acid levels but further work will need to be performed to establish if these variants also predispose these individuals to a particular disease. Furthermore, the presence of variants in URAT1 may occur in an ethnic specific fashion; currently few if any loss-of-function variants that result in hypouricemia have been observed in Caucasian subjects[36]. The significance of this observation is debatable and may be due to the limited number of subjects examined to this point. The presence of distinct uric acid reabsorption statuses between ethnic groups may however indicate differing environmental pressures or perhaps a requisite need for elevated uric acid levels in Caucasians that prevent deleterious mutations from propagating in the population.

Finally, additional studies (Chapter 5) have found that URAT1 is capable of uptake of AMP and ADP under conditions similar to those used to characterize

uptake of uric acid. While speculative, this observation is suggestive of a broader role of OATs, and in particular URAT1, in the reabsorption of endogenous adenine derivatives from the urine. Interestingly, this appears to be a paired effect with OAT2 which preferentially transports guanine-derivatives[37], although the net effect of the pairing of these two transporters may be negligible as they are expressed in differing membranes in the kidney.

Transport of guanine and related nucleotides

Nucleic acid derivatives play an integral role in numerous physiological responses throughout the body. In addition to the previously detailed reclamation of uric acid, a number of related compounds, both exogenous and endogenous, have been identified as substrates of OATs. Organic anion transporter 2 (OAT2) was one of the earliest SLC22 proteins isolated, originally cloned from rat liver in 1994 but not functionally characterized until 1998 where it was subsequently found to function in a manner similar to other OATs[38, 39]. Human OAT2 is a 556 amino acid protein (with a 558 amino acid non-functional isoform[37]) expressed predominantly in the liver (although the subcellular localization of human OAT2 in the liver is presently unclear) with lower expression in the basolateral membrane of proximal tubules in the kidney[40, 41]. Measurable levels of OAT2 are also found in a number of other tissues including placenta, brain, heart, intestine, and testis making its distribution fairly ubiquitous, especially in comparison to other OATs[37]. Currently the mechanism of OAT2 transport activity remains unclear but it has been suggested that both exchanger and facilitator transport mechanisms are potentially valid. In particular, it has

been proposed that OAT2 acts as a NA^+-independent organic anion/dimethylcarboxylate exchanger[42]. Cropp, et al. also highlighted an alternative efflux transport mechanism wherein OAT2 acts as a bidirectional facilitative transporter when intracellular cGMP concentrations are high but dicarboxylate concentration gradients remain outwardly directed, further suggesting that transport via OAT2 is not strictly coupled to a dicarboxylate gradient[37].

The majority of the physiological relevance pertaining to OAT2 comes from its ability to transport cGMP with great affinity and in a bidirectional fashion[37]. cGMP is known to function as a secondary signaling molecule resulting from activation of a number of signaling pathways, predominantly the nitric oxide signaling pathway and the transduction of visual signals in the retina. While it is known that much of the cGMP to GMP turnover is the result of phosphodiesterase activity, it has been postulated that compartmentalization, intracellularly or extracellularly, could also be an effective mechanism to regulate cellular signaling mediated by cGMP. Recently, this effect has been evidenced in developing neurons wherein highly localized concentrations of cAMP and cGMP influence the development of axons and dendrites[43]. Anecdotally, localized transport of cGMP by OAT2 may function in a similar capacity, although it's unlikely to be responsible for such a highly specialized developmental effect. cGMP is also known to regulate the expression of numerous genes in vascular smooth muscle cells[44]. OAT2 therefore may also contribute to the regulation of gene expression in tissues with active cGMP signaling.

In addition to cGMP, OAT2 also transports 2'-deoxyguanosine and GMP with high affinity and GDP, GTP, guanine, with more moderate affinity[37]. Taken together, the collective uptake of a large number of guanine-derived molecules also suggests additional prospects for OAT2, functioning as either a recycling mechanism for guanine-based small molecules or the regulation of an as-yet-unknown homeostatic process for guanine nucleotides. As mentioned previously, URAT1 also demonstrated appreciable uptake of other adenine-based small molecules lending further support to the idea that OATs may function in a general sense to maintain adequate or proper levels nucleic acids, nucleosides, and nucleotides.

Hypotension

Hypotension, or abnormally low blood pressure, occurs due to a variety of physiological and pharmacological reasons. A link between hypotension and OATs was recently uncovered using the recently developed mouse knockout models for various OATs. In mice deficient for Oat3, a 10-15% decrease in blood pressure was observed in knockout mice compared to wildtype whereas no significant difference was observed in either Oat1 or Urat1 knockout mice[45]. Importantly, no change in renal hemodynamics was observed suggesting that the reduced blood pressure is the result of a direct physiological consequence of the loss of organic anion transport by OAT3. Subsequent metabolomics experiments found elevated levels of thymidine, an endogenous nucleoside, in the plasma with concordant decreased levels in the urine which was also shown to be a substrate of Oat3but not Oat1. Interestingly, exogenous administration of

thymidine in Oat3 knockout mice produced a dose-dependent decrease in blood pressure[45]. Additional experiments investigating other potential mechanisms of blood pressure regulation via Oat3 confirmed that the likely mechanism of action is based upon the transport of specific endogenous molecules, including but perhaps not limited to thymidine. Some evidence suggests that the transport of prostaglandins and/or cyclic nucleotides (namely PGE_2 and cGMP respectively) in vascular smooth muscle may also contribute to the observed blood pressure difference[46], however the low levels of expression of OAT3 in smooth muscle and its low affinity for both of these substrates cast some doubt on this possibility. Given this evidence, however, it appears that the physiological significance of OATs is not limited to renal functions or the simple movement of small molecules into and out of cells. Likewise, genetic variants leading to altered OAT3 function may allow for a duality of risk for cardiac events wherein loss-of-function variants would mimic the knockout state and lead to a generally hypotensive state whereas gain-of-function variants would have the opposite effect, potentially leading to increased blood pressure and a concomitant increased risk of cardiac events. While no gain-of-function variants in OAT3 have been identified to date, the possibility remains that these variants could still exist either at an exceedingly low frequency or as substrate-specific effects that have been overlooked.

<u>"Remote sensing and signaling hypothesis"</u>

Given the exceedingly specific yet incredibly overlapping functions of members of the OAT family, including substrate specificities, transport mechanisms, and tissue expression, a more unified theory of the ultimate purpose of the OATs was

inevitable. Proposed by Ahn and Nigam, the “remote sensing and signaling hypothesis” describes the theory that aside from simply transporting anionic molecules with little to no tissue or organismal impact, members of the OAT family act as a sensory and communication system within the body, receiving and sending signals in the form of circulating substrate concentrations[47]. This theory touches on many of the topics mentioned previously, in particular, observations on the tissue localization of OATs point to potential networks of transporters in the brain, kidney, liver, and other tissues where substrates transported in one tissue are shuttled to another via another transporter which ultimately elicits a physiological response. One such example of this is the OAT6-OAT1 olfactory pathway where volatile anionic compounds in the urine, mediated initially by transport into the renal epithelia by OAT1, are transported into the olfactory epithelium by OAT6 in a different organism where they eventually relate environmental cues to the brain. Additionally, the near universal transport of certain small molecules by OATs, specifically carboxylates/dicarboxylates and uric acid, suggest something beyond a simple redundancy mechanism; it’s postulated that these redundancy mechanisms are in fact far more complicated systems where perturbations in homeostatic states are translated to changes in gene expression, post-translational modifications, and chemical gradients designed to restore homeostasis or prevent a catastrophic organ failure in the case of injury[47]. While early and largely speculative, this theory intrinsically makes sense and points towards a significant role of OATs in mammals that has evolved over time and exemplifies a common

paradigm in biology: using the same available proteins in slightly different ways, with slightly different regulation, allowing for an infinitely redundant and ultimately robust physiology.

Summary

Aside from the well-characterized xenobiotic interactions that occur with members of the OAT family, a number of distinct physiological and pathophysiological roles have been demonstrated or hypothesized. Based largely on unique substrate interaction or tissue expression, some of these roles potentially have great bearing on human health and further investigation could lead to both a greater understanding of transporter-influenced physiology as well as potential avenues to modulate said physiology.

Within the family of SLC22 transporters, the OATs inhabit a unique functional niche, allowing for the transport of a diverse set of small molecules in numerous tissues and with an inordinate amount of physiological implications which are only now beginning to be studied with any fervor. Renal excretion, the earliest identified OAT function, is increasingly recognized to be a multi-faceted process with OATs responsible for the initial transport of anionic compounds from the blood into a cell and additional OATs reclaiming these same substrates from the urine. Maintenance of elevated uric acid concentrations, a unique feature amongst higher order primates, is believed to act as an antioxidant pool, potentially preventing numerous maladies including cardiovascular disease and

multiple sclerosis. Cardiovascular health, intricately linked to the content and regulation of the small molecule content of the blood, is directly linked to OAT function and is only now beginning to be discovered, along with the numerous implications in everything from medical intervention in patients to new models of drug design to treat cardiovascular disease. Transport of numerous nucleic acid-based molecules provides a unique method to regulate signal transduction and maintain homeostasis of the molecules responsible for everything from DNA to the basic cellular energy source, ATP.

With the increasing focus on preventative, personalized medicine, components of numerous physiological processes are being reevaluated to determine their worth as biomarkers, with the hope of providing earlier recognition of detrimental states of health or in identifying novel, specific targets for pharmacological intervention. The OATs already benefit from being well-recognized drug transporters and further focus on their physiological functions will surely result in a better understanding of both the negative and positive effects of drug treatment as well as provide increasing insight into potential off-target effects, many of which may not have been previously attributed to transporter activity or inhibition. In line with this new approach, continued discovery and evaluation of genetic variants of OATs will also allow for an improved evaluation of the causes of variability in physiology commonly seen within and between human populations.

References

1. Roth M, Obaidat A, Hagenbuch B. OATPs, OATs and OCTs: The organic anion and cation transporters of the SLCO and SLC22A gene superfamilies. *Br J Pharmacol* 2011.

2. Eraly SA, Hamilton BA, Nigam SK. Organic anion and cation transporters occur in pairs of similar and similarly expressed genes. *Biochem Biophys Res Commun* 2003; **300**(2)**:** 333-342.

3. Eraly SA, Monte JC, Nigam SK. Novel slc22 transporter homologs in fly, worm, and human clarify the phylogeny of organic anion and cation transporters. *Physiol Genomics* 2004; **18**(1)**:** 12-24.

4. VanWert AL, Gionfriddo MR, Sweet DH. Organic anion transporters: discovery, pharmacology, regulation and roles in pathophysiology. *Biopharm Drug Dispos* 2010; **31**(1)**:** 1-71.

5. Felsenstein J (2010). In: *PHYLIP (Phylogeny Interface Package)*. Self Published: University of Washington.

6. Sekine T, Watanabe N, Hosoyamada M, Kanai Y, Endou H. Expression cloning and characterization of a novel multispecific organic anion transporter. *J Biol Chem* 1997; **272**(30)**:** 18526-18529.

7. Sweet DH, Wolff NA, Pritchard JB. Expression cloning and characterization of ROAT1. The basolateral organic anion transporter in rat kidney. *J Biol Chem* 1997; **272**(48)**:** 30088-30095.

8. Motohashi H, Sakurai Y, Saito H, Masuda S, Urakami Y, Goto M*, et al*. Gene expression levels and immunolocalization of organic ion transporters in the human kidney. *J Am Soc Nephrol* 2002; **13**(4)**:** 866-874.

9. Hilgendorf C, Ahlin G, Seithel A, Artursson P, Ungell AL, Karlsson J. Expression of thirty-six drug transporter genes in human intestine, liver, kidney, and organotypic cell lines. *Drug Metab Dispos* 2007; **35**(8)**:** 1333-1340.

10. Kusuhara H, Sekine T, Utsunomiya-Tate N, Tsuda M, Kojima R, Cha SH*, et al*. Molecular cloning and characterization of a new multispecific organic anion transporter from rat brain. *The Journal of biological chemistry* 1999; **274**(19)**:** 13675-13680.

11. Race JE, Grassl SM, Williams WJ, Holtzman EJ. Molecular cloning and characterization of two novel human renal organic anion transporters

(hOAT1 and hOAT3). *Biochemical and biophysical research communications* 1999; **255**(2)**:** 508-514.

12. Cha SH, Sekine T, Fukushima JI, Kanai Y, Kobayashi Y, Goya T*, et al*. Identification and characterization of human organic anion transporter 3 expressing predominantly in the kidney. *Molecular pharmacology* 2001; **59**(5)**:** 1277-1286.

13. Asif AR, Steffgen J, Metten M, Grunewald RW, Muller GA, Bahn A*, et al*. Presence of organic anion transporters 3 (OAT3) and 4 (OAT4) in human adrenocortical cells. *Pflugers Archiv : European journal of physiology* 2005; **450**(2)**:** 88-95.

14. Srimaroeng C, Perry JL, Pritchard JB. Physiology, structure, and regulation of the cloned organic anion transporters. *Xenobiotica* 2008; **38**(7-8)**:** 889-935.

15. Eraly SA, Vallon V, Vaughn DA, Gangoiti JA, Richter K, Nagle M*, et al*. Decreased renal organic anion secretion and plasma accumulation of endogenous organic anions in OAT1 knock-out mice. *J Biol Chem* 2006; **281**(8)**:** 5072-5083.

16. Sweet DH, Miller DS, Pritchard JB, Fujiwara Y, Beier DR, Nigam SK. Impaired organic anion transport in kidney and choroid plexus of organic anion transporter 3 (Oat3 (Slc22a8)) knockout mice. *J Biol Chem* 2002; **277**(30)**:** 26934-26943.

17. Nagle MA, Truong DM, Dnyanmote AV, Ahn SY, Eraly SA, Wu W*, et al*. Analysis of three-dimensional systems for developing and mature kidneys clarifies the role of OAT1 and OAT3 in antiviral handling. *J Biol Chem* 2011; **286**(1)**:** 243-251.

18. Eraly SA, Bush KT, Sampogna RV, Bhatnagar V, Nigam SK. The molecular pharmacology of organic anion transporters: from DNA to FDA? *Mol Pharmacol* 2004; **65**(3)**:** 479-487.

19. Pritchard JB, Sweet DH, Miller DS, Walden R. Mechanism of organic anion transport across the apical membrane of choroid plexus. *J Biol Chem* 1999; **274**(47)**:** 33382-33387.

20. Fujita T, Brown C, Carlson EJ, Taylor T, de la Cruz M, Johns SJ*, et al*. Functional analysis of polymorphisms in the organic anion transporter, SLC22A6 (OAT1). *Pharmacogenet Genomics* 2005; **15**(4)**:** 201-209.

21. Erdman AR, Mangravite LM, Urban TJ, Lagpacan LL, Castro RA, de la Cruz M*, et al*. The human organic anion transporter 3 (OAT3; SLC22A8):

genetic variation and functional genomics. *Am J Physiol Renal Physiol* 2006; **290**(4)**:** F905-912.

22. Hooper DC, Spitsin S, Kean RB, Champion JM, Dickson GM, Chaudhry I*, et al*. Uric acid, a natural scavenger of peroxynitrite, in experimental allergic encephalomyelitis and multiple sclerosis. *Proc Natl Acad Sci U S A* 1998; **95**(2)**:** 675-680.

23. Nakagawa T, Hu H, Zharikov S, Tuttle KR, Short RA, Glushakova O*, et al*. A causal role for uric acid in fructose-induced metabolic syndrome. *Am J Physiol Renal Physiol* 2006; **290**(3)**:** F625-631.

24. Johnson RJ, Kang DH, Feig D, Kivlighn S, Kanellis J, Watanabe S*, et al*. Is there a pathogenetic role for uric acid in hypertension and cardiovascular and renal disease? *Hypertension* 2003; **41**(6)**:** 1183-1190.

25. Enomoto A, Kimura H, Chairoungdua A, Shigeta Y, Jutabha P, Cha SH*, et al*. Molecular identification of a renal urate anion exchanger that regulates blood urate levels. *Nature* 2002; **417**(6887)**:** 447-452.

26. Hosoyamada M, Ichida K, Enomoto A, Hosoya T, Endou H. Function and localization of urate transporter 1 in mouse kidney. *J Am Soc Nephrol* 2004; **15**(2)**:** 261-268.

27. Sica DA, Schoolworth AC. Renal handling of organic anions and cations: excretion of uric acid. In: Brenner BM, Rector F. (ed). *The Kidney*, 6th edn. Saunders Company: Philadelphia, 2000, pp 680-700.

28. Ichida K, Hosoyamada M, Kimura H, Takeda M, Utsunomiya Y, Hosoya T*, et al*. Urate transport via human PAH transporter hOAT1 and its gene structure. *Kidney Int* 2003; **63**(1)**:** 143-155.

29. Eraly SA, Vallon V, Rieg T, Gangoiti JA, Wikoff WR, Siuzdak G*, et al*. Multiple organic anion transporters contribute to net renal excretion of uric acid. *Physiol Genomics* 2008; **33**(2)**:** 180-192.

30. Proctor PH. Uric acid: neuroprotective or neurotoxic? *Stroke* 2008; **39**(5)**:** e88; author reply e89.

31. Waring WS, McKnight JA, Webb DJ, Maxwell SR. Uric acid restores endothelial function in patients with type 1 diabetes and regular smokers. *Diabetes* 2006; **55**(11)**:** 3127-3132.

32. Kim SY, Guevara JP, Kim KM, Choi HK, Heitjan DF, Albert DA. Hyperuricemia and coronary heart disease: a systematic review and meta-analysis. *Arthritis Care Res (Hoboken)* 2010; **62**(2)**:** 170-180.

33. Ichida K, Hosoyamada M, Hisatome I, Enomoto A, Hikita M, Endou H*, et al*. Clinical and molecular analysis of patients with renal hypouricemia in Japan-influence of URAT1 gene on urinary urate excretion. *J Am Soc Nephrol* 2004; **15**(1)**:** 164-173.

34. Iwai N, Mino Y, Hosoyamada M, Tago N, Kokubo Y, Endou H. A high prevalence of renal hypouricemia caused by inactive SLC22A12 in Japanese. *Kidney Int* 2004; **66**(3)**:** 935-944.

35. Komatsuda A, Iwamoto K, Wakui H, Sawada K, Yamaguchi A. Analysis of mutations in the urate transporter 1 (URAT1) gene of Japanese patients with hypouricemia in northern Japan and review of the literature. *Ren Fail* 2006; **28**(3)**:** 223-227.

36. Tasic V, Hynes AM, Kitamura K, Cheong HI, Lozanovski VJ, Gucev Z*, et al*. Clinical and Functional Characterization of URAT1 Variants. *PLoS One* 2011; **6**(12)**:** e28641.

37. Cropp CD, Komori T, Shima JE, Urban TJ, Yee SW, More SS*, et al*. Organic anion transporter 2 (SLC22A7) is a facilitative transporter of cGMP. *Mol Pharmacol* 2008; **73**(4)**:** 1151-1158.

38. Sekine T, Cha SH, Tsuda M, Apiwattanakul N, Nakajima N, Kanai Y*, et al*. Identification of multispecific organic anion transporter 2 expressed predominantly in the liver. *FEBS Lett* 1998; **429**(2)**:** 179-182.

39. Sun W, Wu RR, van Poelje PD, Erion MD. Isolation of a family of organic anion transporters from human liver and kidney. *Biochem Biophys Res Commun* 2001; **283**(2)**:** 417-422.

40. Kojima R, Sekine T, Kawachi M, Cha SH, Suzuki Y, Endou H. Immunolocalization of multispecific organic anion transporters, OAT1, OAT2, and OAT3, in rat kidney. *J Am Soc Nephrol* 2002; **13**(4)**:** 848-857.

41. Enomoto A, Takeda M, Shimoda M, Narikawa S, Kobayashi Y, Yamamoto T*, et al*. Interaction of human organic anion transporters 2 and 4 with organic anion transport inhibitors. *J Pharmacol Exp Ther* 2002; **301**(3)**:** 797-802.

42. Kobayashi Y, Ohshiro N, Sakai R, Ohbayashi M, Kohyama N, Yamamoto T. Transport mechanism and substrate specificity of human organic anion transporter 2 (hOat2 [SLC22A7]). *J Pharm Pharmacol* 2005; **57**(5)**:** 573-578.

43. Shelly M, Lim BK, Cancedda L, Heilshorn SC, Gao H, Poo MM. Local and long-range reciprocal regulation of cAMP and cGMP in axon/dendrite formation. *Science* 2010; **327**(5965)**:** 547-552.

44. Pilz RB, Casteel DE. Regulation of gene expression by cyclic GMP. *Circ Res* 2003; **93**(11)**:** 1034-1046.

45. Vallon V, Eraly SA, Wikoff WR, Rieg T, Kaler G, Truong DM*, et al*. Organic anion transporter 3 contributes to the regulation of blood pressure. *Journal of the American Society of Nephrology : JASN* 2008; **19**(9)**:** 1732-1740.

46. Eraly SA. Organic anion transporter 3 inhibitors as potential novel antihypertensives. *Pharmacological research : the official journal of the Italian Pharmacological Society* 2008; **58**(5-6)**:** 257-261.

47. Ahn SY, Nigam SK. Toward a systems level understanding of organic anion and other multispecific drug transporters: a remote sensing and signaling hypothesis. *Molecular pharmacology* 2009; **76**(3)**:** 481-490.

Chapter 2

Organic Anion Transporter 4 is the Predominant Organic Anion Transporter in the Human Male Reproductive Tract

Introduction

Infertility affects nearly 10% of the reproductive-age population in the United States. Of the many possible causes of infertility, nearly half can be ascribed to a male factor and roughly 20% are idiopathic[1-3]. Of paramount importance in male fertility is the production and maturation of functionally competent spermatozoa and their transit through the male reproductive tract, outlined in Figure 2.1. The sole site of gametogenesis in the male and primary focus in cases of male infertility is the testis, in which diploid spermatogonia undergo mitotic and meiotic divisions and produce haploid spermatozoa (spermatogenesis). At the conclusion of spermatogenesis, spermatozoa are passively transported from the testis to the epididymis, the site of sperm concentration and maturation: human spermatozoa are immotile and incapable of independently fertilizing an ovum upon exiting the testis[4]. While in transit through the epididymis, spermatozoa must retain their viability while gaining additional functional properties. During transit through the length of the epididymis immature spermatozoa gain the requisite biochemical and morphological features commonly identified with sperm such as full motility, the loss of the majority of cytoplasmic volume, and the development of an enzymatically complete acrosome[5]. There are many points in this complex process in which

altered physiological conditions, hormonal signaling, or toxicological exposure could result in a cessation of spermatogenesis or the loss of the carefully maintained environment conducive to sperm production, maturation, or survival which in turn can lead to sub- or infertility.

While the testis is responsible for the creation of haploid gametes in the male, the epididymis is crucial in providing an adequate environment for recently released spermatozoa to biochemically and morphologically mature. Of particular importance is the change in the fluid microenvironment as sperm exit the testis and enter the efferent ductules in the caput epididymis; within the epididymis and along its length, spermatozoa are subject to a unique microenvironment wherein the majority (~90%) of the testicular fluid is reabsorbed by epididymal epithelial cells and replaced with a smaller volume of fluid with a markedly different composition[6]. Establishment and maintenance of the luminal microenvironment of the epididymis thus becomes crucial for spermatozoa survival and male fertility. A number of solutes in the epididymal fluid have been identified thus far including carnitine[7], glutamate and taurine[8], myo-inositiol[9], and a variety of androgenic and estrogenic hormones as well as a multitude of lipid and protein components[6]. In spite of the efforts to characterize the components of epididymal fluid, a significant fraction of the total solutes remain unidentified as do the mechanisms of solute secretion into and reabsorption from the epididymal lumen[10]. Previous work over the last two decades has shown that the epididymis, in particular the efferent ductules and caput epididymis, has an

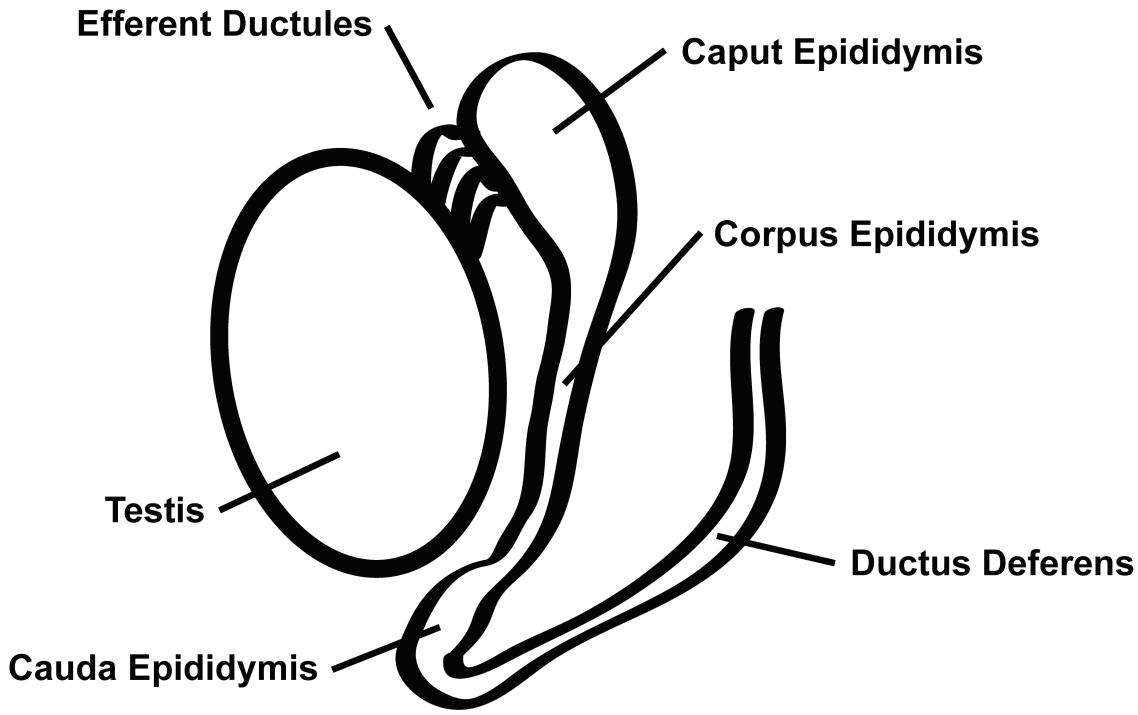

Figure 2.1: Schematic diagram of the human male reproductive tract. Representation of the major tissues involved in the production, maturation, and transit of spermatozoa.

exceedingly high capacity for water and small molecule absorption[11, 12] and that much of this interchange occurs via transporter-mediated mechanisms[13, 14]. However, the identity and functional roles of many of these transporter-mediated processes in the epididymis remain poorly understood and incompletely characterized.

Whereas knowledge of the molecular routes for small molecules to enter or exit the epididymis is limited to only a small number of channels and transporters for a fraction of the total constituents of the epididymal luminal fluid, one prominent example of the consequences of a deficit in a single small molecule component of epididymal fluid is exemplified in the juvenile visceral steatosis (*jvs*) mouse line. This spontaneous line resulted from the loss of proper carnitine transport

vis à vis a loss-of-function mutation in *SLC22A5* (OCTN2), a member of the Solute Carrier (SLC) family of transport proteins and the widely recognized plasma membrane "carnitine transporter" in many tissues[15, 16]. The *jvs* mouse model demonstrates an extreme epididymal phenotype wherein disruption of a single transport mechanism alters the levels of presumably a single constituent of the luminal fluid in the epididymis and results in obstruction of the proximal epididymis and consequentially male infertility[17]. The complex milieu found in the luminal fluid would suggest that many transporters are involved in its maintenance and overall composition as well as the dramatic changes that occur in the transition from testicular to epididymal fluid in the proximal epididymis.

The current study identified OAT4 (*SLC22A11*) in the human epididymis and found that it is expressed in abundance whereas prior to this work its expression was limited to the kidney and the placenta[18]. OAT4 has previously been demonstrated to play a role in the transport of a number of endogenous compounds in both the kidney and placenta, most notably steroid conjugates such as estrone sulfate (ES) and dehydroepiandrosterone sulfate (DHEAS)[18]. Contemporary studies have suggested that OAT4 is responsible for the transport of steroid sulfates, in particular DHEAS and 16α-OH DHEAS, from the fetal compartment into the placenta, which in turn produces the majority of the placenta-derived estrogens found during pregnancy[19]. However, a role for OAT4 outside of traditional barrier or excretory tissues has not been described thus far.

A more detailed investigation of the role of OAT4 in the epididymis could produce insights into the factors necessary for sperm maturation and survival, but also

provide further information regarding the potential causes of idiopathic male infertility and even a new target for treatment of infertility. In particular, these studies may open up another avenue of research into male infertility based on the idea that some small molecules are requisite for normal fertility and have only one way in or out of the epididymal microenvironment – through a transporter.

Materials and Methods

Reagents

Radiolabeled [^{3}H]-estrone sulfate (ES) was purchased from Perkin Elmer Life Sciences (Waltham, MA, USA) and radiolabeled [^{3}H]-AMP, [^{3}H]-adenine, [^{3}H]-adenosine, and [^{3}H]-cAMP were purchased from Moravek (Brea, CA, USA). Unlabeled (±)-carnitine, (±)-acetylcarnitine, and (±)-propionylcarnitine were purchased from Tocris Bioscience (Ellisville, MO, USA). Other chemicals were purchased from Sigma (St. Louis, MO, USA). All cell culture media and reagents were purchased from the University of California, San Francisco Cell Culture Facility (San Francisco, CA, USA).

Quantitative reverse-transcriptase PCR

Total RNA from normal, adult human tissues was obtained from commercial sources: brain, colon, kidney, liver, ovary, placenta, uterus, ductus deferens, and prostate from Clontech (Mountain View, CA, USA), ductus deferens from BioChain (Hayward, CA, USA), and epididymis and seminal vesicle from

Cytomyx (Lexington, MA, USA). cDNA was synthesized from 1 µg of RNA from each sample using a SuperScript III® reverse transcriptase kit (Invitrogen, Carlsbad, CA, USA) following the manufacturer's default procedure employing oligo dT primers. The samples were diluted 1:5 in sterile water and used for quantitative reverse-transcriptase PCR (qRT-PCR). qRT-PCR utilized Taqman® primers and probes (Applied Biosystems, Foster City, CA, USA) specific to each organic anion transporter examined (*SLC22A6*, *SLC22A7*, *SLC22A8*, *SLC22A9*, *SLC22A10*, *SLC22A11*, *SLC22A12*, and *SLC22A13*). Measurements of mRNA levels were performed using 10 µL reaction volumes in a 384-well plate format with 2 µL of diluted cDNA and 0.5 µL of the gene-specific probe and primer reagent per well. A standard curve was developed for each gene using a serial dilution of mammalian expression vectors containing a full-length cDNA of each respective transporter. The results were normalized to *GAPDH* levels in each sample and were run in triplicate wells on each plate. The results are expressed as the absolute number of copies per microgram of total RNA as determined using the standard curve.

Immunohistochemistry

Paraffin-embedded sections of adult human efferent ductules of the epididymis, kidney, and testis were obtained from a commercial source (BioChain). Paraffin-embedded sections from the caput, corpus, and cauda epididymis were kindly provided by Ms. Julie Dufresne and Dr. Daniel Cyr (INRS-Institut Armand-Frappier, Laval, Québec, Canada). Kidney sections were used as a positive control for OAT4 while testis sections were used as a negative control, based on

the presence and absence of *SLC22A11* mRNA in those tissues respectively[18]. Tissue sections were deparaffinized in xylenes and rehydrated using a graded series of ethanol. The sections were incubated in absolute methanol containing 3% hydrogen peroxide for 10 minutes to quench any residual peroxidase activity. Each slide was subsequently incubated in citrate buffer (10 mM sodium citrate, 0.05% Tween 20, pH 6.0) heated to 95°C for 20 minutes. Detection of OAT4 protein was attained using a polyclonal rabbit anti-human antibody (US Biological, Swampscott, MA, USA) at a concentration of 10 µg/mL for 20 minutes at room temperature. Staining for OAT4 used the chromogen 3,3'-diaminobenzidine (DAB) in conjunction with a rabbit immunohistochemistry kit employing a biotin-conjugated goat anti-rabbit secondary antibody and horseradish peroxidase coupled to streptavidin following the recommended protocol from the manufacturer (US Biological). All slides were counterstained using VECTOR Hematoxylin QS® (Vector Laboratories, Burlingame, CA, USA) for 15 seconds at room temperature and were mounted using VectaMount® mounting medium (Vector Laboratories) and standard glass coverslips.

Tissue procurement and metabolite isolation

Whole human plasma from a single male donor was purchased from Innovative Research (Novi, MI, USA) and was stored at -80°C until used in experiments. Intact frozen bovine testes were procured from abattoirs and were a generous gift from Ms. Nada Cummings and Dr. Derek McLean (Washington State University, Pullman, WA, USA). Tissues were stored at -80°C until used for metabolite extraction. Bovine testes were used as a source of metabolites in

place of human tissue due to their easy availability and large amount of starting material.

Polar small molecules were extracted from twelve 130-150 mg samples of whole bovine testes using the two-step with supplemental water method established and described by Wu, et al[20]. The extracted polar fraction was dried under nitrogen at room temperature and stored at -20°C until use. No extraction of human plasma was performed for these experiments.

Metabolomic profiling

Human embryonic kidney (HEK-293) cells overexpressing human OAT4 or transfected with empty vector were created as described elsewhere (J.E. Shima et al, manuscript in submission; Chapter 3). Cells were grown on poly-D-lysine coated 30 mm cell culture dishes (BD Biosciences, San Jose, CA, USA) until 90-95% confluent. Cells were grown in a humidified cell culture incubator at 37°C and 5% CO_2 in Dulbecco's modified Eagle's medium (DMEM H-21) supplemented with 10% fetal bovine serum, 100 U/mL penicillin, 100 µg/mL streptomycin, and 100 µg/mL hygromycin B.

Cells used for experiments were washed with warm chloride-free uptake buffer (125 mM sodium gluconate, 4.8 mM potassium gluconate, 1.2 mM K_2HPO_4, 1.2 mM $MgSO_4$, 1.3 mM calcium gluconate, and 25 mM HEPES/Tris; pH ≈ 7.4) and the residual buffer aspirated off after 5 minutes. The cells then were incubated with either human plasma diluted 1:4 in chloride-free uptake buffer or a 1 mL aliquot of the extracted bovine testicular small molecule isolates resuspended in

12.5 mL of uptake buffer for 1 hour at 37°C. The experiments were terminated by rapidly cooling the plates on ice and aspirating the buffer containing plasma or testicular isolates. Each plate was subsequently washed three times with ice-cold choline buffer (128 mM choline chloride, 4.73 mM KCl, 1.25 mM $MgSO_4$, 1.25 mM $CaCl_2$, and 5 mM HEPES/Tris; pH ≈ 7.4) and any remaining buffer was aspirated prior to resuspension and lysis of the cells. The cells were scraped off the plates on ice and resuspended using 1 mL of ice-cold phosphate-buffered saline (PBS). Cell samples were then centrifuged at 3000 rpm for 4 minutes at 1°C and the supernatant aspirated off. The cell pellet was then resuspended in 200 µL of absolute methanol and sonicated three times on ice in 5 second pulses on a low setting three separate times in the course of 15 minutes. The lysed cells were then incubated on ice for an additional 10 minutes and then stored at -80°C overnight. Following cold storage, the cell lysate was centrifuged at 14,000 rpm for 5 minutes at 1°C. The resulting supernatant was then collected for metabolomic analysis. Six individual experimental samples were used for each condition (EV and OAT4 incubated with human plasma or bovine testicular lysate; 24 samples total). All analyses were performed by the University of California, Davis Metabolomics Core Facility (Davis, CA, USA) using a Surveyor HPLC module (Thermo Scientific, Waltham, MA, USA) in combination with a Finnigan LTQ ion trap mass spectrometer (Thermo Scientific) following the guidelines and procedures outlined elsewhere[21]. Metabolite profiling, identification, and statistical validation of potential hits were performed using MarkerView 1.1 software (Applied Biosystems).

Transport studies

HEK-293 EV and OAT4 cell lines were seeded in 24 well poly-D-lysine coated cell culture plates (BD Biosciences) and grown in standard cell culture media until 90-95% confluent as described previously. Uptake experiments commenced by removing the growth media and washing the cells with warm chloride-free uptake buffer (125 mM sodium gluconate, 4.8 mM potassium gluconate, 1.2 mM K_2HPO_4, 1.2 mM $MgSO_4$, 1.3 mM calcium gluconate, and 25 mM HEPES/Tris; pH ≈ 7.4) for 5 minutes. Experiments were performed by incubating the cells with either 17 nM [^{3}H]-estrone sulfate, 70 nM [^{3}H]-AMP, 50 nM [^{3}H]-adenine, 50 nM [^{3}H]-adenosine, or 50 nM [^{3}H]-cAMP as indicated in the figure legends. Inhibition of ES uptake was achieved by performing the uptake in the presence of 1.0 mM of (±)-carnitine, (±)-acetylcarnitine, or (±)-propionylcarnitine. Inhibition of endogenous equilibrative nucleoside transporter uptake was achieved by incubation with 10 μM 6-S-[(4-Nitrophenyl)methyl]-6-thioinosine (NBMPR) in all experiments that examined uptake of adenine or adenine-derived compounds. After 2 minutes, the uptake buffer was quickly removed and cells were immediately washed three times with ice-cold choline buffer (128 mM choline chloride, 4.73 mM KCl, 1.25 mM $MgSO_4$, 1.25 mM $CaCl_2$, and 5 mM HEPES/Tris; pH ≈ 7.4). Residual choline buffer was aspirated and 1 mL of warm lysis buffer (0.1% SDS/0.1 N NaOH) was added to the cells. The cells were lysed for a minimum of 45 minutes at room temperature with shaking prior to determination of intracellular radioactivity by liquid scintillation counting. Levels of total protein were determined using a BCA assay (Pierce

Biotechnology, Rockford, IL, USA) and used to normalize the levels of radioactivity measured in each well. Uptake experiments were performed in duplicate or triplicate as indicated in the figure legends. Statistical significance was determined using a one-way ANOVA followed by a Dunnett's post-hoc test using Graphpad Prism 5.1 (Graphpad, La Jolla, CA, USA) with a false discovery rate of 0.05.

Results

mRNA expression of *SLC22A11* in human tissues

Quantitative reverse transcriptase PCR (qRT-PCR) examining *SLC22A11* (OAT4) in 13 normal adult human tissues identified high expression levels in the kidney and placenta, as previously reported[18, 19, 22]. In addition, *SLC22A11* was expressed at very high levels in the epididymis, with the number of copies per microgram of total RNA exceeding that found in the kidney, as shown in Figure 2.2A. This is a novel finding previously unreported in the literature. All other male and female reproductive tissues examined showed very low levels of *SLC22A11* expression with the seminal vesicles displaying the next highest level after the epididymis and placenta, although only a fraction of the level in the epididymis. Evaluation of other organic anion transporters, specifically OAT1 (*SLC22A6*), OAT2 (*SLC22A7*), OAT3 (*SLC22A8*), OAT5 (*SLC22A10*), OAT7 (*SLC22A9*), OAT10 (*SLC22A13*), and URAT1 (*SLC22A12*) in the epididymis established that *SLC22A11* is also the predominant epididymal OAT with levels

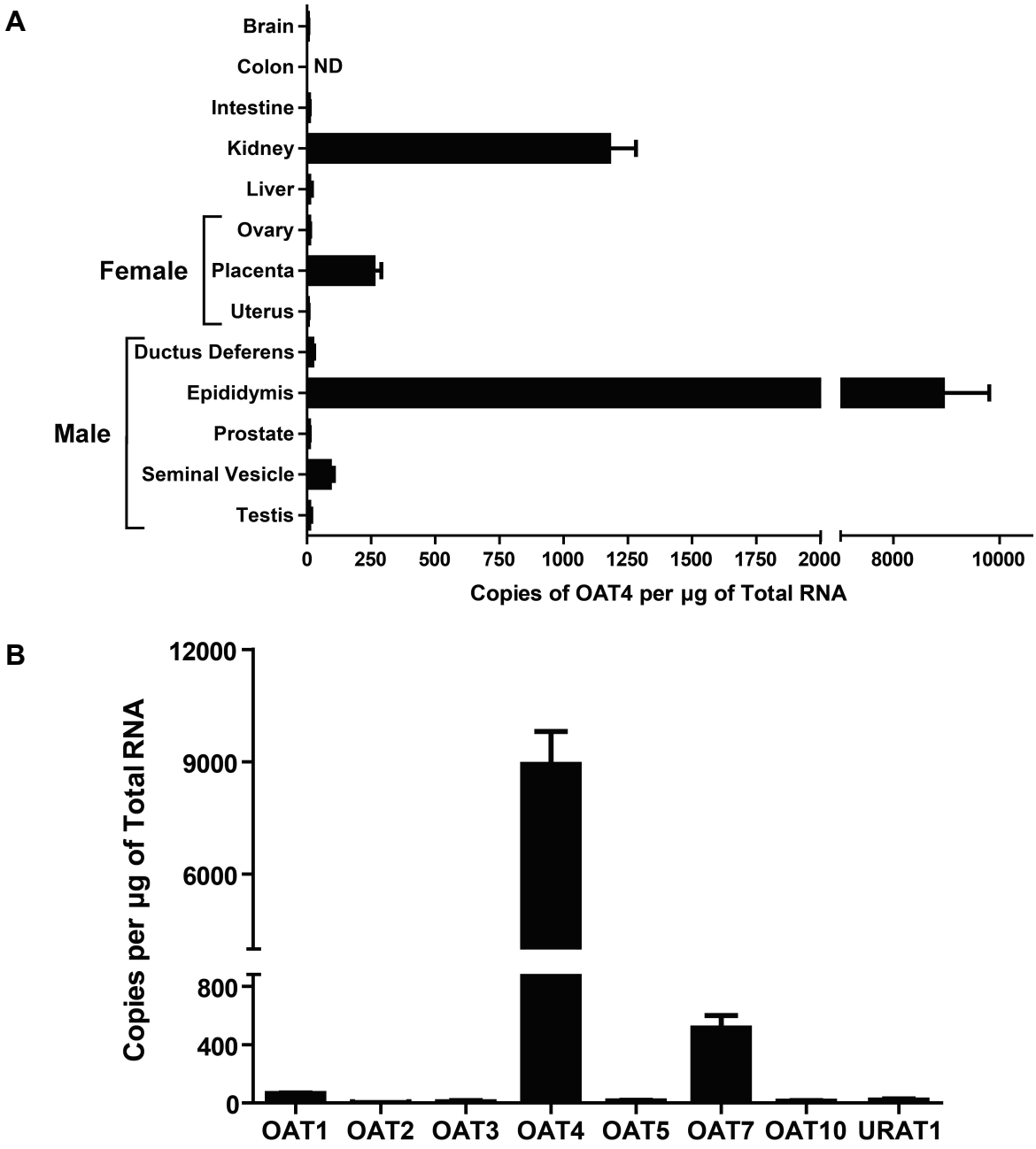

Figure 2.2: mRNA expression of *SLC22A11* and other organic anion transporters in human tissues. A) mRNA expression levels of *SLC22A11* (OAT4) in a normal adult human tissue panel and B) expression levels of organic anion transporters (OATs) in the human epididymis. Expression levels were determined using Taqman® assays specific to each OAT. Expression data were normalized to *GAPDH* expression and copy number was determined using a standard curve for each transporter. Each bar represents the mean ± SD of three independent measurements of single RNA samples. ND = none detected.

approximately 18-fold higher than the next highest expressed OAT, OAT7 (*SLC22A9*) as indicated in Figure 2.2B. Outside of the epididymis, other male reproductive tract tissues demonstrated similar OAT expression levels with the exception of the prostate; OAT2 and OAT3 were moderately expressed in the prostate but at a noticeably lower level than OAT4 expression in the epididymis (data not shown).

OAT4 localization in the human epididymis

Immunohistochemistry experiments to determine the localization of OAT4 protein in the epididymis used a poly-clonal antibody specific to human OAT4 and revealed high expression in the more proximal regions of the epididymis, in particular the efferent ductules (data not shown) and the caput and corpus epididymis as shown in Figure 2.3, panels A and B. Expression of OAT4 was absent in the cauda epididymis (Figure 2.3, panel C) with staining similar to that found in testis sections used as a negative control (data not shown). The quality of commercially available epididymal tissue sections, in particular those of the efferent ductules, was poor and precluded detailed evaluation of the cellular localization of OAT4 in the efferent ductules, however staining was evident and suggestive of high OAT4 expression in this region as well. The greatest degree of staining occurred at the most luminal regions of the cells; in particular the staining of the stereocilia suggests that OAT4 is localized to the principal cells of the epididymis and expressed on the apical membrane. This is most readily observed in panel B of Figure 2.3, which is representative of the corpus epididymis, and is indicated with the arrow in the figure.

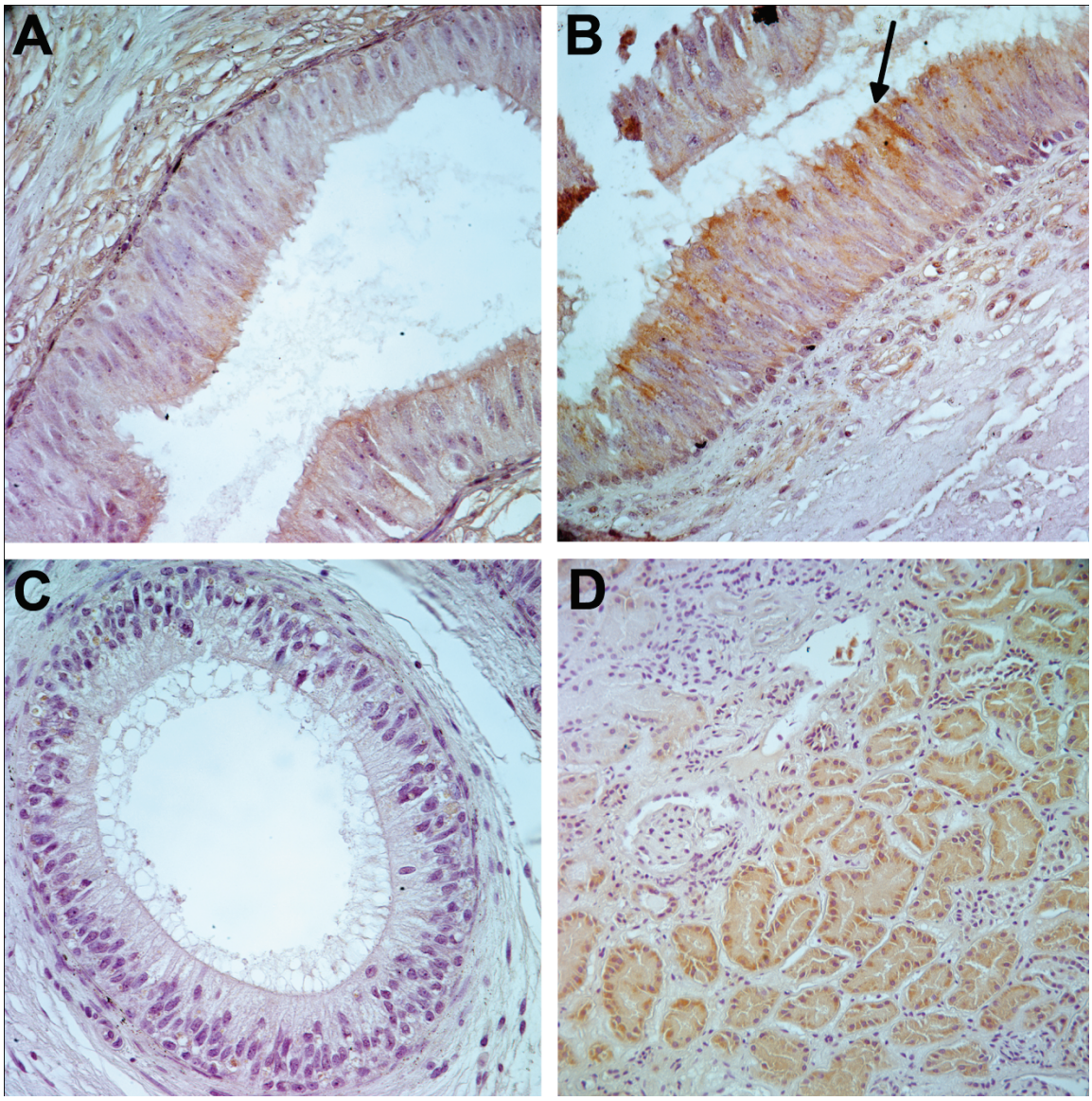

Figure 2.3: OAT4 is expressed in principal cells of the human epididymis. OAT4 was localized in various regions of the human epididymis using a polyclonal antibody specific to OAT4. Staining is indicative of expression on the apical (luminal) membrane of the principal cells of the epididymis. Expression appears to be limited to the apical membrane and is at the highest level in the corpus epididymis and is absent from the cauda epididymis. Sections were counterstained with hematoxylin. Kidney section is shown as an OAT4 positive control. A: caput epididymis, 400X magnification; B: corpus epididymis, 400X magnification; C: cauda epididymis, 400X magnification; D: kidney, 200X magnification.

Metabolomic profiling for potential endogenous substrates of OAT4

The high expression level of OAT4 in the epididymis would seem to be indicative of an important role in the epididymis, either in the reabsorption of components of the testicular fluid or in maintaining homeostasis of a particular anionic component of epididymal fluid required for normal sperm maturation. Metabolomic profiling of bovine testicular lysate was used in an attempt to identify potential endogenous substrates of OAT4, including those that may be in abundance in the male reproductive tract. Bovine testicular lysate was used in this study, as opposed to the equivalent fluid or tissue from a human source, due to its ready availability and the large amount of starting material available from a single testis. Complementary experiments using human plasma were also performed to both corroborate the findings from the bovine testicular lysate and provide alternative substrates for OAT4 that may not be present at relevant concentrations in the epididymis. Furthermore, bovine epididymal samples were positive for bovine OAT4 expression as determined by qRT-PCR (data not shown). The results from screening the bovine testicular lysate are outlined in Table 2.1 and the results from screening human plasma are outlined in Table 2.2. A number of statistically significant hits were identified as higher in the OAT4 expressing cells compared to empty vector cells in both samples, however, the majority were lipid and phospholipid derivatives which were unlikely to be true substrates of OAT4 as they are usually associated with cellular and plasma membranes. The zwitterion propionylcarnitine was identified in both

Table 2.1: Small molecules present at higher levels in OAT4-expressing HEK-293 cells vs. empty vector HEK-293 cells after incubation with polar isolates from bovine testes

M/Z	RT (min)	Identification
177.14	7.98	unknown
218.21	15.12	propionylcarnitine
348.06	27.38	adenosine monophosphate
351.14	7.37	unknown (estrone sulfate)
408.08	2.08	unknown
482.23	14.47	LysoPC (15:0)
496.24	13.96	LysoPC (16:0)
522.24	13.75	LysoPC(18:1:0)
524.21	13.66	LysoPC (18:0)
603.42	13.69	Diacylglycerol(33:1)
629.44	13.47	Diacylglycerol(37:5)
703.24	12.87	Diacylglycerolphosphate(36:0)
760.41	2.21	PE(38:8)
786.41	2.86	PE(40:9)
788.16	16.28	PS(36:2)
861.43	13.64	PI (36:2)
887.35	13.48	PI (38:3)

M/Z: mass to charge ratio. RT: retention time.

Table 2.2: Small molecules present at higher levels in OAT4-expressing HEK-293 cells vs. empty vector HEK-293 cells after incubation with human plasma

M/Z	RT (min)	Identification
177.14	7.96	unknown
218.21	15.11	propionylcarnitine
351.13	7.37	unknown (estrone sulfate)
496.24	14.03	LysoPC (16:0)
524.21	13.73	LysoPC (18:0)
603.42	13.62	Diacylglycerol(33:1)
760.41	2.8	PE(38:8)
786.41	3.1	PE(40:9)

M/Z: mass to charge ratio. RT: retention time.

samples as were unknowns with M/Z ratios of 177.14 and 351.14 respectively. While the exact identity of the unknown metabolite with the M/Z ratio of 351.13 was not apparent, it is possible that this is in fact ES, which has a predicted M/Z ratio of 351.126 and is a well-characterized substrate of OAT4, and has been found at high concentrations in the reproductive tract of a number of species[23]. Followup fragmentation experiments of the unknown with an M/Z ratio of 177.14 predicted a homocysteine-like entity of unknown origin and identity. Aside from these hits, adenosine monophosphate was also identified in the samples incubated with bovine testicular lysate and was one of only two non-lipid hits unique to the testis samples, the other being an additional unknown metabolite with an M/Z ratio of 408.08 and whose identity remains undetermined.

Interaction between OAT4 and potential endogenous substrates identified using metabolomic profiling

Followup experiments attempted to verify the interaction of the potential metabolomic hits with OAT4 using either direct radiolabeled uptake or inhibition of uptake of a radiolabeled probe for OAT4 ([^{3}H]-ES). As shown in Figure 2.4, neither (±)-carnitine nor its acyl derivatives (±)-acetylcarnitine and (±)-propionylcarnitine inhibited [^{3}H]-ES uptake by OAT4 when co-incubated at a concentration of 1.0 mM for 2 minutes suggesting that they are not likely to be substrates of OAT4, in contradiction to the results of the metabolomic profiling. The presence of adenosine monophosphate in the profiling results from the testicular sample suggested that purine-based molecules may also interact with OAT4. Uptake of radiolabeled adenine-derived endogenous small molecules by

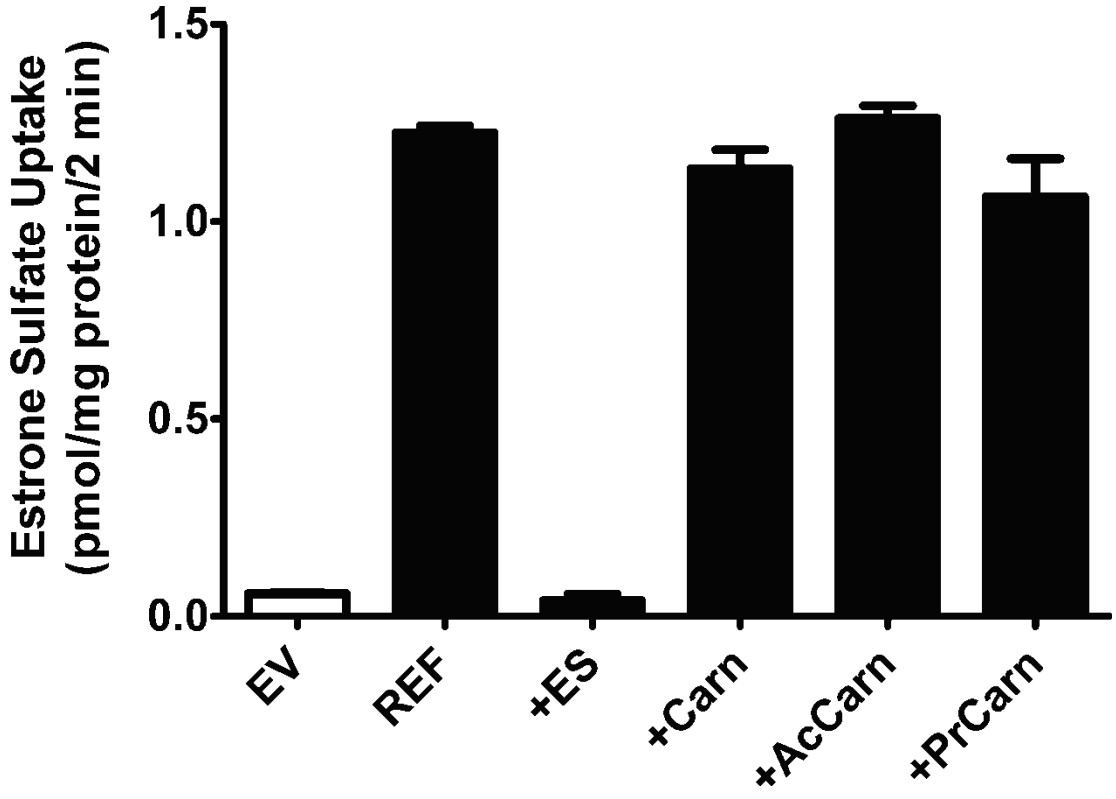

Figure 2.4: Effect of carnitine and acyl carnitines on estrone sulfate uptake by OAT4. Experiments were performed for 2 minutes at 37°C using 17 nM [^{3}H]-estrone sulfate (ES) alone or with coincubation of 1.0 mM unlabeled ES, (±)-carnitine (Carn), (±)-acetylcarnitine (AcCarn), or (±)-propionylcarnitine (PrCarn) using HEK-293 cells stably transfected with empty vector (white bar) or OAT4 (black bars). Uptake values were normalized to the total protein in each well and are presented as the mean uptake ± SEM of three replicate samples.

OAT4 is illustrated in Figure 2.5. While OAT4 transported [^{3}H]-ES to a great extent, no substantial uptake of 50-70 nM of [^{3}H]-adenine and related derivatives was observed after 2 minutes of incubation in the presence of 10 μM of NBMPR, an equilibrative nucleoside transporter (ENT) inhibitor, to block the known interactions between ENTs and purine nucleobases and nucleosides. Thus while OAT4 is capable of transporting ES as expected, it did not appear to interact with

any other of the potential candidates as determined using metabolomic profiling; however, not all the individual candidate compounds or classes of compounds were examined.

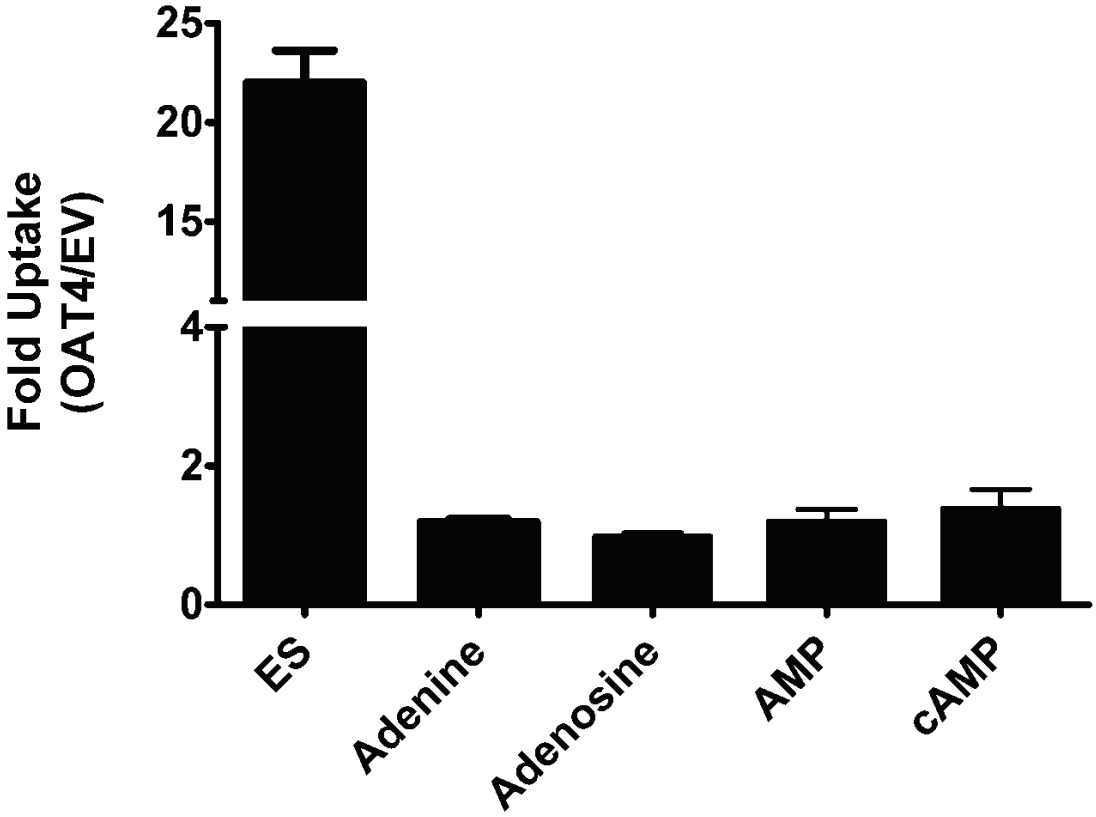

Figure 2.5: Uptake of adenine and endogenous adenine derivatives by OAT4. Uptake experiments using HEK-293 cells expressing OAT4 and empty vector cells were performed for 2 minutes at 37°C using 17 nM [^{3}H]-estrone sulfate, 70 nM [^{3}H]-AMP, or 50 nM of [^{3}H]-adenine, [^{3}H]-adenosine, or [^{3}H]-cAMP in the presence of 10 μM NBMPR. Uptake values were normalized to the total protein in each well and each bar represents the mean uptake ± SEM of three independent replicate experiments.

Discussion

The organic anion transporter OAT4 has been the subject of considerable investigation since its initial characterization in 2000 by Cha, et al[18] and the recognition of its role as an apically expressed renal dicarboxylate exchanger capable of transporting steroid sulfates and other canonical OAT substrates in proximal tubule cells a few years later[22]. Subsequent studies also revealed that OAT4 is capable of interacting with prostaglandins[24], anti-inflammatory drugs[25], and uric acid[26] which furthered the understanding of its functional properties. While the molecular features of OAT4 have been characterized in some detail, the current understanding of the physiological significance of OAT4 remains poorly understood. Studies have found genetic associations between SNPs in OAT4 and uric acid levels[27, 28] and recent investigations have suggested that OAT4 may be important in the synthesis of placenta-derived estrogens[19] and the development of glutaric acidurias[29] but the evidence provided by these studies is more suggestive of a supporting or supplemental role for OAT4 rather than it acting as a primary transporter for a specific physiological process or a causative factor in the development of a disease.

The discovery in the current study of significant OAT4 expression in the epididymis, a critical tissue in the maturation of spermatozoa and resultant male fertility, provides further information relevant to the endogenous role of OAT4. Of particular significance, and in stark contrast to the kidney and placenta, OAT4 appears to be the sole organic anion transporter in the SLC22 family that is expressed at a substantial level in the human epididymis. This extends to the

majority of the male reproductive tract as well. The significance of this remains indeterminate but it could be presumed that known and expected OAT4-meditaed transport of substrates would be restricted largely to the epididymis and much more limited in the remainder of the reproductive tract. The localization of OAT4 to the apical membrane of principal cells in the more proximal regions of the epididymis is also noteworthy and suggests that OAT4 plays a role in solute reabsorption in the epididymis. Principal cells are widely acknowledged to be the primary cells responsible for the reabsorption of water and various solutes, as well as protein and lipid components, in the epididymis which tends to occur to the greatest extent in the more proximal regions[6]. Likewise, the presence of OAT4 on the stereocilia of the principal cells further corroborates its role in the reabsorption of anionic solutes from the epididymal fluid microenvironment as these features follow the paradigm of a greater surface area resulting in greater flux across the membrane. Previous experimental evidence has shown that the epididymis functions much like the proximal tubule of the kidney wherein an immense amount of fluid and solute reabsorption occurs, in the case of the epididymis, from the testicular fluid flowing into the proximal epididymis during the migration of spermatozoa[11]. Reabsorption of water and luminal fluid components and maintenance of solute composition are the primary functions of the principal cells, and the presence of a high level of OAT4, a known reabsorptive transporter, in these cells is in agreement with the functional characteristics of OAT4 previously recognized in the kidney and placenta.

The presence of an abundance of OAT4 expressed in a region-specific manner in the epididymis indicates that it may perform a critical function in the maintenance of the fluid microenvironment in the proximal regions of the epididymis where net reabsorption is the highest. Although it can be presumed that OAT4 likely functions in a reabsorptive fashion in the epididymis based on its characterized activity in cellular assays, the identity of its primary physiologically relevant substrates remains largely unknown. By taking advantage of the high throughput methods developed with mass spectrometry, this study attempted to identify potential substrates of OAT4 from two biological sources (human plasma and bovine testis) using metabolomic profiling. Metabolomic profiling produced a limited number of hits with several considered potential OAT4 substrates. Of these hits, estrone sulfate (a previously identified OAT4 substrate), propionylcarnitine, and adenosine monophosphate were believed to be the most likely to interact with an OAT and were examined further.

Results from metabolomic profiling suggest that the most likely endogenous substrate of OAT4 in testicular fluids, as well as from the plasma, is ES and by inference, other steroid sulfates such as DHEAS. ES is the major form of estrogen in both men and women, occurring at concentrations 20-50 times higher than free estradiol in the blood[30, 31]. ES has also been previously described as an excellent substrate of OAT4 in cellular uptake assays and likewise has been found to be subject to absorption and reabsorption in the placenta and kidney respectively[18, 19, 32]. OAT4 has been shown to transport steroid sulfates to a considerable extent with K_m values in the high nanomolar range[18] while no

evidence has been produced thus far to show that free steroids interact appreciably with OAT4 or any other OAT. This is of notable significance as steroid sulfates have generally been observed at substantially higher concentrations in the male reproductive tract compared to free, biologically active steroids[33], akin to observations made in the blood. This allows for the possibility that signaling events derived from steroids may be mediated through the sulfate conjugates of steroids present in the male reproductive tract.

It is well recognized that the epididymis is reliant on steroid signaling for normal physiologic function and is regulated by both androgens (mainly testosterone and dihydrotestosterone) and estrogens (mainly estradiol), thus the regulation of the pools of these steroids is of critical importance. The impact of steroid regulation on epididymal function is particularly evident in knockout models for the androgen receptor, which result in the complete absence of the epididymis[34, 35], and estrogen receptor alpha in which significant functional anomalies have been observed specifically related to reabsorptive properties leading to infertility[36, 37]. Additionally, the epididymal epithelial cells are known to express the requisite enzymes needed to convert DHEAS and ES into active androgens and estrogens[38, 39], in particular steroid sulfatase (STS). Likewise, a precedent for this mechanism of steroid action has been observed in breast cancer[40] and bone tissue[41] wherein exposure to ES elicits similar effects compared to exposure to free estradiol, indicative of a strong likelihood that ES in particular is capable of eliciting steroid signaling when afforded the requisite enzymatic machinery and transport into a cell. Thus it is reasonable to speculate that steroid sulfates can

act as major pools of steroids in the epididymis and may result in significant functional effects given the extent of transport that could be mediated by OAT4. As such, since OAT4 is the sole OAT expressed in the epididymis, it may be a significant modulator of steroid signaling based on the transport of steroid sulfates and their conversion intracellularly to active steroids as depicted in Figure 2.6.

The presence of ES in metabolomic profiling of OAT4 cell lines exposed to both bovine testicular lysate and human plasma and the fact that proper steroid signaling is of considerable importance in the epididymis strongly suggests that steroid sulfates may be the endogenous substrates for OAT4. However, other potential substrates were identified in the screen. These included propionylcarnitine, a zwitterionic carrier of acyl groups across the mitochondrial membrane, and adenosine monophosphate (AMP), an anionic nucleotide. The possible interactions between carnitine or its ester derivatives and OAT4 were examined using inhibition of ES uptake but did not appear to alter uptake of a low concentration of ES. Similarly, direct uptake of radiolabeled adenine, adenosine, AMP, and cAMP demonstrated no appreciable uptake in OAT4-expressing cells compared to empty vector transfected cells. While both of these hits are intuitively plausible, they appear to not interact with OAT4 in a significant manner. The reasons for these false positives are not entirely clear; the potential causes may be related to the differential expression of transporters capable of direct uptake of these compounds between OAT4 and empty vector cell lines

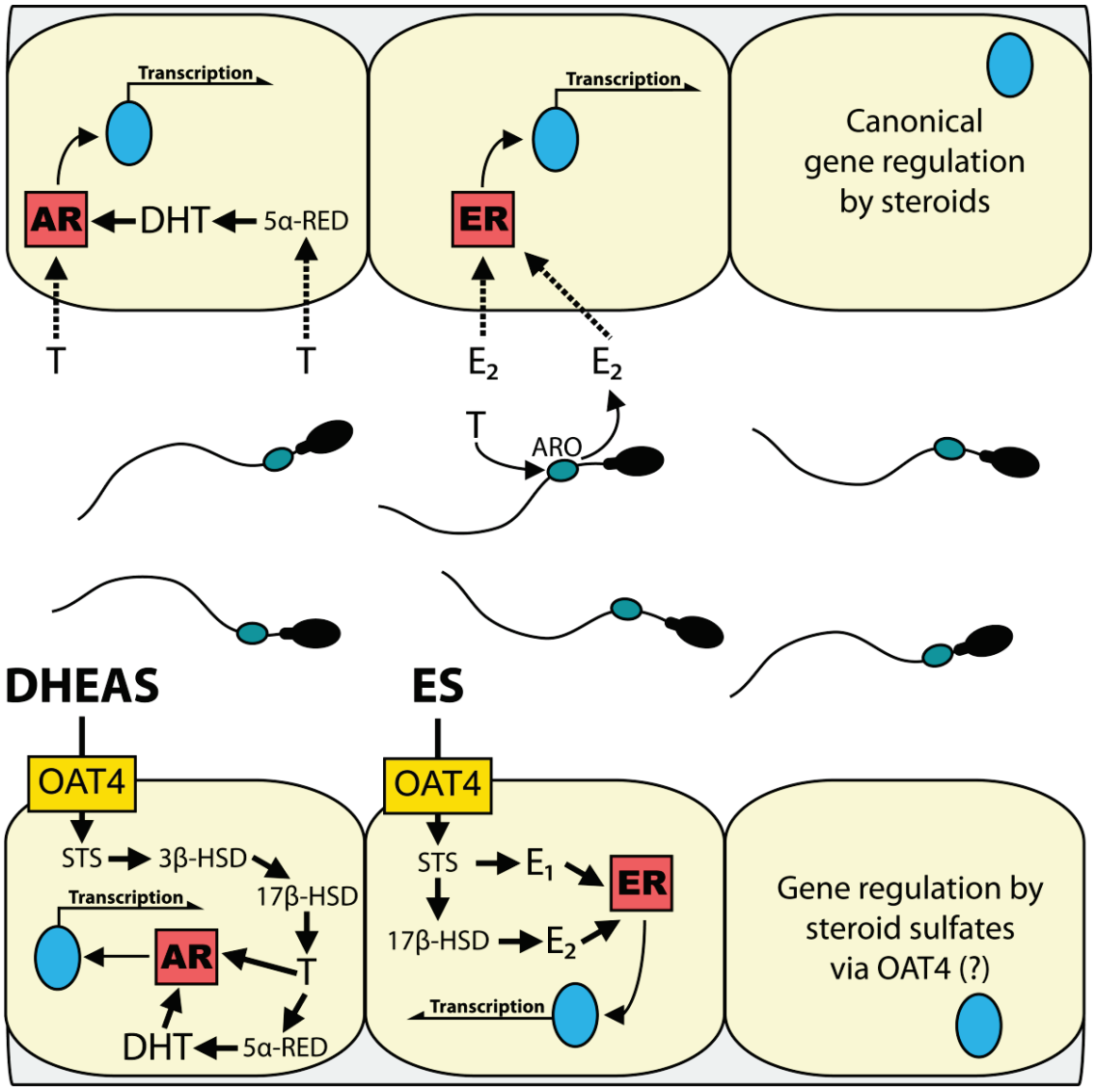

Figure 2.6: Hypothetical function of OAT4 in steroid sulfate-mediated signaling in the epididymis. Depiction of the potential role of OAT4 in androgen and estrogen signaling in epididymal epithelial cells (principal cells) wherein estrone sulfate (ES) or dehydroepiandrosterone sulfate (DHEAS) can be transported by OAT4 and converted to the active estrogens, estrone (E_1) and estradiol (E_2) or active androgens, testosterone (T) and dihydrotestosterone (DHT). Blue ovals represent nuclei and green ovals represent the cytoplasmic droplets. AR: androgen receptor. ER: estrogen receptor. STS: steroid sulfatase. ARO: aromatase (CYP19A1). 17β-HSD: 17β-hydroxysteroid dehydrogenase. 5α-RED: 5α-reductase. Aspects of this figure were adapted from Hess, R.A.[33].

such as other OATs or nucleoside transporters or the regulation of other cellular processes that may result in increased cellular accumulation of carnitine or purine based small molecules. Alternatively, OAT4 has been previously described as capable of secreting metabolic intermediates such as α-ketoglutarate and succinate due to its capacity for bidirectional exchange of dicarboxylates with organic anion substrates[22, 29]. Thus the secretion of intracellular metabolic intermediates for an appreciable amount of time may produce an altered metabolic state in OAT4-expressing cells that would result in the observed increase in propionylcarnitine and AMP, both of which are markers for a depleted cellular energy state[42, 43] and are consistent with both increased beta oxidation and alteration of the AMP:ATP ratio. Finally, the methods utilized in this study may predispose the results to false positives due to either the duration of experimental incubation or biases in the small molecule purification procedures. The consistency of the false positives between both biological samples would suggest that it is a systematic issue, perhaps due to global metabolic changes elicited by OAT4 overexpression, and not directly related to the source or composition of the biological samples used for OAT4 substrate discovery.

This study demonstrated for the first time substantial expression of OAT4 in the male reproductive tract with the highest expression levels in the proximal regions of the epididymis. The presence of OAT4 on the apical membrane of the principal cells suggests an important role in solute reabsorption, consistent with OAT4's purported role in the kidney. While the metabolomic methods utilized in

this study did not identify a novel substrate of OAT4 with potential implications in the fluid microenvironment of the epididymis, these studies revealed the previously known substrate ES as a potential key physiological substrate of OAT4 in the male reproductive tract. The results from the current study suggest that OAT4 may function as a regulator of steroid signaling by mediating the transport of steroid sulfates and subsequent activation to free steroids in the epididymal epithelium.

Clearly, a more refined approach or more stringent examination of the potential hits identified in this study may provide further insights into the role of OAT4 in the male reproductive tract and possibly illuminate more subtle roles in the epididymis in particular. In addition it cannot be ruled out that OAT4 may have a significant role in the reabsorption of other as of yet unidentified epididymal fluid components and potentially facilitate typical sperm maturation by removing a specific anionic solute from the luminal space or by maintaining the epididymal epithelium in a state conducive to sperm maturation and survival. Additional experiments are needed to assess the physiological significance of OAT4 expression in the epididymis and address the fundamental questions of the impact of steroid sulfate-mediated signaling in the epididymis and whether the function of OAT4 in particular is critical to the maturation or survival of spermatozoa in the epididymis and resultant male fertility.

References

1. Abma JC, Chandra A, Mosher WD, Peterson LS, Piccinino LJ. Fertility, family planning, and women's health: new data from the 1995 National Survey of Family Growth. *Vital and health statistics* 1997;(19)**:** 1-114.

2. Bhasin S, de Kretser DM, Baker HW. Clinical review 64: Pathophysiology and natural history of male infertility. *The Journal of clinical endocrinology and metabolism* 1994; **79**(6)**:** 1525-1529.

3. Schmidt L, Munster K, Helm P. Infertility and the seeking of infertility treatment in a representative population. *British journal of obstetrics and gynaecology* 1995; **102**(12)**:** 978-984.

4. Jones RC. To store or mature spermatozoa? The primary role of the epididymis. *International journal of andrology* 1999; **22**(2)**:** 57-67.

5. Yanagimachi R. Mammalian Fertilization. In: Knobil E, Neill JD (eds). *The Physiology of Reproduction*. Raven Press: New York, 1994, pp 189-317.

6. Robaire B, Hinton BT, Orgebin-Crist MC. *The epididymis : from molecules to clinical practice : a comprehensive survey of the efferent ducts, the epididymis, and the vas deferens*. Kluwer Academic/Plenum Publishers: New York, 2002, xiii, 575 p.pp.

7. Yeung CH, Cooper TG, Waites GM. Carnitine transport into the perfused epididymis of the rat: regional differences, stereospecificity, stimulation by choline, and the effect of other luminal factors. *Biol Reprod* 1980; **23**(2)**:** 294-304.

8. Hinton BT. The testicular and epididymal luminal amino acid microenvironment in the rat. *Journal of andrology* 1990; **11**(6)**:** 498-505.

9. Hinton BT, White RW, Setchell BP. Concentrations of myo-inositol in the luminal fluid of the mammalian testis and epididymis. *J Reprod Fertil* 1980; **58**(2)**:** 395-399.

10. Hinton BT, Palladino MA. Epididymal epithelium: its contribution to the formation of a luminal fluid microenvironment. *Microscopy research and technique* 1995; **30**(1)**:** 67-81.

11. Clulow J, Jones RC, Hansen LA, Man SY. Fluid and electrolyte reabsorption in the ductuli efferentes testis. *Journal of reproduction and fertility* 1998; **53:** 1-14.

12. Ilio KY, Hess RA. Structure and function of the ductuli efferentes: a review. *Microscopy research and technique* 1994; **29**(6)**:** 432-467.

13. Clulow J, Jones RC, Hansen LA. Micropuncture and cannulation studies of fluid composition and transport in the ductuli efferentes testis of the rat: comparisons with the homologous metanephric proximal tubule. *Experimental physiology* 1994; **79**(6)**:** 915-928.

14. Hansen LA, Clulow J, Jones RC. The role of Na+-H+ exchange in fluid and solute transport in the rat efferent ducts. *Experimental physiology* 1999; **84**(3)**:** 521-527.

15. Tamai I, Ohashi R, Nezu J, Yabuuchi H, Oku A, Shimane M*, et al*. Molecular and functional identification of sodium ion-dependent, high affinity human carnitine transporter OCTN2. *The Journal of biological chemistry* 1998; **273**(32)**:** 20378-20382.

16. Vaz FM, Scholte HR, Ruiter J, Hussaarts-Odijk LM, Pereira RR, Schweitzer S*, et al*. Identification of two novel mutations in OCTN2 of three patients with systemic carnitine deficiency. *Hum Genet* 1999; **105**(1-2)**:** 157-161.

17. Toshimori K, Kuwajima M, Yoshinaga K, Wakayama T, Shima K. Dysfunctions of the epididymis as a result of primary carnitine deficiency in juvenile visceral steatosis mice. *FEBS letters* 1999; **446**(2-3)**:** 323-326.

18. Cha SH, Sekine T, Kusuhara H, Yu E, Kim JY, Kim DK*, et al*. Molecular cloning and characterization of multispecific organic anion transporter 4 expressed in the placenta. *The Journal of biological chemistry* 2000; **275**(6)**:** 4507-4512.

19. Ugele B, St-Pierre MV, Pihusch M, Bahn A, Hantschmann P. Characterization and identification of steroid sulfate transporters of human placenta. *Am J Physiol Endocrinol Metab* 2003; **284**(2)**:** E390-398.

20. Wu H, Southam AD, Hines A, Viant MR. High-throughput tissue extraction protocol for NMR- and MS-based metabolomics. *Anal Biochem* 2008; **372**(2)**:** 204-212.

21. Fiehn O, Wohlgemuth G, Scholz M, Kind T, Lee do Y, Lu Y*, et al*. Quality control for plant metabolomics: reporting MSI-compliant studies. *Plant J* 2008; **53**(4)**:** 691-704.

22. Ekaratanawong S, Anzai N, Jutabha P, Miyazaki H, Noshiro R, Takeda M*, et al*. Human organic anion transporter 4 is a renal apical organic

anion/dicarboxylate exchanger in the proximal tubules. *Journal of pharmacological sciences* 2004; **94**(3)**:** 297-304.

23. Hess RA, Zhou Q, Nie R, Oliveira C, Cho H, Nakaia M*, et al*. Estrogens and epididymal function. *Reprod Fertil Dev* 2001; **13**(4)**:** 273-283.

24. Kimura H, Takeda M, Narikawa S, Enomoto A, Ichida K, Endou H. Human organic anion transporters and human organic cation transporters mediate renal transport of prostaglandins. *The Journal of pharmacology and experimental therapeutics* 2002; **301**(1)**:** 293-298.

25. Takeda M, Khamdang S, Narikawa S, Kimura H, Hosoyamada M, Cha SH*, et al*. Characterization of methotrexate transport and its drug interactions with human organic anion transporters. *The Journal of pharmacology and experimental therapeutics* 2002; **302**(2)**:** 666-671.

26. Hagos Y, Stein D, Ugele B, Burckhardt G, Bahn A. Human renal organic anion transporter 4 operates as an asymmetric urate transporter. *J Am Soc Nephrol* 2007; **18**(2)**:** 430-439.

27. Kolz M, Johnson T, Sanna S, Teumer A, Vitart V, Perola M*, et al*. Meta-analysis of 28,141 individuals identifies common variants within five new loci that influence uric acid concentrations. *PLoS Genet* 2009; **5**(6)**:** e1000504.

28. van der Harst P, Bakker SJ, de Boer RA, Wolffenbuttel BH, Johnson T, Caulfield MJ*, et al*. Replication of the five novel loci for uric acid concentrations and potential mediating mechanisms. *Human molecular genetics* 2010; **19**(2)**:** 387-395.

29. Hagos Y, Krick W, Braulke T, Muhlhausen C, Burckhardt G, Burckhardt BC. Organic anion transporters OAT1 and OAT4 mediate the high affinity transport of glutarate derivatives accumulating in patients with glutaric acidurias. *Pflugers Arch* 2008; **457**(1)**:** 223-231.

30. *The Merck Manual of Diagnosis and Therapy*, vol. 17. John Wiley & Sons: Whitehouse Station, NJ, 1999, 2833pp.

31. Zumoff B, Troxler RG, O'Connor J, Rosenfeld RS, Kream J, Levin J*, et al*. Abnormal hormone levels in men with coronary artery disease. *Arteriosclerosis* 1982; **2**(1)**:** 58-67.

32. Smith OW. Free and conjugated estrogens in blood and urine before and during parturition in normal human pregnancy. *Acta Endocrinol (Copenh)* 1966; **51:** Suppl 104:101-131.

33. Hess RA. Oestrogen in fluid transport in efferent ducts of the male reproductive tract. *Rev Reprod* 2000; **5**(2)**:** 84-92.

34. De Gendt K, Swinnen JV, Saunders PT, Schoonjans L, Dewerchin M, Devos A*, et al*. A Sertoli cell-selective knockout of the androgen receptor causes spermatogenic arrest in meiosis. *Proceedings of the National Academy of Sciences of the United States of America* 2004; **101**(5)**:** 1327-1332.

35. Yeh S, Tsai MY, Xu Q, Mu XM, Lardy H, Huang KE*, et al*. Generation and characterization of androgen receptor knockout (ARKO) mice: an in vivo model for the study of androgen functions in selective tissues. *Proceedings of the National Academy of Sciences of the United States of America* 2002; **99**(21)**:** 13498-13503.

36. Hess RA, Bunick D, Lubahn DB, Zhou Q, Bouma J. Morphologic changes in efferent ductules and epididymis in estrogen receptor-alpha knockout mice. *Journal of andrology* 2000; **21**(1)**:** 107-121.

37. Zhou Q, Clarke L, Nie R, Carnes K, Lai LW, Lien YH*, et al*. Estrogen action and male fertility: roles of the sodium/hydrogen exchanger-3 and fluid reabsorption in reproductive tract function. *Proceedings of the National Academy of Sciences of the United States of America* 2001; **98**(24)**:** 14132-14137.

38. Lemazurier E, Seralini GE. Evidence for sulfatase and 17beta-hydroxysteroid dehydrogenase type 1 activities in equine epididymis and uterus. *Theriogenology* 2002; **58**(1)**:** 113-121.

39. Wiszniewska B. Steroidogenic characteristics of in vitro cultured epididymal epithelial cells of the rat. *Reprod Biol* 2001; **1**(1)**:** 60-66.

40. Nozawa T, Suzuki M, Takahashi K, Yabuuchi H, Maeda T, Tsuji A*, et al*. Involvement of estrone-3-sulfate transporters in proliferation of hormone-dependent breast cancer cells. *The Journal of pharmacology and experimental therapeutics* 2004; **311**(3)**:** 1032-1037.

41. Muir M, Romalo G, Wolf L, Elger W, Schweikert HU. Estrone sulfate is a major source of local estrogen formation in human bone. *The Journal of clinical endocrinology and metabolism* 2004; **89**(9)**:** 4685-4692.

42. Winder WW, Hardie DG. AMP-activated protein kinase, a metabolic master switch: possible roles in type 2 diabetes. *Am J Physiol* 1999; **277**(1 Pt 1)**:** E1-10.

43. Brass EP, Stabler SP. Carnitine metabolism in the vitamin B-12-deficient rat. *Biochem J* 1988; **255**(1)**:** 153-159.

Chapter 3

Genetic Variants of Human Organic Anion Transporter 4 Demonstrate Altered Transport of Endogenous Substrates†

Introduction

Understanding the role of organic anion transporters (OATs) in the kidney has become increasingly important given their demonstrated roles in drug disposition, adverse drug interactions, and xenobiotic-induced toxicities[1-3]. Currently, the majority of this research has focused on the basolateral membrane transporters OAT1 (*SLC22A6*) and OAT3 (*SLC22A8*), which mediate the initial uptake of xenobiotics from the blood into the proximal tubule cells in the process of renal secretion. A number of studies have shown that these transporters can facilitate the uptake of numerous drugs and toxins[4], likely providing a significant mechanism for renal toxicity, and that these transporters in particular respond to renal injury[5]. While renal secretion of endogenous small molecules and xenobiotics is an important facet of the physiological and pharmacological functions of the kidney, the reabsorption of organic anions from the urine is also a substantial process that occurs in the kidney. Passive and facilitated reabsorption can influence both the pharmacokinetic profile of a drug and the circulating levels of important metabolic intermediates and precursors in the

---

† This chapter has been published previously: Shima J.E., Komori T., Taylor T.R., Stryke D., Kawamoto M., Johns S.J., Carlson E.J., Ferrin T.E., Giacomini K.M. "Genetic variants of human organic anion transporter 4 demonstrate altered transport of endogenous substrates." *American Journal of Physiology – Renal Physiology* 2010; 299(4):F767-775. doi: 10.1152/ajprenal.00312.2010. The Am Physiol Soc, used with permission.

blood[6, 7]. To date, comparatively little has been done to evaluate and understand the potential impact of apical organic anion transporters that play a role in reabsorptive mechanisms of drugs and other xenobiotics in the renal proximal tubule.

OAT4 (*SLC22A11*) is a solute carrier (SLC) family transporter which functions primarily as an organic anion/dicarboxylate exchanger[8]. *SLC22A11* transcripts are expressed at appreciable levels in the kidney, similar to OCT2 (*SLC22A2*) and OCTN2 (*SLC22A5*) but at a substantially lower level compared to OAT1 and OAT3[9, 10]. OAT4 has been localized to the apical membrane of renal proximal tubules, accordant with its function as a reabsorptive transporter in the kidney[8]. Previous studies have demonstrated that OAT4 is capable of transporting or interacting with both endogenous compounds and xenobiotics including steroid sulfates[11], non-steroidal anti-inflammatory drugs[12], angiotensin II and leukotriene receptor antagonists[13], prostaglandins[14], and uric acid[6] and thus could affect homeostatic processes occurring in the kidney and the body as a whole as well as impact the efficacy or safety of commonly used drugs. Similarly, OAT4 is expressed on the basolateral membrane of the syncytiotrophoblast of the placenta and is postulated to be important in the removal of steroid sulfates from the fetal compartment and thereby promoting appropriate steroid signaling and minimizing toxic effects for the developing fetus[11, 15, 16]. Prior studies have also identified associations between genetic variants of OAT4 and the clearance of the loop diuretic torsemide[17] as well as plasma uric acid levels[18, 19] suggesting that function-altering variants of OAT4 may be responsible for differences

observed in the clearance of xenobiotics and the reabsorption of important endogenous metabolites.

Previous studies have identified a number of genetic variants in OAT4, including multiple variants that result in a change in the amino acid sequence. Variants have been described in studies that examined a small number of individuals from diverse ethnic groups[20] and also in specific populations such as osteoporotic Korean women[21], the latter of which identified a nonfunctional variant only in those suffering from osteoporosis. A recent article by Zhou, et al has functionally characterized a number of previously described naturally occurring genetic variants of OAT4[20], however these variants were discovered by analyzing a limited number of DNA samples. The current study analyzed a large sample of DNA samples (n=272) from four distinct ethnic groups to identify coding variants in OAT4 in healthy individuals. A number of variants were identified and underwent subsequent functional assessments using model substrates of OAT4. Many of these variants demonstrated altered functionality and may significantly affect the renal excretion of a number of xenobiotics and anionic metabolites.

Materials and Methods

Reagents

Radiolabeled [^{3}H]-estrone sulfate was purchased from Perkin Elmer Life Sciences (Waltham, MA, USA). Radiolabeled [^{3}H]-ochratoxin A and [^{14}C]-uric acid were purchased from Moravek (Brea, CA, USA). All other chemicals were

purchased from Sigma (St. Louis, MO, USA). All cell culture media and reagents were purchased from the University of California, San Francisco Cell Culture Facility (San Francisco, CA, USA).

Identification of OAT4 SNPs

Nonsynonymous variants of OAT4 were identified from submissions in the NCBI dbSNP database (http://www.ncbi.nlm.nih.gov/snp) or through resequencing of genomic DNA as part of the Studies of Pharmacogenetics in Ethnically Diverse Populations (SOPHIE) project. DNA samples from the SOPHIE project were collected and analyzed in 68 healthy individuals from four ethnic groups: Caucasian, African American, Asian American, and Mexican American. Variants in the coding and flanking intronic regions in OAT4 were identified following methodologies described previously[22]. A complete list of OAT4 variants found in the SOPHIE project can be accessed at http://pharmacogenetics.ucsf.edu/.Use of genomic DNA from healthy volunteers was performed according to procedures reviewed and approved by the UCSF Committee on Human Research and informed consent was obtained from all subjects enrolled in the study.

Computational Analysis

All complete mammalian OAT4 sequences were downloaded from the ENSEMBL database (http://www.ensebml.org). Alignments of OAT4 protein sequences were created using MUSCLE 3.6[23] and the resulting alignment was visualized using the BioEdit software suite. Prediction of OAT4 SNP effects was done using pre-existing tools including SIFT[24], PolyPhen[25], PhD-SNP[26], and

SNAP[27], which use a variety of sequence and evolutionary analysis methods to predict whether a SNP would be potentially deleterious to the function of the protein.

Cell Line Construction

A full-length human OAT4 transcript (GenBank Accession # NM_018484) was PCR amplified from cDNA synthesized from a commercially available adult kidney RNA sample purchased from Clontech (Mountain View, CA, USA). The reference OAT4 coding sequence was subcloned into the mammalian expression vector pcDNA5/FRT (Invitrogen, Carlsbad, CA, USA) and variants of OAT4 were created using site-directed mutagenesis utilizing Pfu Ultra® DNA polymerase (Stratagene, La Jolla, CA, USA) and the pcDNA5/FRT-OAT4 vector as a template. All plasmid sequences were verified via direct sequencing of the complete open reading frame, including the variant locations. Cell lines stably transfected with pcDNA5/FRT (empty vector control), reference OAT4, or its variants were created using FLP-In-293 cells (Invitrogen) as previously described[28]. All stably transfected cell lines were grown in a humidified 37°C incubator with 5% CO_2 and cultured in DMEM H-21 supplemented with 10% heat-inactivated FBS, 100 U/mL penicillin, 100 µg/mL streptomycin, and 100 µg/mL hygromycin B.

RNA Isolation and qRT-PCR

Stable cell lines expressing reference OAT4 or its variants were grown in 6-well poly-D-lysine coated plates (BD Biosciences, San Jose, CA, USA) until reaching

90-95% confluency. Upon reaching confluency, cell culture media was aspirated and the cells were washed once with cold PBS. After removal of the PBS wash, TRIzol® reagent (Invitrogen) was added to the cells and RNA was isolated following the manufacturer's standard protocol. RNA purity and quality was assessed spectrophotometrically and by examination of 28S and 18S bands via agarose gel electrophoresis. cDNA was synthesized using a Superscript III® Reverse Transcription kit (Invitrogen) from 1 µg of purified total RNA samples following the manufacturer's standard protocol. The resulting cDNA was then diluted and used for quantitative determination of *SLC22A11* mRNA levels.

qRT-PCR was performed using Taqman® reagents and specific primer and probe sets for human *SLC22A11* and *GAPDH* (Applied Biosystems, Foster City, CA, USA). Reactions were performed in a 384 well plate with a 10 µL reaction volume using an ABI 7900HT Fast Real-time PCR system (Applied Biosystems) using the default instrument settings. Expression levels were determined from three independent biological samples using the $\Delta\Delta C_t$ method after normalization to endogenous levels of *GAPDH*. The results were expressed as a percentage of the mRNA level determined for the OAT4 reference cell line.

Protein Isolation and Western Blotting

Total protein was isolated from OAT4 expressing cells by culturing them to 90-95% confluency in T75 flasks and lysing them using radio-immunoprecipitation assay buffer (Sigma) following the manufacturer's standard protocol. Plasma membrane protein was isolated using a cell surface biotinylation kit (Pierce

Biotechnology, Rockford, IL, USA) following the manufacturer's standard protocol with slight modifications. Briefly, stably transfected OAT4 reference and variant cells lines were grown in T75 cell culture flasks, washed with ice-cold PBS, and incubated with Sulfo-NHS-SS-Biotin (Pierce Biotechnology) for 60 minutes at 4°C with gentle shaking. The cells were subsequently scraped off the flask, washed with ice-cold PBS supplemented with protease inhibitor cocktail (Pierce Biotechnology), and lysed. Biotinylated protein was isolated by incubating the lysate with streptavidin-linked agarose for 60 minutes at room temperature and eluted using 50mM dithiothreitol in standard SDS-PAGE buffer. Protein concentration was determined using a bicinchoninic acid (BCA) assay (Pierce Biotechnology).

Comparable amounts of protein from each cell line were run on a 4-20% gradient Tris-HCl polyacrylamide gel and transferred to an Immobilon® polyvinylidene fluoride (PVDF) membrane (Millipore, Billerica, MA, USA). The membranes were incubated in 5% nonfat milk in Tris-buffered saline with 0.05% Tween (TBST) for 1 hour followed by incubation with 5 µg/mL of rabbit anti-human polyclonal OAT4 antibody (US Biological, Swampscott, MA, USA) overnight at 4°C. Membranes were subsequently washed with TBST buffer and incubated with a 1:2000 dilution of a goat anti-rabbit IgG horseradish peroxidase-coupled secondary antibody (Santa Cruz Biotechnology, Santa Cruz, CA, USA) diluted in 5% nonfat milk in TBST buffer for 1 hour at room temperature. Following secondary antibody incubation, the membrane was washed with TBST buffer and protein detection was performed using ECL Plus® reagents (GE Healthcare, Piscataway,

NJ, USA). The membranes were stripped for 45 minutes using a β-mercaptoethanol based buffer and the procedure repeated using an antibody specific to the α-subunit of the Na^+/K^+ ATPase (US Biological) at a 1:1000 dilution to assess gel loading.

Uptake Studies

Cellular uptake of canonical substrates by OAT4 and its variants was determined using [^{3}H]-estrone sulfate, [^{3}H]-ochratoxin A, and [^{14}C]-uric acid. Cells were seeded on 24 well poly-D-lysine coated cell culture plates (BD Biosciences) in standard cell culture media as described previously and experiments commenced 24 hours after cell seeding. Uptakes were performed at 37°C for 2 minutes (estrone sulfate and ochratoxin A) or 4 minutes (uric acid) and began after the media was removed and cells were washed with warm Cl-free uptake buffer (125 mM sodium gluconate, 4.8 mM potassium gluconate, 1.2 mM K_2HPO_4, 1.2 mM $MgSO_4$, 1.3 mM calcium gluconate, and 25 mM HEPES/Tris; pH ≈ 7.4) for 3 minutes. Experiments were initiated by incubating the cells with warm Cl-free uptake buffer containing radiolabeled compound as indicated in the figure legends. At the completion of the incubation time period, cells were quickly washed with ice-cold choline buffer (128 mM choline chloride, 4.73 mM KCl, 1.25 mM $MgSO_4$, 1.25 mM $CaCl_2$, and 5 mM HEPES/Tris; pH ≈ 7.4) three times. Any remaining buffer was aspirated and the cells were lysed with 1 mL of warm 0.1% SDS/0.1 N NaOH solution for a minimum of 45 minutes. Intracellular levels of radioactive compound were determined using liquid scintillation counting. All resulting levels of substrate uptake were normalized to the total

protein in each well using a BCA protein assay. All uptake experiments were performed in triplicate and using empty vector transfected cell lines to establish background levels of uptake in HEK-293 cells. Statistically significant differences in uptake were evaluated using Graphpad Prism 5.1 (Graphpad, La Jolla, CA, USA) using a one-way ANOVA followed by a Dunnett's post-hoc test with a false discovery rate of 0.05.

Kinetic studies were performed in a similar fashion with supplemental amounts of unlabeled substrates included in the uptake buffer to produce the final concentration of substrate. At least three independent experiments were performed using empty vector transfected cells and OAT4 reference and variant cell lines. Kinetic values (K_m and V_{max}) were determined using non-linear regression analysis in Graphpad Prism 5.1 (Graphpad) after subtracting the uptake observed in the empty vector cell line from the uptake in stably transfected OAT4 cell lines at each concentration. Curves were fit to the Michaelis-Menten equation $V = V_{max}[S]/(K_m + [S])$ where V is the rate of uptake, V_{max} is the maximal uptake rate of the substrate, K_m is the substrate concentration at half the V_{max}, and [S] is the substrate concentration.

Results

Variant Identification

Variants of OAT4 were identified for further study by both querying the dbSNP database and by resequencing 272 DNA samples from four distinct ethnic groups

within the SOPHIE project. Resequencing of the ten exons and adjacent flanking regions of *SLC22A11* within SOPHIE identified 27 variable positions which included seven nonsynonymous and six synonymous variants with the remaining 14 variants occurring in intronic regions. Two additional nonsynonymous variants were identified in the dbSNP database. The majority of the

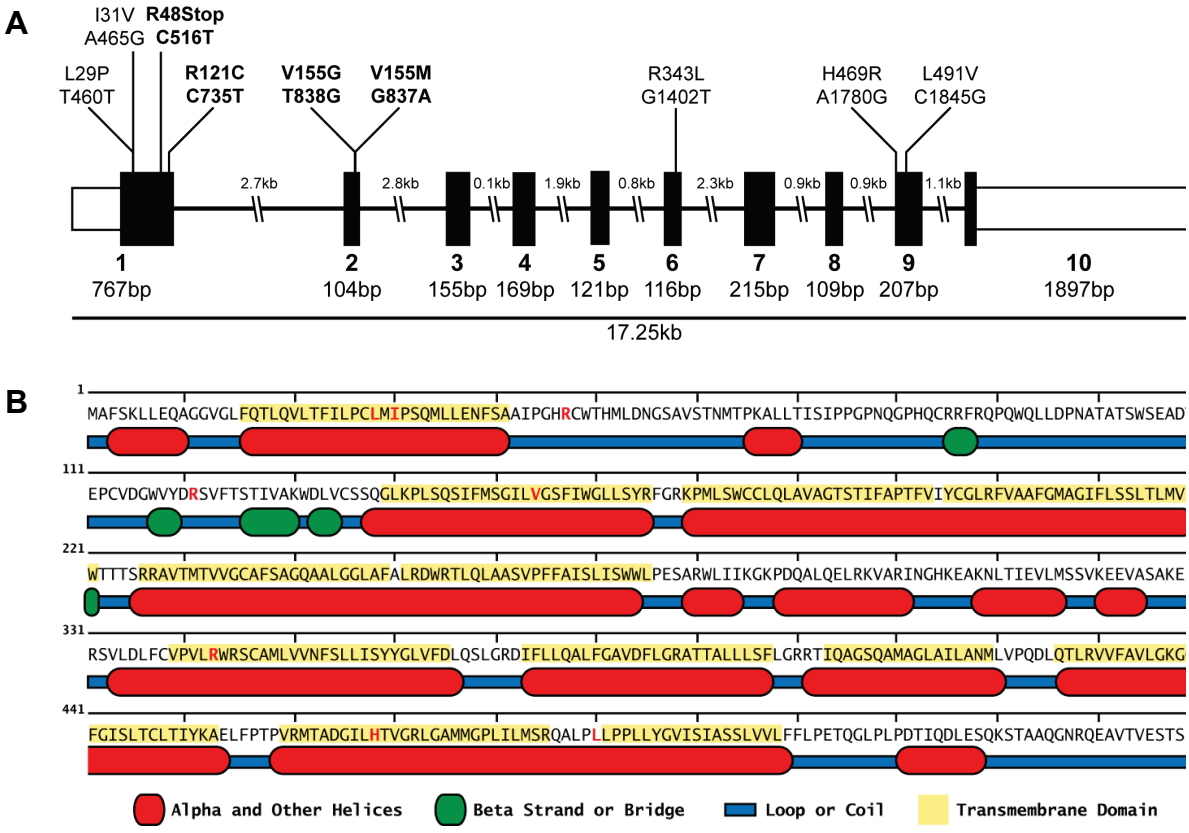

Figure 3.1: Location of nonsynonymous variants in human *SLC22A11*. A) Sites of nonsynonymous variants in the exonic structure of OAT4 (*SLC22A11*). Bold indicates variants that occur at a frequency of at least 1% in at least one ethnic group. B) Location of nonsynonymous variants in *SLC22A11* secondary structural elements based on predictions using MINNOU (http://minnou.cchmc.org/). Red amino acids indicate the positions of *SLC22A11* nonsynonymous variants.

nonsynonymous variants occurred in the first two exons of *SLC22A11* as shown in Figure 3.1A. Additionally, five of the nine amino acid altering variants were found in predicted transmembrane helix regions while two were found in the large extracellular loop occurring between the first two transmembrane domains. The L491V variant occurred in the small loop region between the predicted transmembrane helix 11 and 12.The location of these variants is further detailed in Figure 3.1B and Table 3.1.Four of the nonsynonymous variants (R121C, R343L, H469R, and L491V) were previously unidentified while the remaining three (R48Stop, V155M, and V155G) have been identified in either independent resequencing efforts[20] or as part of the HapMap and 1000 Genomes projects. The novel variant R121C occurred at a frequency of 2.3% in African Americans within the SOPHIE project. Similarly, the R48Stop and V155M variants were present at higher frequencies (2.3 and 1.7% respectively) in the SOPHIE cohort than previously reported[20]. However, the V155G variant, while a singleton in the Mexican American arm of SOPHIE, was found at 2.3% in the Han Chinese group within the HapMap genotyping project. All other nonsynonymous variants were found as singletons. All of the nonsynonymous variants identified in Mexican Americans were found as singletons while no nonsynonymous variants were found in the Asian American samples within SOPHIE; the majority of OAT4 nonsynonymous variants were found in a single ethnic group. A complete listing of the allele frequencies of these variants is shown in Table 3.2. In spite of the apparent discrepancy in allele frequency between the SOPHIE results and other

Table 3.1: Nonsynonymous variants of human *SLC22A11*

ID*	Exon	Genomic Position	mRNA Position	Base Change	Protein Position	Amino Acid Change
rs11231819	1	64080133	460	T→C	29	Leu→Pro
rs11231820	1	64080138	465	A→G	31	Ile→Val
rs35008345	1	64080189	516	C→T	48	Arg→Stop
PMT-2945	1	64080408	735	C→T	121	Arg→Cys
rs61744144	2	64083252	837	G→A	155	Val→Met
rs12785832	2	64083253	838	T→G	155	Val→Gly
PMT-2917	6	64089355	1402	G→T	343	Arg→Leu
PMT-2910	9	64093723	1780	A→G	469	His→Arg
PMT-2911	9	64093788	1845	C→G	491	Leu→Val

* indicates dbSNP or Pharmacogenetics of Membrane Transporters (PMT) IDs.

genotyping projects, these results suggest that nonsynonymous variants of OAT4 are not uncommon and may occur at higher frequencies than previously reported. Two nonsynonymous variants were previously listed in dbSNP (L29P and I31V) and while these variants lacked allele frequency data they were reported by multiple sequencing groups suggesting that they are not sequencing artifacts. However they were not found in any of the ethnic groups comprising SOPHIE or in the HapMap or 1000 Genomes projects. Of note, OAT4 possesses variants that result in two possible alternate amino acids at the same position and a nonsense change that produces a stop codon early in the protein sequence, both of which are considered rare events when examining variation within the SLC22 transporter family[29].

Conservation of OAT4 and *in silico* Functional Assessment

A large number of variants found to possess altered function have been shown to occur in evolutionarily conserved positions in membrane transporters[29, 30]. When the OAT4 nonsynonymous variants were mapped to multiple alignments of available complete OAT4 sequences, including human, chimpanzee, macaque, bovine, and canine orthologs, only two variants occurred in positions of conservation (R343L and L491V). However, and not without expectation, all of the variable positions are conserved when examining primate sequences only. Alignment of primate OATs expressed in the kidney (OAT4, OAT3, and OAT1) identified an additional position of conservation in OAT4 (L29P).

Further analysis using various computational algorithms designed to predict the functional consequences of amino acid substitutions was undertaken as well; four different algorithms were used to predict potential functional effects of variants of OAT4. These algorithms, which base their evaluations on calculations of protein stability, amino acid substitution matrices, and evolutionary constraints, largely predicted that most of the variants identified in OAT4 would result in a change in protein function. The results of these predictions are shown in Table 3.3. In fact, the only variants consistently predicted to have no functional consequences were I31V and L491V, at the extreme termini of OAT4. There was also a consensus among the four methods that the L29P, R121C, and R343L variants would cause a detrimental change in function. The R48Stop variant was not included in these analyses as the accepted assumption is that a premature stop codon will undoubtedly cause a change in protein function due to

Table 3.2: Allele frequency of nonsynonymous human *SLC22A11* variants

ID*	Variant	dbSNP MAF/Ethnicity	1K Genomes MAF			PMT MAF			
			CEU	CHB-JPT	YRI	AA	CA	AS	ME
rs11231819	Leu29Pro	N/A†	NA	NA	NA	NA	NA	NA	NA
rs11231820	Ile31Val	N/A†	NA	NA	NA	NA	NA	NA	NA
rs35008345	Arg49Stop	0.029/CA+AA	NA	NA	NA	0.000	0.023	0.000	0.008
PMT-2945	Arg121Cys	N/A	NA	NA	NA	0.023	0.000	0.000	0.000
rs61744144	Val155Met	N/A†	0.000	0.000	0.027	0.015	0.000	0.000	0.000
rs12785832	Val155Gly	0.023/CHB	NA	NA	NA	0.000	0.000	0.000	0.007
PMT-2917	Arg343Leu	N/A	0.009	0.000	0.000	0.000	0.000	0.000	0.007
PMT-2910	His469Arg	N/A	NA	NA	NA	0.000	0.008	0.000	0.000
PMT-2911	Leu491Val	N/A	NA	NA	NA	0.000	0.000	0.000	0.007

* indicates dbSNP or Pharmacogenetics of Membrane Transporters (PMT) IDs. † indicates presence of the SNP in the database but lacking any frequency data. MAF: Minor Allele Frequency; CA: Caucasian; AA: African American; AS: Asian American; ME: Mexican American; CHB: Han Chinese from Beijing, China; CEU: Northern and Western European ancestry from Utah; CHB-JPT: Han Chinese from Beijing, China and Japanese from Tokyo, Japan; YRI: Yoruban from Ibadan, Nigeria. NA: Not identified in the project or database.

Table 3.3: Predicted effect of nonsynonymous variants on OAT4 function

ID*	Variant	Mammalian Conservation†	OAT Family Conservation‡	Prediction of Variant Effect			
				SIFT	PolyPhen	PhD-SNP	SNAP
rs11231819	Leu29Pro	Unconserved	Conserved	Damaging	Damaging	Disease	Non-neutral
rs11231820	Ile31Val	Unconserved	Unconserved	Neutral	Benign	Neutral	Neutral
rs35008345	Arg49Stop	Unconserved	Unconserved	ND	ND	ND	ND
PMT-2945	Arg121Cys	Unconserved	Unconserved	Damaging	Damaging	Disease	Non-neutral
rs61744144	Val155Met	Unconserved	Unconserved	Damaging	Damaging	Neutral	Neutral
rs12785832	Val155Gly	Unconserved	Unconserved	Damaging	Benign	Disease	Non-neutral
PMT-2917	Arg343Leu	Conserved	Conserved	Damaging	Damaging	Disease	Non-neutral
PMT-2910	His469Arg	Unconserved	Unconserved	Neutral	Damaging	Disease	Non-neutral
PMT-2911	Leu491Val	Conserved	Conserved	Neutral	Benign	Neutral	Neutral

* indicates dbSNP or Pharmacogenetics of Membrane Transporters (PMT) IDs. † consists of human, chimpanzee, gorilla, macaque, dog, and cow OAT4 sequences. ‡ consists of human, chimpanzee, gorilla, and macaque OAT1, OAT3, and OAT4 sequences. ND: not determined.

the truncation of the protein. There was also no obvious correlation between the conservation status of the residue and the predicted effect of these variants; variants at both conserved and unconserved sites were predicted to be detrimental to the function of OAT4.

Functional Effects of OAT4 Nonsynonymous Variants

The functional consequences of nonsynonymous OAT4 variants were evaluated using stably transfected HEK-293 cells overexpressing either reference OAT4 or one of the coding variants. The effect of all nine nonsynonymous variants was investigated using uptake assays with the canonical OAT4 substrates estrone sulfate, ochratoxin A, and uric acid. Preliminary experiments demonstrated that the uptake of all three substrates was in the linear range up to 5 minutes (data not shown); all subsequent experiments were performed within this time frame of linear uptake. Incubation with estrone sulfate for 2 minutes produced the highest level of intracellular substrate accumulation with 13.8 ± 1.59 fold greater levels in the OAT4 reference cell line compared to empty vector (EV) transfected cells ($p \leq 0.001$). In comparison to the estrone sulfate uptake in the OAT4 reference cell line, the L29P, R48Stop, and H469R variant cell lines all demonstrated drastically reduced levels of uptake ($p \leq 0.001$). These levels were comparable to that in empty vector transfected cells, strongly suggesting that these variants result in the complete loss of function of OAT4 (Figure 3.2A). Similar patterns of uptake

A

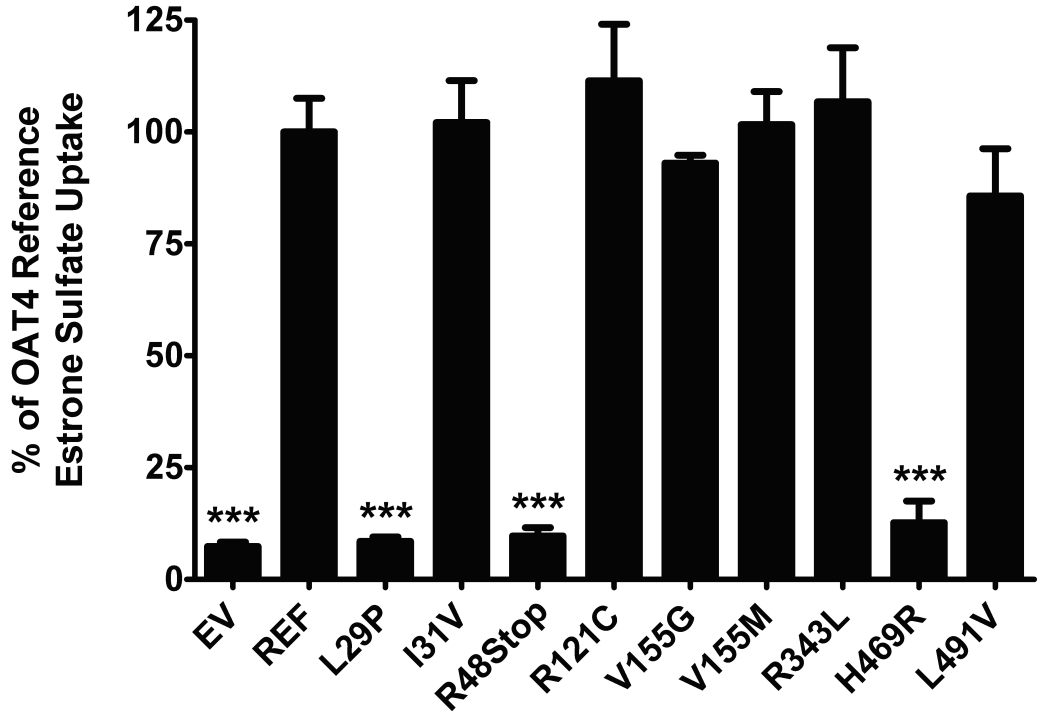
% of OAT4 Reference
Estrone Sulfate Uptake
125
100
75
50
25
0
***
***
***
***
EV
REF
L29P
I31V
R48Stop
R121C
V155G
V155M
R343L
H469R
L491V

B

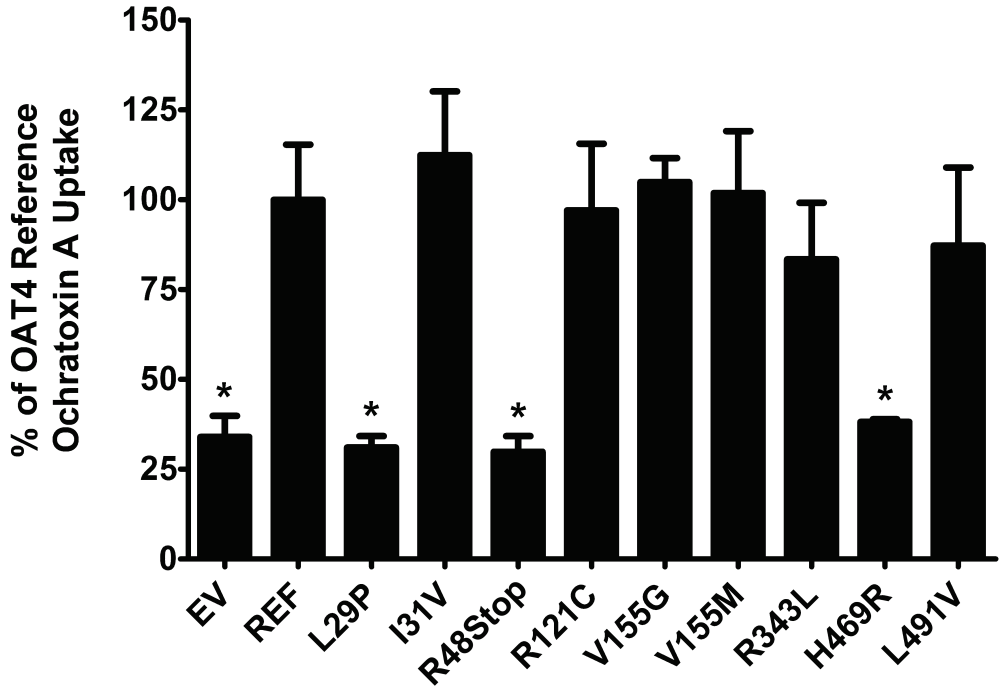
% of OAT4 Reference
Ochratoxin A Uptake
150
125
100
75
50
25
0
*
*
*
*
EV
REF
L29P
I31V
R48Stop
R121C
V155G
V155M
R343L
H469R
L491V

C

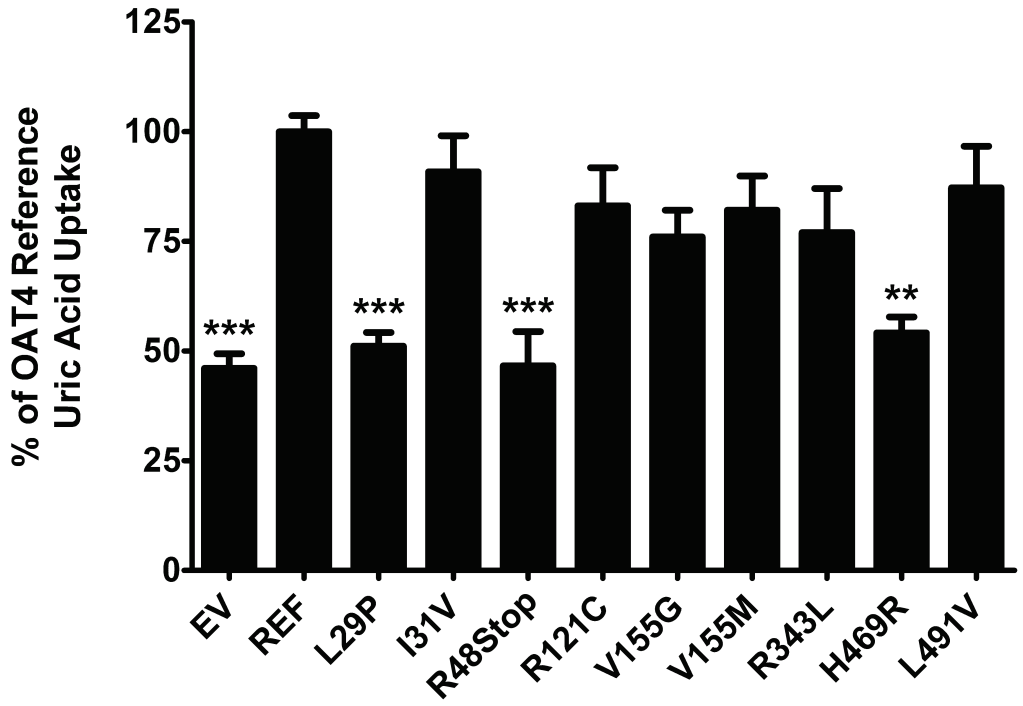

Figure 3.2: Functional characterization of genetic variants of OAT4 using uptake of canonical substrates. OAT4 mediated uptake of A) estrone sulfate, B) ochratoxin, and C) uric acid. Experiments were performed for 2 minutes (estrone sulfate and ochratoxin A) or 4 minutes (uric acid) at 37°C using 17 nM [^{3}H]-estrone sulfate, 200 μM [^{3}H]-ochratoxin A, or 400 μM uric acid (100 μM[^{14}C]-uric acid + 300 μM unlabeled uric acid). Uptake values are expressed as a percentage of OAT4 reference sequence uptake and were normalized to total protein in each well. Each bar represents the mean uptake ± SEM of three independent experiments.*** indicates p-value ≤ 0.001, ** a p-value ≤ 0.01, and * a p-value ≤ 0.05 when compared to reference uptake levels using one-way ANOVA analysis and Dunnett's post-hoc test.

were also observed in transiently transfected HEK-293 cells incubated with estrone sulfate (data not shown). The remaining variants did not show a noticeable decrease in estrone sulfate uptake and were all comparable to the reference sequence level of uptake. Uptake of ochratoxin A and uric acid, while not as extensive as that of estrone sulfate, consistently produced 2-3 fold greater

intracellular accumulation in reference cells than in EV cells after 2 minutes of substrate incubation. The effect of the variants was similar to that observed in the estrone sulfate uptake experiments (Figure 3.2B and 3.2C). Specifically, the L29P, R48Stop, and H469R variants all showed a complete loss of function and their levels of uptake were comparable to that observed in the EV cell line ($p \leq 0.05$ for ochratoxin A; $p \leq 0.001$ for uric acid). None of variants displayed differential uptake due to the substrate used which is suggestive that none of these variants cause a substrate selectivity change in OAT4.

Four nonsynonymous variants in OAT4 were found with frequencies greater than 1% in at least one ethnic group. Of these variants, only the R48Stop variant was found to impair OAT4 uptake capacity. Kinetic analysis of the remaining variants (R121C, V155G, and V155M) using estrone sulfate was performed to ascertain if there were subtle differences in function in these higher frequency variants that were not observable in uptake assays. As shown in Figure 3.3 and Table 3.4, all of these high frequency variants showed altered kinetics compared to the reference cell line. While all of the K_m values were close to the reference cell line value of 5.65 μM, the R121C and V155G variants both had statistically significant decreases in their V_{max} values with the V155G variant having a V_{max} of 0.113 ± 0.0138 pmol/μg protein/min and the R121C variant having a V_{max} of 0.209 ± 0.0264 pmol/μg protein/min compared to the reference value of 0.341 ± 0.0442 pmol/μg protein/min ($p \leq 0.001$ and $p \leq 0.05$ respectively). The ratios of V_{max} to K_m for all of the variants were not substantially different from the reference cell line however. Kinetic values were not determined for the complete loss of

function variants due to the inability to measure any increase in uptake beyond that observed in the EV cell line.

Effect of Variants on OAT4 mRNA and Protein Expression

The underlying mechanism occurring in the loss of function variants and the kinetic variability observed in the most common OAT4 nonsynonymous variants was investigated initially using qRT-PCR. The level of expression of *SLC22A11* in each of the cell lines was determined in relation to the expression of the control gene *GAPDH*. The expression of *SLC22A11* mRNA was routinely 30,000-40,000 fold higher in the stably transfected cell lines than in the empty vector transfected cell lines. While the I31V, R48Stop, and R121C variants showed slight decreases in mRNA levels compared to the reference cell line, only the R48Stop variant mRNA levels were significantly lower ($p \leq 0.05$), as shown in Figure 3.4. The use of stable cell lines created using the Flp-In system ensured that any differences in mRNA levels would most likely not be due to multiple integration sites of the expression vector, positional effects from random integration in the genome, or variability in the amount of vector successfully transfected transiently.

Plasma membrane protein levels resulting from each of the OAT4 variants were assessed using biotinylation of surface proteins in HEK-293 stably transfected cells expressing the reference and common variants forms of OAT4 followed by

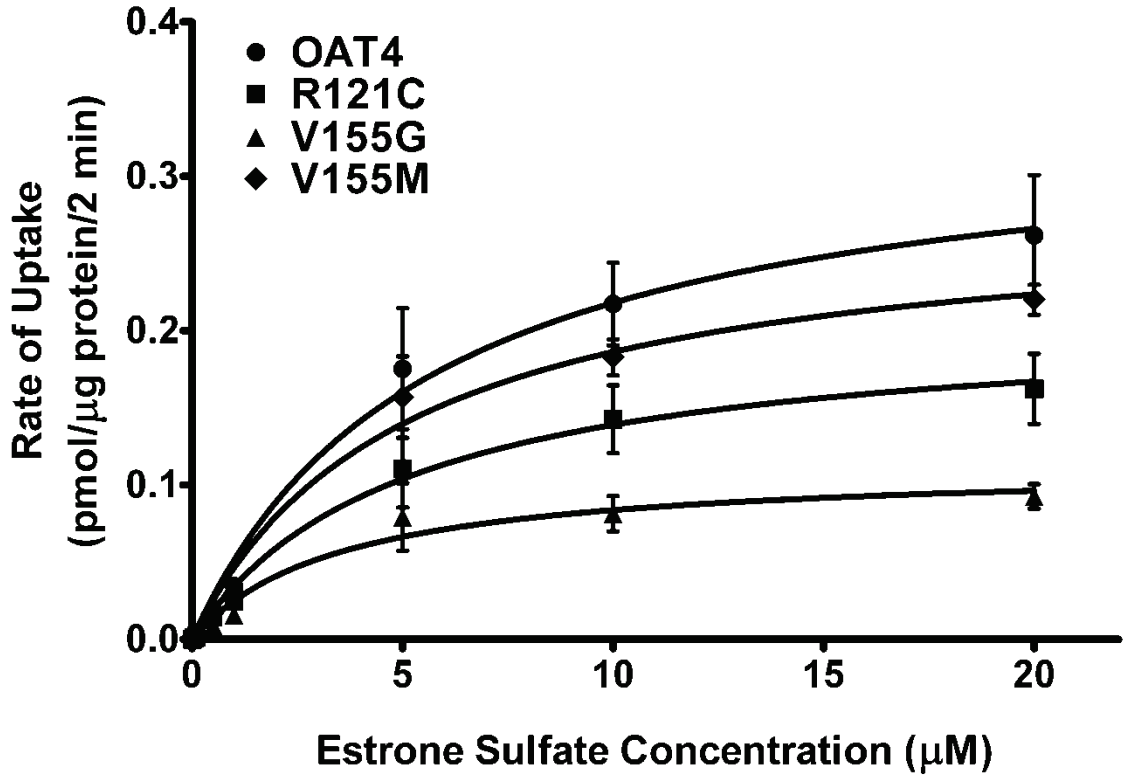

Figure 3.3: Saturable uptake of estrone sulfate in HEK-293-Flp cells overexpressing OAT4 and three high frequency nonsynonymous variants. Experiments were performed for 2 minutes at 37°C using 20 nM [^{3}H]-estrone sulfate and unlabeled estrone sulfate for the remainder. Uptake values were normalized to total protein and adjusted for the uptake of estrone sulfate in empty vector transfected cells. Curves were generated using non-linear regression with automatic removal of outliers in Graphpad Prism 5.1.

Table 3.4: Kinetic parameters of estrone sulfate uptake by common OAT4 nonsynonymous variants

Variant	K_m (μM)	V_{max} (pmol/ug protein/min)	V_{max}:K_m Ratio (pmol mg protein^{-1} min^{-1}/μM)
REF	5.65 ± 2.02	0.341 ± 0.0442	60.4 ± 12.2
R121C	5.07 ± 1.84	0.209 ± 0.0265*	41.2 ± 8.98
V155G	3.52 ± 1.41	0.113 ± 0.0138†	31.6 ± 9.27
V155M	5.01 ± 1.16	0.280 ± 0.0224	55.7 ± 10.7

* indicates p value < 0.05. † indicates p value < 0.001.

Western blotting. Figure 3.5 shows a representative blot of the nonfunctional variants of OAT4 with an expected band detected at approximately 90kDa. The reference OAT4 band was the most intense whereas minimal to no OAT4 protein was detected in either the L29P or the R48Stop cell lines (lanes 3 and 4). It should be noted that the OAT4 antibody is based on an epitope of the protein that occurs at the C-terminus of OAT4 thus making the R48Stop variant

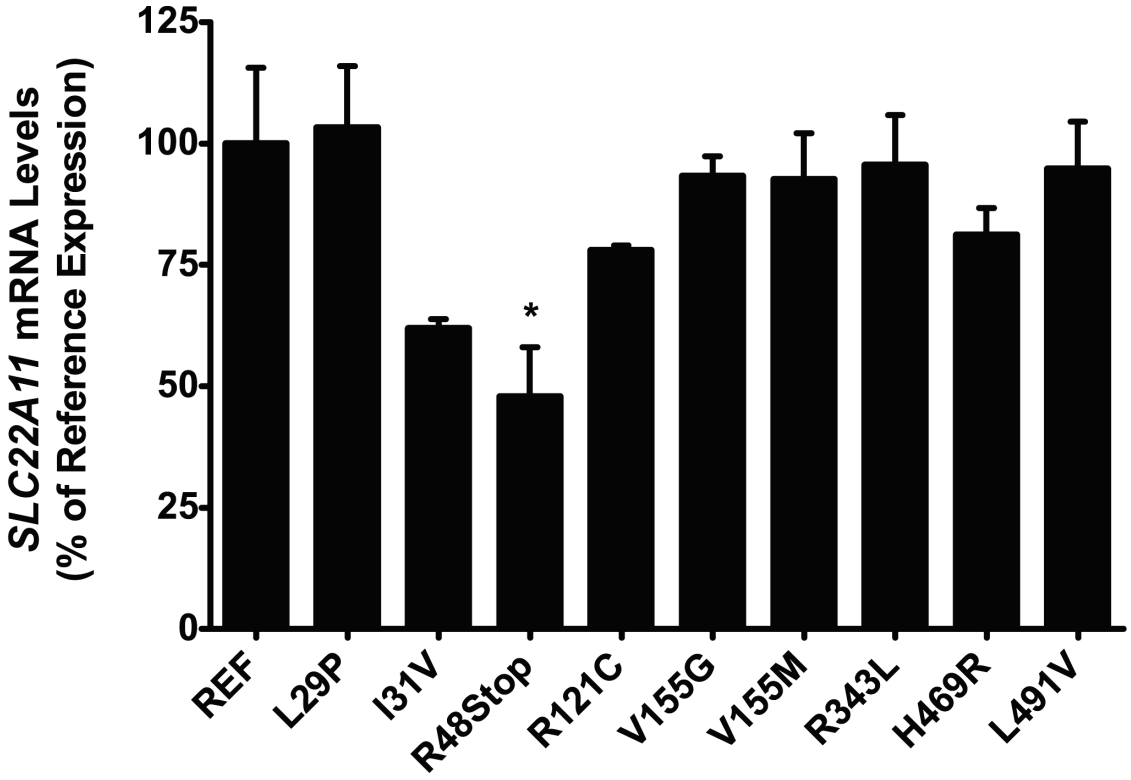

Figure 3.4: mRNA expression levels of *SLC22A11* and its variants in stably transfected HEK-293-Flp cells. Total RNA was extracted from each cell line, reverse transcribed to cDNA, and subsequently used to determine mRNA levels of each variant of *SLC22A11* using quantitative real-time PCR with a Taqman® assay specific to human *SLC22A11*. Expression levels were normalized to endogenous expression of *GAPDH* and are shown as a percentage of reference *SLC22A11* expression. Bars represent the mean ± SEM from two independent experiments. * indicates a p-value ≤ 0.05 compared to expression in the reference cell line.

undetectable. Repeat experiments using alternative antibodies derived from epitopes near the N-terminus were unsuccessful. OAT4 was detected in the H469R variant cell line, albeit at an apparently lower level than the reference cell line. Similar results were also obtained in blots of total protein wherein no protein was detected in either the L29P or R48Stop variants and the H469R variant showed decreased levels compared to the reference cell line. Reprobing the blot with an antibody specific for the Na^+/K^+ ATPase α-subunit revealed the abundance of membrane protein in the sample and approximately even loading of protein (Figure 3.5). Additionally, reprobing of the blot with a β–actin antibody showed very faint to no bands in the plasma membrane fraction whereas abundant staining was present in the total protein blot, indicating that the membrane fraction was largely free of cytoplasmic protein (data not shown).

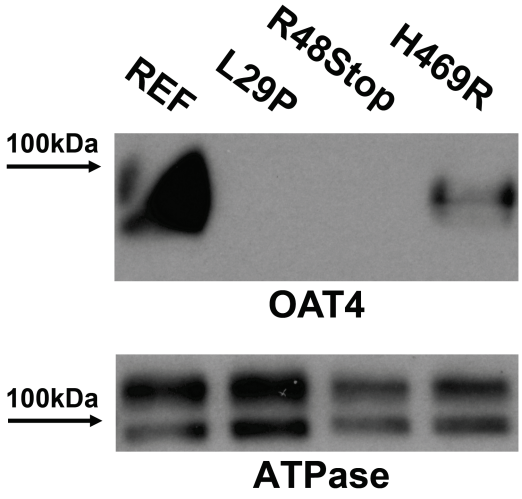

Figure 3.5: Levels of plasma membrane protein in HEK-293-Flp cells expressing reference and non-functional forms of OAT4. Upper Panel: plasma membrane protein was isolated via biotinylation, separated using SDS-PAGE and probed with an antibody specific to OAT4. Lower Panel: the same membrane was stripped and reprobed with an antibody specific to the α-subunit of the Na^+/K^+ ATPase.

Discussion

Human OAT4 is present on the apical membrane of the renal proximal tubule and as such, is known or suspected to be an important factor in the disposition of a variety of drugs and biologically relevant metabolites. Accordingly, several studies have focused on the identification and characterization of natural variants that occur in OAT4[20, 21]. Unlike these previous studies, however, this study used DNA samples from a large number of unrelated, ethnically diverse subjects to provide greater confidence in allele frequencies and to identify potential population specific variants in OAT4. Overall, the variation in the amino acid sequence of OAT4 was low, limited to 12 total variable positions and resulting in only seven nonsynonymous variants, only four of which occur on more than one chromosome and none of which occur at frequencies greater than 3%. While this is a low level of variability, these levels are similar to that observed in other renal SLC22 family transporters including OAT1[31] and OAT3[32]. The extent of amino acid conservation at variant positions was also relatively low with only two completely conserved variant locations when compared to multiple mammalian species (R343L and L491V) and only three sites when compared to other human OATs expressed in the kidney (L29P, R343L, and L491V). Furthermore, the majority of OAT4 nonsynonymous variants were predicted to be deleterious based on four distinct prediction algorithms. However, when examined using uptake of multiple substrates, the uptake results were concordant with only a third of the computational predictions. Examination of the kinetic properties of the higher frequency variants, all predicted to be damaging to some extent, also

found slight reductions in V_{max}, however reductions in V_{max} values may reflect differences in surface expression of OAT4. In spite of indications of intolerance to variation in OAT4 based on low variability and computational methodologies, neither the conservation of specific residues nor the change in physiochemical properties appeared to be strong predictors of functional consequences as evidenced by the R343L and L491V variants, which occurred at conserved sites yet retained complete functionality and the three most common variants which, in spite of a slight reduction in V_{max}, were largely functional. This suggests that the conservation of residues is important to the preservation of function among orthologous OAT4 proteins, but that the precise residues responsible for OAT4's specific functional capacity are not fully defined nor understood. Recent studies examining the role of histidine and glycine residues in OAT4 have made similar assessments and shed light on potentially critical regions for OAT4 function; systematic alteration of these residues produced distinct functional phenotypes related to membrane trafficking and substrate recognition[33, 34].

Of the nonsynonymous variants examined in this study, three resulted in a complete loss of function (L29P, R48Stop, and H469R) whereas the remainder demonstrated either no change in uptake (I31V, R343L, and L491V) of model substrates or only modest changes in the kinetic properties (R121C, V155G, and V155M) of estrone sulfate uptake. This "all-or-nothing" phenotype is unique among the SLC22 transporters examined thus far in that there were no observed variants possessing intermediate function or altered substrate specificity.

It is interesting to note that one of the highest frequency nonsynonymous variants observed in this study is the replacement of an arginine with a stop codon at position 48 (R48Stop) immediately after the first transmembrane domain. While the introduction of stop codons is an exceedingly rare event, and such nonsense variants are selected against for obvious reasons[35], variants producing premature termination of an SLC22 membrane transporter have been observed in OAT3[32] and OCTN1[28]. In contrast, both of these variants were exceedingly low frequency, unlike the R48Stop variant in OAT4 which occurs at 2.3% in Caucasians and was also observed in the Mexican American group as a singleton. Whole genome surveys of stop codons have recently found that while comprising an exceedingly small percentage of known variants, they do occur throughout the genome; these variants are believed to more often than not result in a severe truncation of the protein and some are readily identified as strongly causal alleles for certain diseases such as Legionnaires' disease-induced pneumonia[36]. Additionally, it is well recognized that premature termination variants such as R48Stop are subject to nonsense-mediated mRNA decay (NMD). The fact that the mRNA of the R48Stop variant was reduced by nearly 50% compared to the expression of reference OAT4 suggests that NMD may be a mechanism contributing to the observed decreased level of mRNA expression, though this was not specifically investigated in the current study. The remaining mRNA that is translated would be expected to produce a severely truncated protein incapable of transporting any of the model substrates, consistent with the observed variant effect in Figure 3.2A-C. Of note, a recent paper by Zhou, et al

described a R48Y variant occurring in OAT4 that results in a complete loss of function as well as a potentially altered glycosylation state[37]. However, this variant was not identified in the larger SOPHIE, HapMap, or 1000 Genomes projects; rather a stop codon was identified at the 48 position of OAT4 in these and other smaller sequencing projects[20]. While the impact in a clinical context of the premature termination codon resulting from the R48Stop variant is unknown, it would be expected that individuals possessing this variant would have altered reabsorption of small molecules such as estrone sulfate, uric acid, and renally eliminated drugs that are substrates of OAT4.

The L29P variant is also of interest due to its complete loss of function. This variant occurs within the first transmembrane domain of OAT4 and while it was not found in the SOPHIE or 1000 Genomes projects, it was identified prior to these efforts by two separate sequencing groups and was deposited in dbSNP. This position is not conserved in other mammalian OAT4 sequences but is conserved among other primate OATs including OAT1 and OAT3, suggesting that this position may be important for the translation of the protein, protein stability, or for localization to the plasma membrane in primates. The mRNA expression of the L29P variant was similar to the reference but no plasma membrane protein was detected in the L29P cell line, which explains its loss of function. The mechanism by which a leucine to proline change at this position results in a loss of protein expression on the plasma membrane may be related to general protein instability or a failure of the protein to be inserted in the membrane; extreme angles induced by proline residues in helical structures may

result in drastically unstable or significantly impaired proteins[38]. Conversely, the presence of a leucine residue at this position may also confer protein stability based on the conserved nature of this N-terminal residue in other primate OATs. Further inquiry would be needed to determine whether this variant is detrimental due to the introduction of a proline residue or the loss of a leucine residue.

Within the set of singleton variants, only the H469R variant elicited a complete loss of function phenotype. Systematic replacement of histidine residues in OAT4 by Zhou, et al, however, did find that the conversion of these residues to alanine resulted in the preservation of comparable uptake activity of estrone sulfate in the majority of mutants compared to unmodified OAT4[33]. This suggests that histidine residues are not critical to the optimal function of OAT4. However, the presence of an arginine at this position resulted in a complete loss of function of OAT4 in the present study which can be partly explained by the loss of a significant fraction of OAT4 on the plasma membrane as shown in Figure 3.5. This suggests that while this position may not be of critical importance to OAT4 function in general, the presence of a residue with the properties of arginine may be detrimental to protein stability or trafficking.

Three common variants of OAT4 also displayed altered kinetic properties when tested with estrone sulfate. While the K_m values of each of these variants for estrone sulfate were all comparable to the reference value determined for OAT4, the V_{max} for each of these variants was lower than that of the reference with the V155G variant demonstrating the greatest difference at ~33% of the reference value. Consistent with the results of this study, Zhou, et al observed a reduction

in function of the V155G variant and a concomitant reduction in protein level[37] although the degree of decreased uptake was greater than in the current study. Each of these variants had frequencies above 2% in at least one ethnic group, suggesting that a number of individuals possessing these variants may also be subject to a lower absolute level of reabsorption of OAT4 substrates although the effect may not be readily observable in human subjects.

The impact of transporters located on the apical membrane of proximal tubule cells has been demonstrated previously but is a growing area of interest with numerous implications in pharmacokinetics and pharmacogenetics. The characterization of naturally occurring genetic variants of these transporters, such as OAT4, is a necessary and informative step to better define the potential genetic causes of drug-induced renal toxicities and perturbations in the urinary excretion of endogenous metabolites. This study provides an extensive examination of variants found to occur naturally in 4 ethnically diverse populations and how these variants may affect the ability of OAT4 to control the levels of drug and metabolite substrates reabsorbed from the urine. Three nonsynonymous variants of OAT4 demonstrated a complete loss of function in uptake experiments with multiple chemically diverse substrates while an additional three variants that occurred at a frequency of at least 2% displayed reduced V_{max} values in the transport of estrone sulfate. A loss of protein expression and/or localization to the plasma membrane was a hallmark of the loss of function variants and can explain, at least in part, the observed lack of function in cellular uptake studies. Future studies examining the impact of

nonsynonymous variants on the pharmacokinetics of drug substrates of OAT4 in a clinical setting would be particularly interesting considering the high frequency of the loss of function variants and would provide useful information regarding the effect of transporters primarily involved in the reabsorption of small molecules in the body.

References

1. Robertson EE, Rankin GO. Human renal organic anion transporters: characteristics and contributions to drug and drug metabolite excretion. *Pharmacol Ther* 2006; **109**(3)**:** 399-412.

2. Enomoto A, Niwa T. Roles of organic anion transporters in the progression of chronic renal failure. *Ther Apher Dial* 2007; **11 Suppl 1:** S27-31.

3. Giacomini KM, Huang SM, Tweedie DJ, Benet LZ, Brouwer KL, Chu X*, et al*. Membrane transporters in drug development. *Nat Rev Drug Discov* 2010; **9**(3)**:** 215-236.

4. Bakhiya N, Monien B, Frank H, Seidel A, Glatt H. Renal organic anion transporters OAT1 and OAT3 mediate the cellular accumulation of 5-sulfooxymethylfurfural, a reactive, nephrotoxic metabolite of the Maillard product 5-hydroxymethylfurfural. *Biochem Pharmacol* 2009; **78**(4)**:** 414-419.

5. Zhang R, Yang X, Li J, Wu J, Peng WX, Dong XQ*, et al*. Upregulation of rat renal cortical organic anion transporter (OAT1 and OAT3) expression in response to ischemia/reperfusion injury. *Am J Nephrol* 2008; **28**(5)**:** 772-783.

6. Hagos Y, Stein D, Ugele B, Burckhardt G, Bahn A. Human renal organic anion transporter 4 operates as an asymmetric urate transporter. *J Am Soc Nephrol* 2007; **18**(2)**:** 430-439.

7. Ganapathy ME, Brandsch M, Prasad PD, Ganapathy V, Leibach FH. Differential recognition of beta -lactam antibiotics by intestinal and renal peptide transporters, PEPT 1 and PEPT 2. *J Biol Chem* 1995; **270**(43)**:** 25672-25677.

8. Ekaratanawong S, Anzai N, Jutabha P, Miyazaki H, Noshiro R, Takeda M*, et al*. Human organic anion transporter 4 is a renal apical organic anion/dicarboxylate exchanger in the proximal tubules. *J Pharmacol Sci* 2004; **94**(3)**:** 297-304.

9. Hilgendorf C, Ahlin G, Seithel A, Artursson P, Ungell AL, Karlsson J. Expression of thirty-six drug transporter genes in human intestine, liver, kidney, and organotypic cell lines. *Drug Metab Dispos* 2007; **35**(8)**:** 1333-1340.

10. Nishimura M, Naito S. Tissue-specific mRNA expression profiles of human ATP-binding cassette and solute carrier transporter superfamilies. *Drug Metab Pharmacokinet* 2005; **20**(6)**:** 452-477.

11. Cha SH, Sekine T, Kusuhara H, Yu E, Kim JY, Kim DK*, et al*. Molecular cloning and characterization of multispecific organic anion transporter 4 expressed in the placenta. *J Biol Chem* 2000; **275**(6)**:** 4507-4512.

12. Takeda M, Khamdang S, Narikawa S, Kimura H, Hosoyamada M, Cha SH*, et al*. Characterization of methotrexate transport and its drug interactions with human organic anion transporters. *J Pharmacol Exp Ther* 2002; **302**(2)**:** 666-671.

13. Yamashita F, Ohtani H, Koyabu N, Ushigome F, Satoh H, Murakami H*, et al*. Inhibitory effects of angiotensin II receptor antagonists and leukotriene receptor antagonists on the transport of human organic anion transporter 4. *J Pharm Pharmacol* 2006; **58**(11)**:** 1499-1505.

14. Kimura H, Takeda M, Narikawa S, Enomoto A, Ichida K, Endou H. Human organic anion transporters and human organic cation transporters mediate renal transport of prostaglandins. *J Pharmacol Exp Ther* 2002; **301**(1)**:** 293-298.

15. Ugele B, St-Pierre MV, Pihusch M, Bahn A, Hantschmann P. Characterization and identification of steroid sulfate transporters of human placenta. *Am J Physiol Endocrinol Metab* 2003; **284**(2)**:** E390-398.

16. Zhou F, Illsley NP, You G. Functional characterization of a human organic anion transporter hOAT4 in placental BeWo cells. *Eur J Pharm Sci* 2006; **27**(5)**:** 518-523.

17. Vormfelde SV, Schirmer M, Hagos Y, Toliat MR, Engelhardt S, Meineke I*, et al*. Torsemide renal clearance and genetic variation in luminal and basolateral organic anion transporters. *Br J Clin Pharmacol* 2006; **62**(3)**:** 323-335.

18. Kolz M, Johnson T, Sanna S, Teumer A, Vitart V, Perola M*, et al*. Meta-analysis of 28,141 individuals identifies common variants within five new loci that influence uric acid concentrations. *PLoS Genet* 2009; **5**(6)**:** e1000504.

19. van der Harst P, Bakker SJ, de Boer RA, Wolffenbuttel BH, Johnson T, Caulfield MJ*, et al*. Replication of the five novel loci for uric acid concentrations and potential mediating mechanisms. *Hum Mol Genet* 2010; **19**(2)**:** 387-395.

20. Xu G, Bhatnagar V, Wen G, Hamilton BA, Eraly SA, Nigam SK. Analyses of coding region polymorphisms in apical and basolateral human organic anion transporter (OAT) genes [OAT1 (NKT), OAT2, OAT3, OAT4, URAT (RST)]. *Kidney Int* 2005; **68**(4)**:** 1491-1499.

21. Lee WK, Kwak JO, Hwang JS, Suh CK, Cha SH. Identification and characterization of single nucleotide polymorphisms of SLC22A11 (hOAT4) in Korean women osteoporosis patients. *Mol Cells* 2008; **25**(2)**:** 265-271.

22. Leabman MK, Huang CC, Kawamoto M, Johns SJ, Stryke D, Ferrin TE*, et al*. Polymorphisms in a human kidney xenobiotic transporter, OCT2, exhibit altered function. *Pharmacogenetics* 2002; **12**(5)**:** 395-405.

23. Edgar RC. MUSCLE: multiple sequence alignment with high accuracy and high throughput. *Nucleic Acids Res* 2004; **32**(5)**:** 1792-1797.

24. Ng PC, Henikoff S. SIFT: Predicting amino acid changes that affect protein function. *Nucleic Acids Res* 2003; **31**(13)**:** 3812-3814.

25. Ramensky V, Bork P, Sunyaev S. Human non-synonymous SNPs: server and survey. *Nucleic Acids Res* 2002; **30**(17)**:** 3894-3900.

26. Capriotti E, Calabrese R, Casadio R. Predicting the insurgence of human genetic diseases associated to single point protein mutations with support vector machines and evolutionary information. *Bioinformatics* 2006; **22**(22)**:** 2729-2734.

27. Bromberg Y, Rost B. SNAP: predict effect of non-synonymous polymorphisms on function. *Nucleic Acids Res* 2007; **35**(11)**:** 3823-3835.

28. Urban TJ, Yang C, Lagpacan LL, Brown C, Castro RA, Taylor TR*, et al*. Functional effects of protein sequence polymorphisms in the organic cation/ergothioneine transporter OCTN1 (SLC22A4). *Pharmacogenet Genomics* 2007; **17**(9)**:** 773-782.

29. Urban TJ, Sebro R, Hurowitz EH, Leabman MK, Badagnani I, Lagpacan LL*, et al*. Functional genomics of membrane transporters in human populations. *Genome Res* 2006; **16**(2)**:** 223-230.

30. Leabman MK, Huang CC, DeYoung J, Carlson EJ, Taylor TR, de la Cruz M*, et al*. Natural variation in human membrane transporter genes reveals evolutionary and functional constraints. *Proc Natl Acad Sci U S A* 2003; **100**(10)**:** 5896-5901.

31. Fujita T, Brown C, Carlson EJ, Taylor T, de la Cruz M, Johns SJ*, et al*. Functional analysis of polymorphisms in the organic anion transporter, SLC22A6 (OAT1). *Pharmacogenet Genomics* 2005; **15**(4)**:** 201-209.

32. Erdman AR, Mangravite LM, Urban TJ, Lagpacan LL, Castro RA, de la Cruz M*, et al*. The human organic anion transporter 3 (OAT3; SLC22A8): genetic variation and functional genomics. *Am J Physiol Renal Physiol* 2006; **290**(4)**:** F905-912.

33. Zhou F, Pan Z, Ma J, You G. Mutational analysis of histidine residues in human organic anion transporter 4 (hOAT4). *Biochem J* 2004; **384**(Pt 1)**:** 87-92.

34. Zhou F, Tanaka K, Pan Z, Ma J, You G. The role of glycine residues in the function of human organic anion transporter 4. *Mol Pharmacol* 2004; **65**(5)**:** 1141-1147.

35. Sawyer SL, Berglind LC, Brookes AJ. Negligible validation rate for public domain stop-codon SNPs. *Hum Mutat* 2003; **22**(3)**:** 252-254.

36. Hawn TR, Verbon A, Lettinga KD, Zhao LP, Li SS, Laws RJ*, et al*. A common dominant TLR5 stop codon polymorphism abolishes flagellin signaling and is associated with susceptibility to legionnaires' disease. *J Exp Med* 2003; **198**(10)**:** 1563-1572.

37. Zhou F, Zhu L, Cui PH, Church WB, Murray M. Functional characterization of nonsynonymous single nucleotide polymorphisms in the human organic anion transporter 4 (hOAT4). *Br J Pharmacol* 2010; **159**(2)**:** 419-427.

38. Yohannan S, Yang D, Faham S, Boulting G, Whitelegge J, Bowie JU. Proline substitutions are not easily accommodated in a membrane protein. *J Mol Biol* 2004; **341**(1)**:** 1-6.

Chapter 4

Molecular Effects of Nonsynonymous Polymorphisms in URAT1

Introduction

Purine degradation occurs as part of the normal metabolic processes in all animals during the turnover of DNA, both through the intake of purine-rich foods and via cell death. In higher order primates, including humans, the lack of hepatic uricase activity results in uric acid being the primary purine metabolite and the major form excreted in the urine[1]. Consequently, uric acid levels are particularly high in humans compared to other species with the range in healthy individuals between 200 μM and 500 μM[2]. The reasons for and the effects of elevated uric acid levels are under continuous investigation; there is considerable evidence suggesting that uric acid is a proverbial "double-edged sword" wherein exceedingly low and high levels can have distinct consequences on human health. For instance, low levels of uric acid have been strongly associated with a greater frequency and severity of relapses of multiple sclerosis[3-5] as well as cases of exercise-induced renal failure[6, 7] whereas elevated levels have been associated with the development of metabolic syndrome, gout, and hypertension[8-10]. The mechanisms and factors influencing uric acid levels are thus of considerable interest in regard to the predisposition to and the potential exacerbation of human diseases.

Recent studies have shed light on the network of transporters that function in the kidney to maintain uric acid homeostasis with key transporters located on both

the apical and basolateral membrane of cells comprising the renal proximal tubules[11-14]. Among these uric acid transporters, the Solute Carrier (SLC) family transporter URAT1 (*SLC22A12*) was identified as the primary contributor to the net renal reabsorption of uric acid in the kidney[13]. URAT1 is expressed on the apical membrane of the renal proximal tubule and uptake of uric acid via URAT1 has been shown to be sensitive to a number of uricosuric agents such as benzbromarone and probenecid, providing an explanation for the hypouricemia observed with usage of these and other drugs[13]. The direct control of uric acid levels by URAT1 was further substantiated by the observation that no uricosuric effect was elicited in patients with nonfunctional URAT1 mutations treated with benzbromarone[15].

A number of previously identified nonsynonymous variants in *SLC22A12* have provided the first causal links between heritable variants of uric acid transporters and hypouricemia in humans. In particular, the W258Stop variant, which occurred in 74% of Japanese subjects displaying severe idiopathic hypouricemia, produced a truncated form of URAT1 that completely lost the ability to transport uric acid[13]. Likewise, a previous study reported the discovery of seven nonsynonymous variants in 24 hypouricemic Japanese individuals, three of which were associated with reduced uric acid levels in the blood, including the W258Stop variant[12]. In fact, it has been estimated that 90% of Japanese hypouricemia patients have a mutation in *SLC22A12*[11]. These studies have provided significant insight into the causes of reduced uric acid levels however limitations of the studies, primarily the identification of nonsynonymous variants

exclusively in hypouricemic individuals of Japanese descent, results in an incomplete picture of the extent of URAT1 variation and the potential impact in other ethnic groups. Thus the occurrence of variants of URAT1 in healthy individuals and in a variety of ethnicities is of significant interest considering the higher rates of multiple sclerosis, gout, and metabolic syndrome in other ethnic groups compared to the Japanese and the association of these conditions with altered uric acid levels[16-19]. To date, few studies have attempted to identify nonsynonymous variants in apparently healthy individuals; resequencing of control groups as part of the Japanese hypouricemia studies in fact identified no nonsynonymous variants in subjects that did not present with hypouricemia[12]. Similarly, it is widely recognized that uric acid levels vary considerably among ethnic groups[20] and that these levels have a substantial genetic component[21].

Using subjects enrolled in the Study of Pharmacogenetics in Ethnically Diverse Populations (SOPHIE) project, the present study examined genetic variation in URAT1 by deep resequencing in 265 ethnically diverse individuals comprising four ethnic groups: African American, Asian American, Caucasian, and Mexican American. Discovery of URAT1 variants that may modulate uric acid levels without leading to the extremes of uricemias could provide valuable information about factors that predispose individuals to disease states influenced by the level of circulating uric acid and potentially identify individuals with altered responses to uricosuric agents.

Materials and Methods

Reagents

Radiolabeled [^{14}C]-uric acid was purchased from Moravek (Brea, CA, USA). All other chemicals were purchased from Sigma (St. Louis, MO, USA). All cell culture media and reagents were purchased from the University of California, San Francisco Cell Culture Facility (San Francisco, CA, USA).

Variant Identification

Nonsynonymous variants of *SLC22A12* were identified from either searches of the NCBI dbSNP database (http://www.ncbi.nlm.nih.gov/snp) or by resequencing subjects enrolled in the SOPHIE project. All exons comprising *SLC22A12*, with the exception of exon seven, were resequenced as were the flanking intronic regions; amplification and subsequent direct sequencing of exon seven failed in multiple attempts and thus was excluded from this analysis. The specific PCR procedures relevant to resequencing methodologies have been described in detail previously[22]. The complete protocol and primer sequences as well as a complete listing of the *SLC22A12* variants found as part of the SOPHIE project can be obtained via the Pharmacogenetics of Membrane Transporters (PMT) website (http://pharmacogenetics.ucsf.edu/).

Cell Line Construction

The full-length cDNA for *SLC22A12* (GenBank Accession # NM_144585) was PCR amplified after reverse transcription from a commercially available RNA

sample obtained from adult human kidney (Clontech, Mountain View, CA, USA) and cloned into pcDNA5/FRT (Invitrogen, Carlsbad, CA, USA). Nonsynonymous variants of *SLC22A12* were created by site-directed mutagenesis with Pfu Ultra® DNA polymerase (Stratagene, La Jolla, CA, USA) and the pcDNA5/FRT-URAT1 vector as a template. The cloned*SLC22A12* reading frame contained three synonymous variants which did not alter the amino acid sequence of the URAT1 protein and were present in the reference and variant URAT1 constructs. All plasmid sequences were verified by direct sequencing of the complete open reading frame and the variant locations to ensure that no spurious mutations were introduced. Stable cell lines overexpressing reference URAT1, a nonsynonymous variant form of URAT1, or transfected with pcDNA5/FRT alone were created as previously described[23]. Briefly, Flp-In-293® (HEK-293) (Invitrogen) cells grown at 37°C with 5% CO_2 were simultaneously transfected with the respective pcDNA5/FRT or pcDNA5/FRT-URAT1 vector and 3-fold excess pOG44 vector, passaged 24 hours later, and selected for using 100 µg/mL hygromycin B.

Uptake Studies

Uptake experiments using [^{14}C]-uric acid were performed using cells seeded on 24 well poly-D-lysine coated cell culture plates (BD Biosciences) in standard cell culture media described previously for 2 minutes at 37°C, within the time frame of linear uptake of uric acid by URAT1. Uptake studies commenced with the additions of warm chloride-free uptake buffer (125 mM sodium gluconate, 4.8 mM potassium gluconate, 1.2 mM K_2HPO_4, 1.2 mM $MgSO_4$, 1.3 mM calcium

gluconate, and 25 mM HEPES/Tris; pH ≈ 7.4) containing 10 or 25 μM of radiolabeled uric acid as indicated in the figure legends. The cells were quickly washed with ice-cold choline buffer (128 mM choline chloride, 4.73 mM KCl, 1.25 mM $MgSO_4$, 1.25 mM $CaCl_2$, and 5 mM HEPES/Tris; pH ≈ 7.4) three successive times followed by the addition of 1 mL of warm lysis buffer (0.1% SDS/0.1 N NaOH). Uptake values were determined using liquid scintillation counting and were normalized to the total protein in each well as determined using a bicinchoninic acid (BCA) protein assay. Determination of K_m and V_{max} values for uric acid transport by URAT1 and its nonsynonymous variant forms was performed in a similar fashion using supplemental unlabeled uric acid in the uptake buffer for any concentrations exceeding 10 μM. Three independent experiments were performed using empty vector transfected and URAT1 reference and nonsynonymous variant cell lines.

RNA Isolation and qRT-PCR

Stable cell lines expressing reference URAT1 or its nonsynonymous variants were grown in 6-well poly-D-lysine coated cell culture plates (BD Biosciences, San Jose, CA, USA) until reaching 90-95% confluency. TRIzol® reagent (Invitrogen) was used to purify total RNA following the manufacturer's standard protocol. RNA purity and quality was assessed by spectrophotometry and by examination of 28S and 18S ribosomal band integrity. cDNA was synthesized with a Superscript III® Reverse Transcription kit (Invitrogen) using 1 μg of total RNA following the manufacturer's standard protocol. The resultant cDNA was

diluted and used as template for qRT-PCR and the assessment of *SLC22A12* mRNA levels in each of the cell lines.

qRT-PCR was performed using Taqman® reagents and specific primer and probe sets for human *SLC22A12* and *GAPDH* (Applied Biosystems, Foster City, CA, USA). Reactions were performed in a 384 well plate with a 10 µL reaction volume employing a 7900HT Fast Real-time PCR system (Applied Biosystems) using the default instrument settings. *SLC22A12* expression levels were determined using the $\Delta\Delta C_t$ method after normalization to endogenous levels of *GAPDH*.

Protein Isolation and Western Blotting

Total protein was isolated from cells stably expressing URAT1 or its nonsynonymous variants cultured in T75 flasks until 90-95% confluent. The cells were lysed using radio-immunoprecipitation assay (RIPA) buffer (Sigma) following the manufacturer's standard protocol. Plasma membrane protein was purified using a cell surface biotinylation kit employing the amine-reactive labeling reagent Sulfo-NHS-SS-Biotin (Pierce Biotechnology, Rockford, IL, USA) following the manufacturer's standard protocol with slight modifications. Briefly, the cell lines stably expressing URAT1 or its nonsynonymous variants were grown in T75 cell culture flasks, washed with ice-cold PBS, and incubated with Sulfo-NHS-SS-Biotin for 60 minutes at 4°C with gentle shaking. The cells were subsequently scraped off the flask and washed with ice-cold PBS supplemented with protease inhibitor cocktail (Pierce Biotechnology). Following lysis of the

cells, the lysate was incubated with streptavidin-linked agarose for 60 minutes at room temperature and the biotinylated protein eluted using 50 mM dithiothreitol in standard SDS-PAGE buffer. The protein concentration was determined using a BCA assay (Pierce Biotechnology) following the manufacturer's standard protocol.

Western blotting was performed using a 12-well 4-20% gradient Tris-HCl polyacrylamide gel and was subsequently transferred to an Immobilon® polyvinylidene fluoride (PVDF) membrane (Millipore, Billerica, MA, USA). The membranes were incubated in 5% nonfat milk in Tris-buffered saline buffer with 0.05% Tween (TBST) for 1 hour followed by incubation with 3 µg/mL of a mouse anti-human monoclonal URAT1 antibody (Abnova, Taipei, Taiwan) overnight at 4°C. The membranes were subsequently washed with TBST buffer and incubated with a 1:6000 dilution of a goat anti-mouse IgG horseradish peroxidase-coupled secondary antibody (Santa Cruz Biotechnology, Santa Cruz, CA, USA) diluted in 5% nonfat milk in TBST buffer for 1 hour at room temperature. After rinsing the membrane, protein detection was performed using ECL Plus® reagents (GE Healthcare, Piscataway, NJ, USA) following the standard protocol. Blotting with a 1:1000 dilution of a Na^+/K^+ ATPase α-subunit antibody (US Biological, Swampscott, MA, USA) using the same membrane was performed in a similar fashion to normalize plasma membrane protein levels. Densitometry measurements were performed using Adobe Photoshop® CS4 (Adobe Systems, San Jose, CA, USA), calculated as a ratio of URAT1 to the

98kDa Na^+/K ATPase band and expressed as a percentage of URAT1 reference protein levels.

Sequence Conservation

Complete mammalian URAT1 protein sequences were downloaded from the ENSEMBL database (http://www.ensembl.org). Conservation was assessed using nine sequences representative of human, gorilla, chimpanzee, and macaque, dog, cow, horse, mouse, and rat URAT1. Multiple alignments of URAT1 were performed using MUSCLE 3.6[24] and visualized using the T_EXshade package[25]. The membrane topology diagram was generated using the human reference sequence and the T_EXtopo package[26]. Residues were divided into three groups: 1) "invariable" residues were identical among all species, 2) "conserved" residues were identical among the majority of species, and 3) "similar" residues were chemically similar in the majority of species. All other residues were considered to be unconserved.

Population Genetics and Haplotype Analysis

Population genetic statistics, namely pi (π), a measure of nucleotide diversity, were calculated for numerous regions of *SLC22A12* as previously described[22, 27]. Calculations of π were performed following the methods described by Tajima[28]. *SLC22A12* haplotypes were created using Haploview 4.2[29] with PHASED genotypes derived from the PMT resequencing results. Haplotype variants were selected based on a minor allele frequency of at least 1% in at least one ethnic group and their occurrence in Hardy-Weinberg equilibrium. No nonsynonymous

variants of URAT1 were used due to their low frequency, existence as an indel, or absence from the PMT sample set. The resulting haplotypes were only considered if they occurred at a frequency of at least 1% in at least one ethnic group.

Statistics

A one-way ANOVA test followed by a Dunnett's post-hoc test was performed using Graphpad Prism 5.1 (Graphpad, La Jolla, CA, USA) to determine statistically significant differences in uptake or mRNA and protein expression. The kinetic values K_m and V_{max} were determined by non-linear regression analysis in Graphpad Prism 5.1 (Graphpad) after subtracting the background uptake present in the empty vector cell line at each concentration from the uptake in the URAT1 expressing cell lines. Curves were fit to the Michaelis-Menten equation $V = V_{max}[S]/(K_m + [S])$ where V is the rate of uptake, V_{max} is the maximal uptake rate of the substrate, K_m is the substrate concentration at half the V_{max}, and [S] is the substrate concentration.

Results

SLC22A12 Variant Identification

Variants of *SLC22A12* were identified by resequencing DNA samples from 265 healthy individuals representing four distinct ethnic groups as part of the Studies of Pharmacogenetics of Membrane Transporters (SOPHIE) project and by

searching the dbSNP database (http://www.ncbi.nlm.nih.gov/snp). These efforts identified three novel nonsynonymous variants (I131V, W277R, and R342H), one novel nonsynonymous insertion variant (T542LysfX13, henceforth known as T542INS), and six synonymous variants (two novel and four previously identified) within the SOPHIE cohort. An additional nonsynonymous variant (G65W) was identified as part of the HapMap project and was included for further study. The specific features of these variants are detailed in Table 4.1. All of the nonsynonymous variants, with the exception of W277R, occurred in the extracellular and intracellular loops of URAT1 with a distinct absence of protein-altering variants in the predicted transmembrane regions as depicted in Figure 4.1. The W277R variant is predicted to occur at the interface of the 6th transmembrane domain and a large intracellular loop that follows it. As shown in Table 4.2, all of the nonsynonymous variants of URAT1 found in the SOPHIE cohort were rare with I131V, W277R, and R342H identified as singletons in the African American (I131V and W277R) and Asian American (R342H) samples whereas the T542INS variant occurred at a frequency of 1.5% in the African American sample. In contrast, the G65W variant was found at a frequency of 3.7% in the Japanese arm of the HapMap project and was also present in the Han Chinese group at a frequency of 1.2%; the G65W variant was also found as a singleton in both the Caucasian and Yoruban groups making this variant an infrequent example of a completely pan-ethnic nonsynonymous variant that occurs in a SLC22 transporter[30]. Within SOPHIE, no nonsynonymous variants were identified in samples from either Caucasians or Mexican Americans.

Table 4.1: Nonsynonymous variants of *SLC22A12*

ID†	Exon	Genomic Position	mRNA Position	Base Change	Protein Position	Amino Acid Change	Mammalian Conservation	Primate Conservation
rs12800450	1	64115797	940	G>T	65	Gly→Trp	U	C
PMT-5519	1	64115995	1138	A>G	131	Ile→Val	C	C
PMT-5545	4	64117850	1576	T>C	277	Trp→Arg	C	C
PMT-5539	6	64122926	1772	G>A	342	Arg→His	C	C
PMT-5550	10	64125561	2371	A>AAGAAGGC ACACATGGTA	542	Thr→Lysf*X13*	U	C

†: indicates either dbSNP or Pharmacogenetics of Membrane Transporters (PMT) IDs, U: Unconserved. C: Conserved.

Conservation and Genetic Analysis of URAT1

URAT1 is highly conserved among mammalian species; as depicted in Figure 4.1, 87% of the residues of URAT1 are conserved to some degree among nine URAT1 mammalian orthologs and nearly 60% of residues are invariable across all species examined. In primates, the percentage of invariable residues increases to nearly 99%. Within the secondary structure of URAT1, distinct regions of strong conservation are found; the immediate N-terminal region up to the second transmembrane domain displays a high degree of conservation as does the seventh through tenth transmembrane domains. The converse is also true with noticeable portions of URAT1 lacking strong conservation in the third through fifth transmembrane domain and in the C-terminal region. The nonsynonymous variants of URAT1 were largely found at positions displaying a high degree of conservation with the I131V, W277R, and R342H variants in positions considered to be conserved or invariable in mammalian orthologs. The G65W variant, which did not occur at an invariable or largely conserved position, did arise at a position with chemically similar amino acids in mammalian orthologs. The T542INS variant was also found in a position that showed no conservation among the species examined.

Evaluation of the selective pressures on *SLC22A12* was performed using population genetic statistics, namely average heterozygosity (π) which is representative of the genetic diversity in a gene[31]. *SLC22A12* had π values consistent with that observed in other SLC transporters[30, 32] although the values of π_{Coding} (representing the nucleotide diversity of the coding regions) and π_S

Table 4.2: Allele frequencies of *SLC22A12* nonsynonymous variants

ID†	Variant	HapMap MAF				PMT MAF			
		CEU n=108	CHB n=86	JPT n=82	YRI n=108	AA n=132	CA n=134	AS n=134	ME n=130
rs12800450	Gly65Trp	0.009	0.012	0.037	0.009	NA	NA	NA	NA
PMT-5519	Ile131Val	NA	NA	NA	NA	0.008	0.000	0.000	0.000
PMT-5545	Trp277Arg	NA	NA	NA	NA	0.008	0.000	0.000	0.000
PMT-5539	Arg342His	NA	NA	NA	NA	0.000	0.000	0.008	0.000
PMT-5550	Thr542Lysf*X13*	NA	NA	NA	NA	0.015	0.000	0.000	0.000

†: indicates either dbSNP or Pharmacogenetics of Membrane Transporters (PMT) IDs. NA: Not identified in the respective sequencing project; n: number of chromosomes; MAF: Minor Allele Frequency; CA: Caucasian; AA: African American; AS: Asian American; ME: Mexican American; CHB: Han Chinese from Beijing, China; CEU: Northern and Western European ancestry from Utah; JPT: Japanese from Tokyo, Japan; YRI: Yoruban from Ibadan, Nigeria.

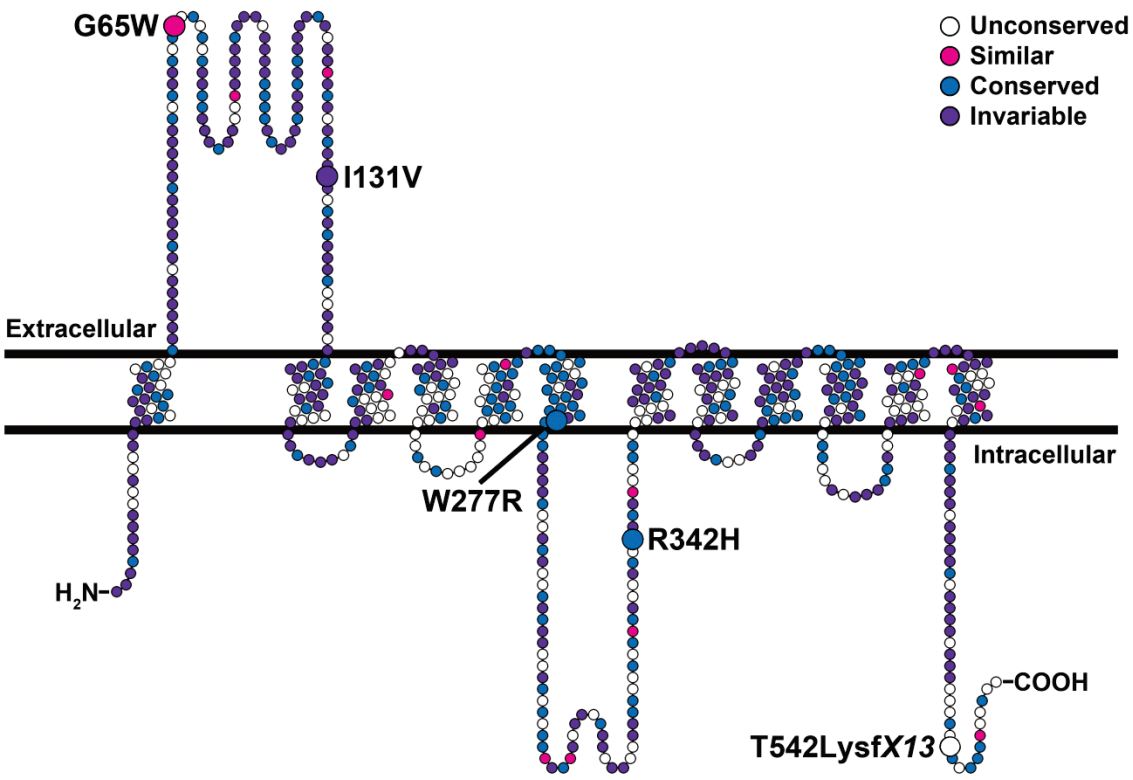

Figure 4.1: Location of human nonsynonymous URAT1 variants and conservation of URAT1 among mammals. Depiction of the predicted membrane topology of URAT1 showing the conservation of residues among nine mammalian species using color-based classification: purple residues are invariable, blue residues are conserved (the residue is identical in most, but not all, species), and magenta residues are chemically similar across the species but not conserved. Sites of human nonsynonymous variants are enlarged and indicated with a corresponding label.

(representing the nucleotide diversity of the synonymous variant sites) were both noticeably higher compared to any other member of the organic anion transporter (OAT) family (shown in Table 4.3) or any other transporter examined previously[30]. Likewise, and consistent with the majority of SLC transporters, the π_S value far exceeded the value of π_{NS} (representing the nucleotide diversity of the nonsynonymous variant sites), which suggested that *SLC22A12* is undergoing significant negative selection. In fact, the π_{NS} to π_S ratio of 0.003 is

the lowest observed in any SLC transporter examined so far by an order of magnitude. Of note, however, the π_{Coding} value of 11.2 x 10^4 is higher than the majority of other SLC transporters and suggests that though under negative selection, the amount of nucleotide variability within the coding regions of *SLC22A12* is substantial.

Analysis of the haplotypes in multiple ethnic groups gave further indication of the extent of genetic variability with *SLC22A12*. A total of 18 haplotypes that occurred at a frequency of at least 1% were identified and are shown in Figure 4.2, which illustrates the observed haplotypes in African Americans, Asian Americans, Caucasians, and Mexican Americans in the SOPHIE project. The haplotypes were ordered and numbered based on both the evolutionary relationships among them and the frequency at which they occurred and were determined for each ethnic group. The low frequency of the nonsynonymous

Table 4.3: Population genetic statistics for members of the OAT family

Gene	Protein	π_{Coding} (x 10^4)	π_{NS} (x 10^4)	π_S (x 10^4)	π_{NS} : π_S
SLC22A6	OAT1	1.24 ± 1.67	0.37 ± 1.00	3.85 ± 5.79	0.096
SLC22A7	OAT2	8.10 ± 5.58	0.64 ± 1.37	28.4 ± 19.9	0.023
SLC22A8	OAT3	4.40 ± 3.66	0.77 ± 1.49	15.7 ± 13.7	0.049
SLC22A11	OAT4	3.04 ± 2.86	1.27 ± 1.95	8.29 ± 9.05	0.153
SLC22A12	URAT1	11.2 ± 7.36	0.11 ± 0.57	43.3 ± 28.4	0.003

Values of π are shown as the mean ± SEM. π_{Coding} is the nucleotide diversity in the entire coding region of each gene, π_{NS} is the nucleotide diversity at nonsynonymous sites and π_S is the nucleotide diversity at synonymous sites.

variants of *SLC22A12*precluded their inclusion in the haplotype analysis. Numerous *SLC22A12* haplotypes were observed with African Americans possessing the greatest number of unique haplotypes (7) as well as the greatest number of total haplotypes (12). In particular both the *1 and *3 haplotypes occurred at a frequency of approximately 20% in African Americans while six haplotypes occurred at a frequency of 5% or less. Caucasians had the fewest number of haplotypes (5) with the *1 haplotype being the most common haplotype in both the Caucasian and Mexican American samples (60% and 54% in Caucasian and Mexican American groups respectively). The Caucasian and Asian American samples also possessed two unique haplotypes (*2A and *3D in Asian Americans and *3B and *3C in Caucasians) found only in their respective ethnic groups albeit with frequencies much lower in comparison to the predominant haplotypes. In contrast to the other ethnic groups, the *3A and *2 haplotypes were predominant in the Asian American ethnic group, accounting for more than 50% of the haplotypes in those subjects. Interestingly, Mexican Americans shared two haplotypes with only one other ethnic group: the *3A haplotype with Asian Americans (where it is the predominant haplotype) and the *5 haplotype with African Americans.

Effect of Nonsynonymous Variants of URAT1 on Uric Acid Uptake

The functional effects of all five nonsynonymous variants of URAT1 were examined using uric acid uptake in stably transfected HEK-293 cells expressing either the reference or a variant form of URAT1. Uptake after 2 minutes using 25

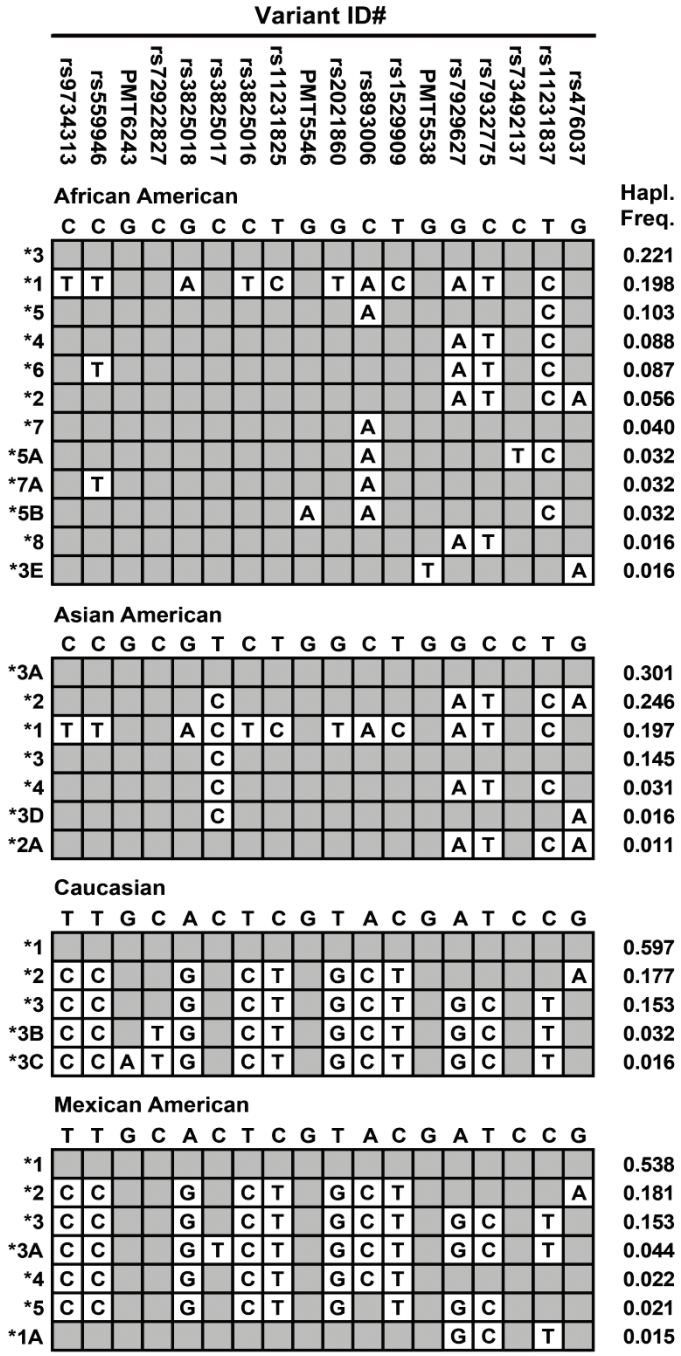

Figure 4.2: Major haplotypes of *SLC22A12* in four ethnic groups. Haplotypes in the exonic and flanking intronic regions of *SLC22A12* in four distinct ethnic groups comprising the PMT project were determined. Variants and haplotypes that occurred at frequencies of less than 1% were omitted. The most common haplotype sequence is shown for each ethnic group. Grey boxes indicate the presence of the common allele whereas the white boxes indicate the base change that occurs at the variable position in the haplotype.

μM of radiolabeled uric acid resulted in an increase of intracellular uric acid in the reference cell line of 22.5 ± 4.4 fold compared to the empty vector transfected cells (0.121 ± 0.017 pmol/μg protein/min vs. 0.00599 ± 0.00163 pmol/μg protein/min; p value ≤ 0.001). Simultaneous experiments with the variant cell lines showed considerable uptake of uric acid by all the variants without any

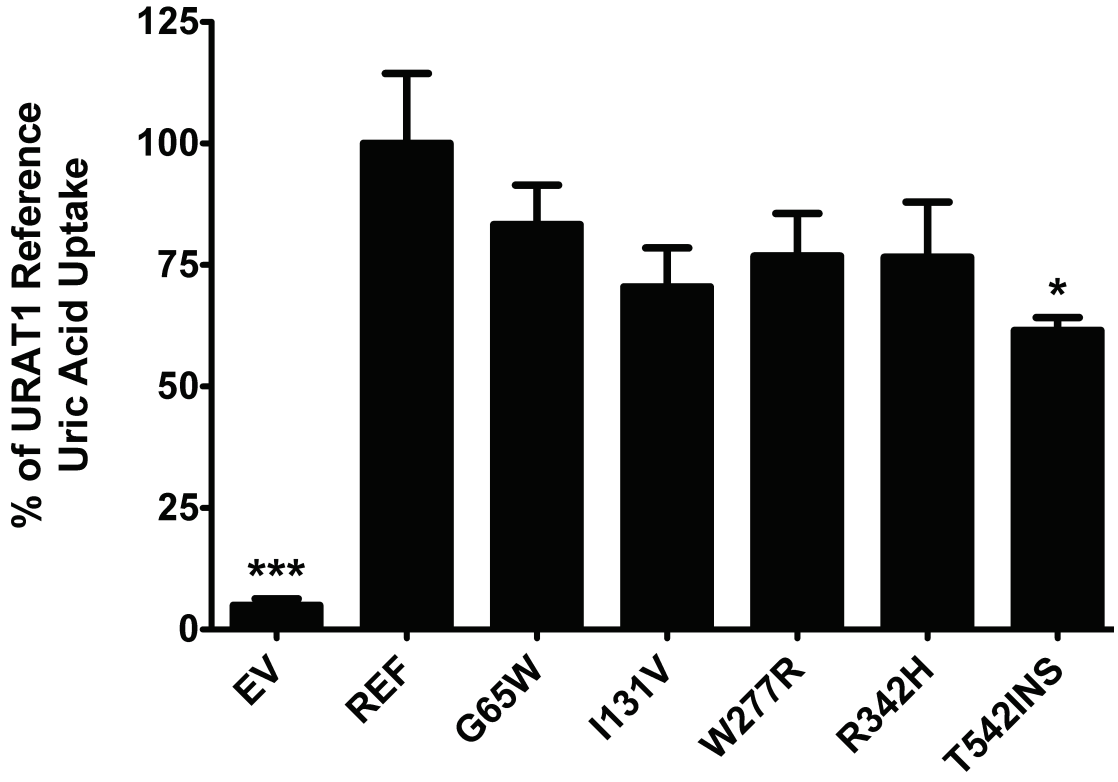

Figure 4.3: Characterization of uric acid uptake by nonsynonymous variants of URAT1. Experiments were performed for 2 minutes at 37°C using 25 μM radiolabeled uric acid. All uptakes used stably transfected HEK-293 Flp-In cells. Uptake values were normalized to total protein per well and expressed as a percentage of URAT1 reference uric acid uptake (0.121 ± 0.017 pmol/μg protein/min). Each bar represents the mean uptake ± SEM of three independent experiments.*** and * indicate a p-value ≤ 0.001 and 0.05 respectively, compared to reference URAT1 using a one-way ANOVA analysis and a Dunnett's post-hoc test.

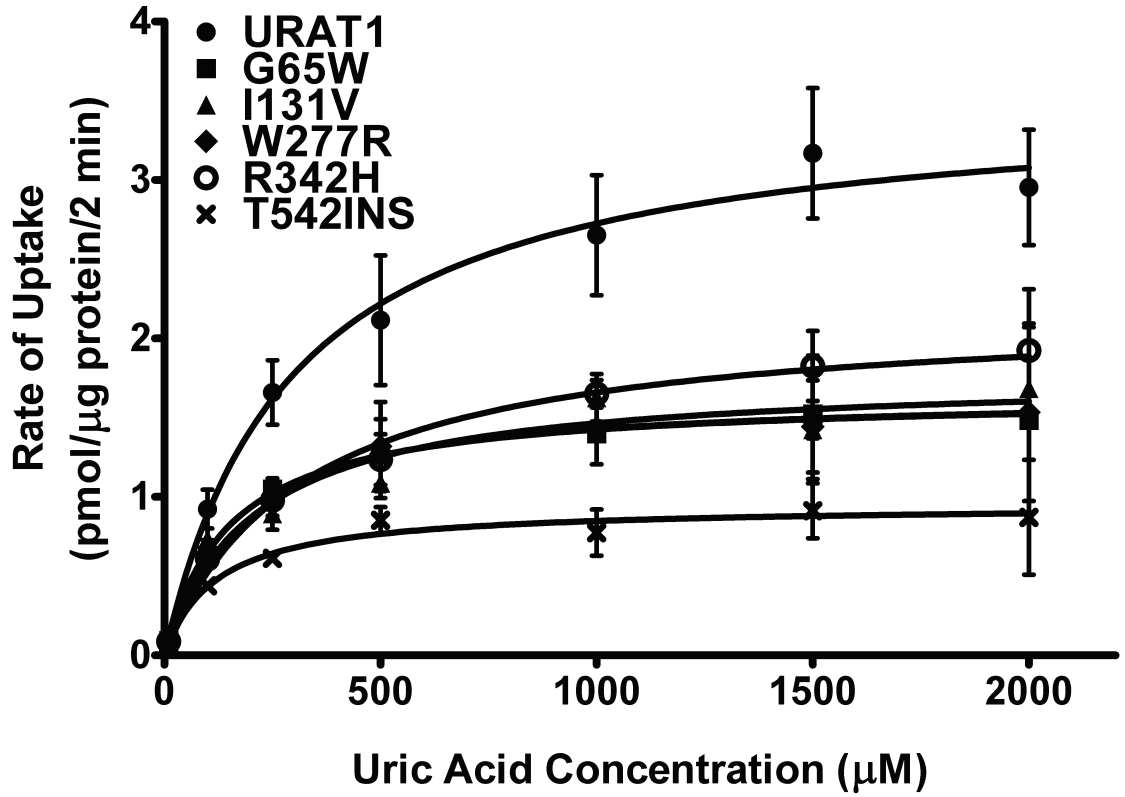

Figure 4.4: Saturable uptake of uric acid in stably transfected HEK-Flp cells expressing URAT1 or its nonsynonymous variants. Experiments were performed for 2 minutes at 37°C using 10 μM radiolabeled uric acid and unlabeled uric acid for the remainder. Uptake values were normalized to total protein per well and adjusted for the uptake of uric acid in empty vector transfected cells. Curves were generated using non-linear regression with automatic removal of outliers in Graphpad Prism 5.1. Kinetic parameters are shown in Table 4.4.

complete loss of function phenotype. However, all the nonsynonymous variants demonstrated a slight, but not significant decrease in uric acid uptake with the exception of the T542INS variant, which resulted in a statistically significant (p value ≤ 0.05) reduction in uric acid uptake compared to the uptake in the URAT1 reference expressing cell line as shown in Figure 4.3.

Table 4.4: Kinetic parameters of uric acid uptake by nonsynonymous variants of URAT1

Variant	K_m (μM)	V_{max} (pmol/μg protein/min)	Normalized V_{max} (pmol/μg protein/min)	Normalized V_{max} : K_m Ratio (pmol/mg protein/min/μM)
REF	305 ± 16.2	4.08 ± 0.338	3.84 ± 0.319	12.6 ± 0.580
G65W	83.7 ± 29.8*	1.27 ± 0.144†	1.37 ± 0.155*	18.0 ± 4.56
I131V	302 ± 73.7	2.23 ± 0.595*	4.25 ± 0.114	14.9 ± 3.26
W277R	179 ± 7.96	1.79 ± 0.282†	3.10 ± 0.487	17.2 ± 1.96
R342H	298 ± 45.3	2.16 ± 0.269*	3.66 ± 0.456	12.6 ± 1.43
T542INS	78.2 ± 19.2*	0.758 ± 0.195†	2.22 ± 0.570*	28.3 ± 0.339*

*: p value ≤ 0.01, †: p value ≤ 0.001 compared to Reference. Values are expressed as the mean ± SEM. Normalized V_{max} indicates the V_{max} values normalized to the amount of URAT1 protein on the plasma membrane determined through Western blotting.

The kinetic parameters of uric acid interaction with each of the URAT1 variant transporters, as displayed in Figure 4.4, indicated differences compared to the reference. As summarized in Table 4.4, the URAT1 reference cells produced a K_m value for uric acid of approximately 300 μM which is close to the established literature value[13]. Two variants, G65W and T542INS, resulted in significantly lower K_m values for uric acid in comparison to the URAT1 reference (83.7 ± 29.8 and 78.2 ± 19.2 μM respectively; p value ≤ 0.01) whereas the K_m value of the W277R variant transporter was lower than the reference value but the difference was not significant. The remaining variants resulted in K_m values comparable to the reference value. Additionally, the V_{max} value for each of the nonsynonymous URAT1 variant transporters was significantly lower than that of the reference (4.08 ± 0.338 pmol/μg protein/min) with a reduction of at least 45% in all the variants; the T542INS variant had the lowest V_{max} with a nearly 80% reduction. Normalization of the V_{max} values to the plasma membrane protein level determined using Western blotting produced values for V_{max} closer to the reference value of 3.84 ± 0.319 pmol/μg protein/min, although the values of the G65W and T542INS variants were still significantly reduced compared to the reference value (1.37 ± 0.155 pmol/μg protein/min and 2.22 ± 0.570 pmol/μg protein/min respectively; p value ≤ 0.01). When the ratios of normalized V_{max} to K_m (a surrogate assessment of transport efficiency) were compared, however, only the T542INS variant demonstrated significantly altered transport efficiency compared to the reference ratio (28.3 ± 0.339 pmol/mg protein/min/μM

versus12.6 ± 0.580 pmol/mg protein/min/μM respectively; p value ≤ 0.01). These results are also summarized in Table 4.4.

Effect of URAT1 Nonsynonymous Variants on mRNA and Protein Expression

Quantitative reverse transcriptase PCR (qRT-PCR) and Western blots were used to assess the molecular effects of nonsynonymous variants on *SLC22A12*expression thus providing potential mechanistic explanations behind the observed decrease in uric acid uptake observed in each of the variants. mRNA expression levels of *SLC22A12* in the reference and variant cell lines verified that it was transcribed at a high level in all cell lines with approximately 500-fold higher *SLC22A12* expression in the reference cell line than in the empty vector transfected cell line. As shown in Figure 4.5, the mRNA levels of all of the variants of *SLC22A12* were similar to the reference expression levels with the exception of the R342H variant which was expressed at nearly 150% of the reference. However, this difference was not statistically significant and did not appear to correspond to higher levels of the R342H variant protein reaching the plasma membrane.

URAT1 protein levels, assessed using Western blotting of biotinylated surface protein, indicated that plasma membrane protein levels of URAT1 were largely decreased among all the variants. As revealed in Figure 4.6A, band intensities of URAT1 were decreased in the cell lines expressing all of the nonsynonymous variant URAT1 transporters, except for the G65W variant. When representative

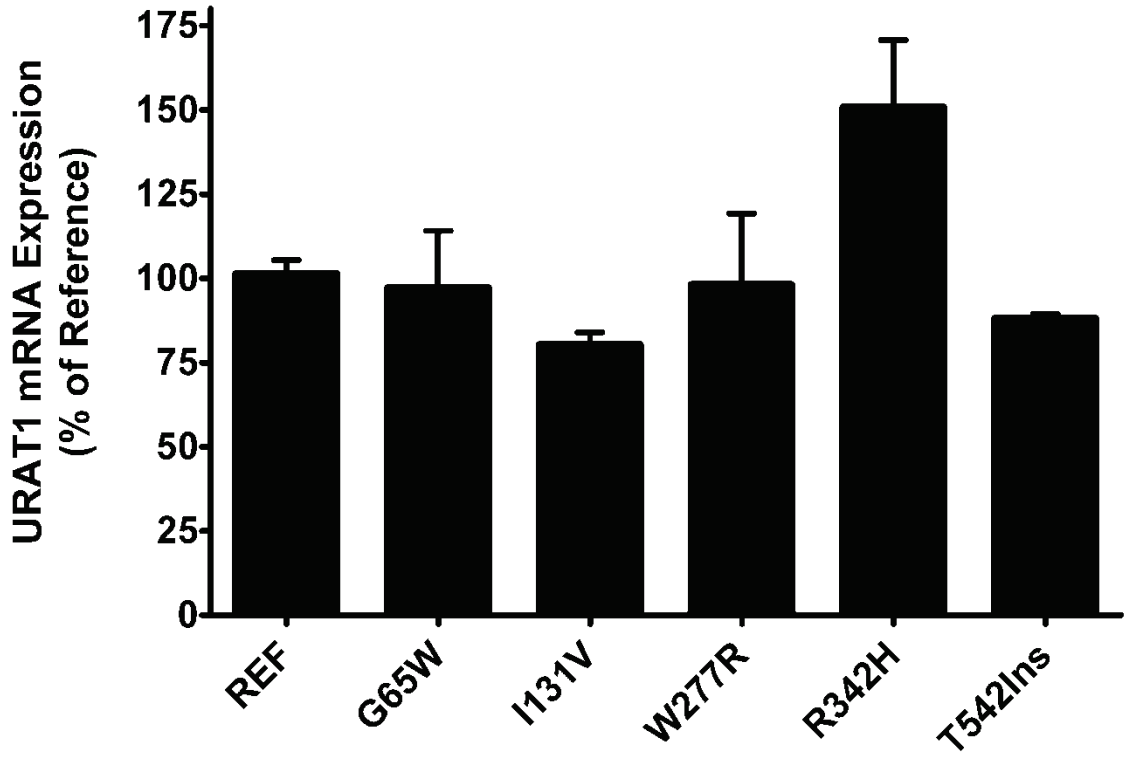

Figure 4.5: mRNA expression levels of *SLC22A12* and its nonsynonymous variants in stably transfected HEK-293-Flp cells. cDNA was synthesized from total RNA extracted from each cell line and used to determine mRNA levels *SLC22A12* and each of its nonsynonymous variants using quantitative real-time PCR with a Taqman® assay specific to *SLC22A12*. Expression levels were normalized to endogenous expression of *GAPDH* and are shown as a percentage of reference *SLC22A12* mRNA expression. Bars represent the mean ± SEM from three independent experiments.

blots were quantified using densitometry and normalized to endogenous levels of the α-subunit of the Na^+/K^+ ATPase present at approximately 98kDa, the levels of URAT1 on the plasma membrane in the variant cell lines were reduced between 40% and 70% with the T542INS variant showing the greatest and only statistically significant decrease (Figure 4.6B). Unlike the other rare variants, the more common G65W variant showed no significant change in plasma membrane URAT1 levels compared to the plasma

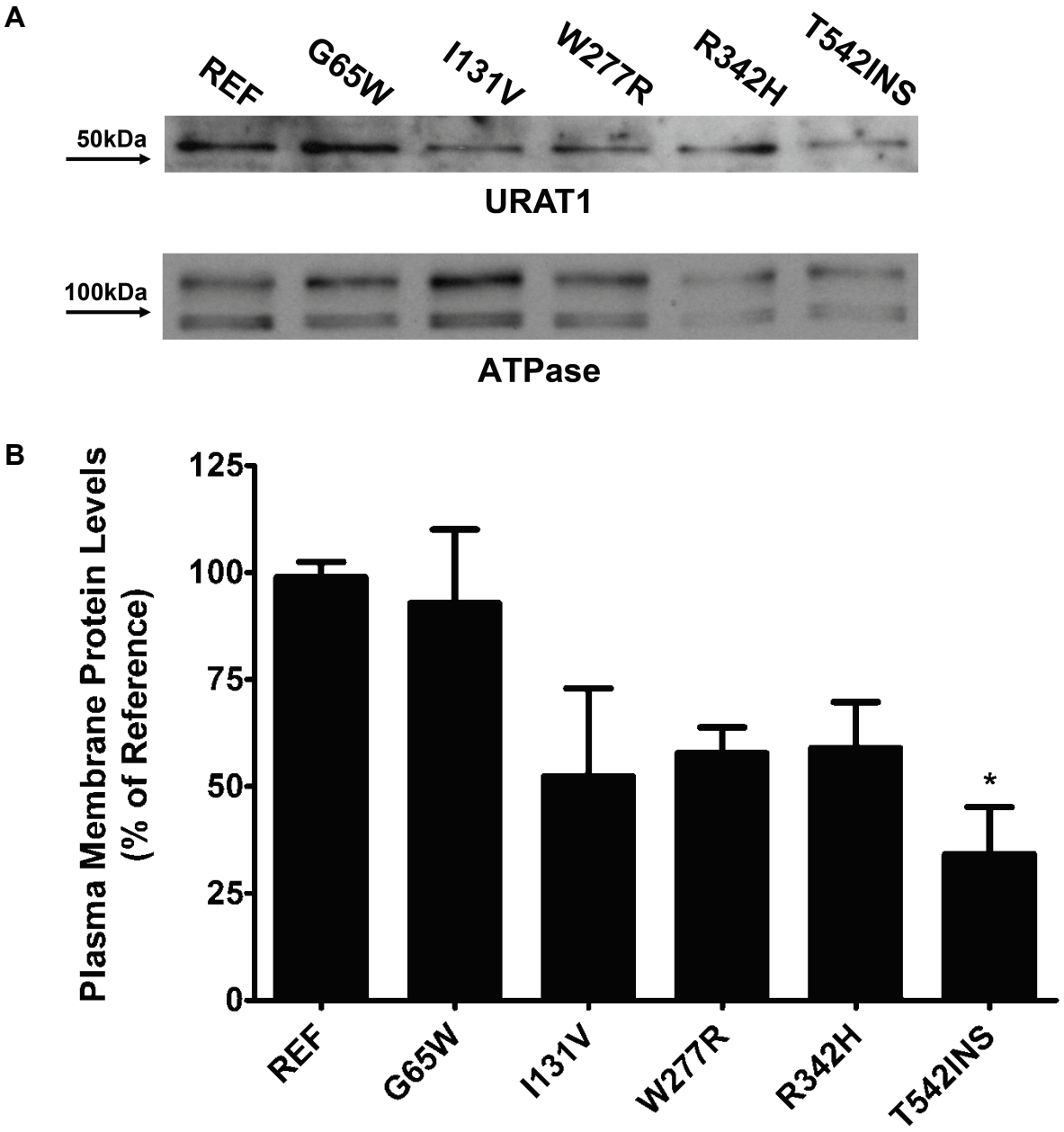

Figure 4.6: Levels of plasma membrane protein in HEK-293 cells expressing URAT1 or its nonsynonymous variants. A) Representative Western blots of plasma membrane protein isolated via biotinylation, separated using SDS-PAGE, and probed with an antibody specific to URAT1. The same membrane was stripped and reprobed with an antibody specific to the α-subunit of Na^+/K^+ ATPase. B) Levels of URAT1 and the α-subunit of Na^+/K^+ ATPase found on the plasma membrane were quantified using densitometry, normalized to the approximately 98kDa band of Na^+/K^+ ATPase in each lane, and expressed as a percentage of the amount of URAT1 present in the reference cell line using two separate protein measurements. * indicates p value ≤ 0.05 compared to reference.

membrane level of URAT1 in the reference cell line. Blots using total protein extracted from each cell line produced similar results (data not shown).

Discussion

Uric acid is a significant small molecule in human health and physiology and the maintenance of appropriate levels in the blood is of considerable importance. The development of a number of health conditions and the predisposition to a wide array of ailments has brought increasing attention to what genetic factors modulate uric acid levels and how changes in these levels can manifest themselves in otherwise healthy individuals. The importance of URAT1 in this process has been previously recognized with a substantial amount of evidence pointing to genetic variants of *SLC22A12* being the primary causal factor behind the development of hypouricemia in the Japanese and Korean populaces[11-13, 33] as well as being the primary target for several pharmacological agents used in the treatment of hyperuricemia, most prominently uricosuric agents such as probenecid[13]. This study expands on the current knowledge of URAT1 specifically through the characterization of nonsynonymous variants of URAT1 that occur in healthy individuals from multiple ethnic groups, thus increasing the understanding of how uric acid levels may be modulated in those not presenting with obvious cases of uricemia.

SLC22A12 is a highly conserved gene within human populations, reflecting its important role in uric acid homeostasis. This is evident by the fact that this study

identified only four previously unknown nonsynonymous variants in the gene with only a single previously identified variant, G65W, occurring at an allele frequency greater than 2%. The identification of only a few rare nonsynonymous variants in URAT1 in healthy populations is in agreement with previous studies in healthy control Japanese populations, which failed to identify any nonsynonymous variants in URAT1[11, 12]. The extent of the coding region conservation is further exemplified by the values of average heterozygosity (π) calculated in *SLC22A12*. The π_{NS} to π_S ratio of 0.003 was the lowest identified in multiple evaluations of SLC22 transporters and is indicative of a protein that performs a critical function and does not readily tolerate detrimental variants[30, 32]. Furthermore and prior to this study, the only nonsynonymous variants of URAT1 characterized were in confirmed hypouricemic individuals where the decrease in URAT1 function is readily apparent[11]. Paradoxically, a large number of haplotypes were identified in four ethnic groups with distinct haplotypes associated with each group, belying the incredibly conserved nature of the protein. These observations are not necessarily mutually exclusive given the fact that the *SLC22A12* haplotypes are largely derived from synonymous and intronic variants and further substantiates the effect of purifying selection on *SLC22A12*: a very diverse set of haplotypes without a corresponding diverse set of protein-altering variants.

In contrast to the majority of URAT1 nonsynonymous variants identified in hypouricemic individuals, which clearly exhibited a near total loss of uric acid uptake[11-13], the URAT1 variants in this study retained some uric acid uptake function. The hallmarks of all the hypomorphic variants in this study are

significant changes in the kinetic properties K_m and V_{max} related to uric acid uptake. Likewise, the majority of these variants resulted in noticeably lower levels of URAT1 protein on the plasma membrane while the mRNA levels remained largely unchanged implying that much of the reduced uric acid uptake may be the result of a reduction in the amount of URAT1 expressed on the cell surface. Though not investigated in this study, reduced surface levels of URAT1 may be due to errors in trafficking of the transporter.

The T542INS variant, which resulted in the most extreme reduction in URAT1 function, is noteworthy as it resulted in the change of a threonine residue to a lysine as well as the replacement of the C-terminus of URAT1 with 13 different amino acids before the occurrence of an alternate stop codon. To date, frameshift mutations that have been characterized in other SLC22 transporters rarely result in proteins with any observable function[30]. In URAT1 and the closely related paralog OAT4, the extreme C-terminal region contains a PDZ binding domain, which plays a role in the expression of these transporters on the plasma membrane. In particular, loss of this domain resulted in a marked reduction in protein on the plasma membrane and resulting functional capacity[34, 35]. Thus this variant represents a naturally occurring form of these same synthetic variants and likely interacts with little to no affinity with PDZ domain-containing scaffold proteins. This mechanism provides a potential explanation for the observed decrease in function and is supported by the observed decrease in URAT1 surface protein as seen in Figure 4.6.

The most frequent variant examined in the present study, G65W, produced a similar although less drastic reduction in uric acid uptake. The G65W variant had a slightly decreased ability to transport uric acid and possessed significantly lower K_m and V_{max} values. The level of plasma membrane protein measured in the G65W variant cells was similar to the reference suggesting that this variant alters a region that is not important for surface expression of URAT1, but that does alter its interaction with uric acid. Variants in the large extracellular loop of related SLC transporters frequently result in a reduction of functional capacity similar to the G65W variant of URAT1[30]. Considering the highly conserved nature of URAT1, the retention of the majority of uric acid uptake activity in the G65W variant likely allowed for the highest allele frequency observed in the nonsynonymous variants identified in this study as well as its occurrence in all of the major ethnic groups examined.

The assessment of the genetic variation of URAT1 is important due to the implications of uric acid levels in a wide variety of conditions affecting human health including multiple sclerosis, metabolic syndrome, heart disease, and gout among others[3, 8, 9, 17]. While it has been definitively shown that loss of function variants in URAT1 can result in hypouricemia, the impact of less severe variants requires further examination. This study provided an assessment of the degree of URAT1 conservation among multiple ethnic groups and characterized the functional consequences of variants that occurred in healthy individuals. While the majority of these variants occurred at an exceedingly low frequency, thus limiting the ability to study them in human subjects, those examined displayed an

appreciable decrease, but not a total loss, in function. Advancing these findings to a clinical setting may reveal important genetic factors controlling uric acid levels in healthy human populations and predisposition to diseases influenced by uric acid levels.

References

1. Wu XW, Muzny DM, Lee CC, Caskey CT. Two independent mutational events in the loss of urate oxidase during hominoid evolution. *J Mol Evol* 1992; **34**(1)**:** 78-84.

2. Johnson RJ, Titte S, Cade JR, Rideout BA, Oliver WJ. Uric acid, evolution and primitive cultures. *Semin Nephrol* 2005; **25**(1)**:** 3-8.

3. Hooper DC, Spitsin S, Kean RB, Champion JM, Dickson GM, Chaudhry I*, et al*. Uric acid, a natural scavenger of peroxynitrite, in experimental allergic encephalomyelitis and multiple sclerosis. *Proc Natl Acad Sci U S A* 1998; **95**(2)**:** 675-680.

4. Toncev G. Therapeutic value of serum uric acid levels increasing in the treatment of multiple sclerosis. *Vojnosanit Pregl* 2006; **63**(10)**:** 879-882.

5. Toncev G, Milicic B, Toncev S, Samardzic G. Serum uric acid levels in multiple sclerosis patients correlate with activity of disease and blood-brain barrier dysfunction. *Eur J Neurol* 2002; **9**(3)**:** 221-226.

6. Ito O, Hasegawa Y, Sato K, Mitsui H, Yuda F, Sato H*, et al*. A case of exercise-induced acute renal failure in a patient with idiopathic renal hypouricemia developed during antihypertensive therapy with losartan and trichlormethiazide. *Hypertens Res* 2003; **26**(6)**:** 509-513.

7. Mima A, Ichida K, Matsubara T, Kanamori H, Inui E, Tanaka M*, et al*. Acute renal failure after exercise in a Japanese sumo wrestler with renal hypouricemia. *Am J Med Sci* 2008; **336**(6)**:** 512-514.

8. Nakagawa T, Hu H, Zharikov S, Tuttle KR, Short RA, Glushakova O*, et al*. A causal role for uric acid in fructose-induced metabolic syndrome. *Am J Physiol Renal Physiol* 2006; **290**(3)**:** F625-631.

9. Johnson RJ, Kang DH, Feig D, Kivlighn S, Kanellis J, Watanabe S*, et al*. Is there a pathogenetic role for uric acid in hypertension and cardiovascular and renal disease? *Hypertension* 2003; **41**(6)**:** 1183-1190.

10. Choi HK, Mount DB, Reginato AM. Pathogenesis of gout. *Ann Intern Med* 2005; **143**(7)**:** 499-516.

11. Ichida K, Hosoyamada M, Hisatome I, Enomoto A, Hikita M, Endou H*, et al*. Clinical and molecular analysis of patients with renal hypouricemia in Japan-influence of URAT1 gene on urinary urate excretion. *J Am Soc Nephrol* 2004; **15**(1)**:** 164-173.

12. Iwai N, Mino Y, Hosoyamada M, Tago N, Kokubo Y, Endou H. A high prevalence of renal hypouricemia caused by inactive SLC22A12 in Japanese. *Kidney Int* 2004; **66**(3)**:** 935-944.

13. Enomoto A, Kimura H, Chairoungdua A, Shigeta Y, Jutabha P, Cha SH*, et al*. Molecular identification of a renal urate anion exchanger that regulates blood urate levels. *Nature* 2002; **417**(6887)**:** 447-452.

14. Eraly SA, Vallon V, Rieg T, Gangoiti JA, Wikoff WR, Siuzdak G*, et al*. Multiple organic anion transporters contribute to net renal excretion of uric acid. *Physiol Genomics* 2008; **33**(2)**:** 180-192.

15. Hamada T, Ichida K, Hosoyamada M, Mizuta E, Yanagihara K, Sonoyama K*, et al*. Uricosuric action of losartan via the inhibition of urate transporter 1 (URAT 1) in hypertensive patients. *Am J Hypertens* 2008; **21**(10)**:** 1157-1162.

16. Pugliatti M, Sotgiu S, Rosati G. The worldwide prevalence of multiple sclerosis. *Clin Neurol Neurosurg* 2002; **104**(3)**:** 182-191.

17. Nuki G, Simkin PA. A concise history of gout and hyperuricemia and their treatment. *Arthritis Res Ther* 2006; **8 Suppl 1:** S1.

18. Nishimura R, Nakagami T, Tominaga M, Yoshiike N, Tajima N. Prevalence of metabolic syndrome and optimal waist circumference cut-off values in Japan. *Diabetes Res Clin Pract* 2007; **78**(1)**:** 77-84.

19. Procopiou M, Philippe J. The metabolic syndrome and type 2 diabetes: epidemiological figures and country specificities. *Cerebrovasc Dis* 2005; **20 Suppl 1:** 2-8.

20. Nan H. Serum uric acid and metabolic risk factors in three ethnic groups: Asian Indians and Creoles in Mauritius and Chinese in Qingdao, China. PhD thesis, University of Helsinki, Helsinki, 2008.

21. Nath SD, Voruganti VS, Arar NH, Thameem F, Lopez-Alvarenga JC, Bauer R*, et al*. Genome scan for determinants of serum uric acid variability. *J Am Soc Nephrol* 2007; **18**(12)**:** 3156-3163.

22. Leabman MK, Huang CC, Kawamoto M, Johns SJ, Stryke D, Ferrin TE*, et al*. Polymorphisms in a human kidney xenobiotic transporter, OCT2, exhibit altered function. *Pharmacogenetics* 2002; **12**(5)**:** 395-405.

23. Urban TJ, Yang C, Lagpacan LL, Brown C, Castro RA, Taylor TR*, et al*. Functional effects of protein sequence polymorphisms in the organic cation/ergothioneine transporter OCTN1 (SLC22A4). *Pharmacogenet Genomics* 2007; **17**(9)**:** 773-782.

24. Edgar RC. MUSCLE: multiple sequence alignment with high accuracy and high throughput. *Nucleic Acids Res* 2004; **32**(5)**:** 1792-1797.

25. Beitz E. TEXshade: shading and labeling of multiple sequence alignments using LATEX2 epsilon. *Bioinformatics* 2000; **16**(2)**:** 135-139.

26. Beitz E. T(E)Xtopo: shaded membrane protein topology plots in LAT(E)X2epsilon. *Bioinformatics* 2000; **16**(11)**:** 1050-1051.

27. Fujita T, Brown C, Carlson EJ, Taylor T, de la Cruz M, Johns SJ*, et al*. Functional analysis of polymorphisms in the organic anion transporter, SLC22A6 (OAT1). *Pharmacogenet Genomics* 2005; **15**(4)**:** 201-209.

28. Tajima F. Statistical method for testing the neutral mutation hypothesis by DNA polymorphism. *Genetics* 1989; **123**(3)**:** 585-595.

29. Barrett JC, Fry B, Maller J, Daly MJ. Haploview: analysis and visualization of LD and haplotype maps. *Bioinformatics* 2005; **21**(2)**:** 263-265.

30. Urban TJ, Sebro R, Hurowitz EH, Leabman MK, Badagnani I, Lagpacan LL*, et al*. Functional genomics of membrane transporters in human populations. *Genome Res* 2006; **16**(2)**:** 223-230.

31. Hartl DL, Clark, AG. *Principles of Population Genetics*. Sinaeur Associates: Sunderland, MA, 1997.

32. Leabman MK, Huang CC, DeYoung J, Carlson EJ, Taylor TR, de la Cruz M*, et al*. Natural variation in human membrane transporter genes reveals evolutionary and functional constraints. *Proc Natl Acad Sci U S A* 2003; **100**(10)**:** 5896-5901.

33. Cheong HI, Kang JH, Lee JH, Ha IS, Kim S, Komoda F*, et al*. Mutational analysis of idiopathic renal hypouricemia in Korea. *Pediatr Nephrol* 2005; **20**(7)**:** 886-890.

34. Anzai N, Miyazaki H, Noshiro R, Khamdang S, Chairoungdua A, Shin HJ*, et al*. The multivalent PDZ domain-containing protein PDZK1 regulates transport activity of renal urate-anion exchanger URAT1 via its C terminus. *J Biol Chem* 2004; **279**(44)**:** 45942-45950.

35. Miyazaki H, Anzai N, Ekaratanawong S, Sakata T, Shin HJ, Jutabha P*, et al*. Modulation of renal apical organic anion transporter 4 function by two PDZ domain-containing proteins. *J Am Soc Nephrol* 2005; **16**(12)**:** 3498-3506.

Chapter 5

Genetic and Functional Divergence Between the Apical Renal Organic Anion Transporters OAT4 and URAT1

Introduction

Homeostasis of critical endogenous metabolites and micronutrients as well as the clearance of many therapeutic drugs is regulated to a considerable degree through reabsorptive processes that occur in the kidney. It has been estimated that 99% of the solutes present in the filtered volume resulting from glomerular filtration is eventually reabsorbed to some extent; this includes solutes such as sodium, calcium, phosphates and sulfates, amino acids, glucose, and uric acid as well as variety of drugs such as antivirals, peptidomimetics, and antibiotics[1]. The majority of these filtrate constituents are subject to reabsorption by passive or active transport mechanisms mediated by membrane transporters. Among these transporters, renally expressed members of the Solute Carrier (SLC) family of transporters include those that transport carnitine[2], uric acid[3], glucose[4], lactic acid[5], free inorganic sulfate[6], and free inorganic phosphate[7] among many others. The importance of these transporters in maintaining the appropriate physiological levels of metabolites and micronutrients is exemplified by deficiencies that develop when detrimental SNPs are found in the transporters responsible for their uptake in the kidney[3, 6-9]. Furthermore, some studies have suggested that many reabsorptive processes in the kidney involve redundant transporters, such as those implicated in the transport of glucose[10, 11], and that these systems

oftentimes involve evolutionarily related genes that arose through processes of gene duplication.

In the renal proximal tubules, members of the organic anion transporter (OAT) family within the greater SLC22 family play a significant role in the excretion and reabsorption of a multitude of xenobiotics and endogenous small molecules. Recent studies have demonstrated that SLC22 transporters, and OATs in particular, followed a unique evolutionary path in mammals and are believed to have arisen from multiple gene duplication events, resulting in numerous sub-families of genes with many commonalities at the genomic and functional levels[12, 13]. Functional assessments of these transporters have also shown that conserved pairs of genes have similar functional characteristics[10, 14, 15], however, it remains to be determined if these sets of transporters truly evolved incidentally as redundant mechanisms for the reabsorption of multiple constituents of the urine or if they perform similar, yet distinct roles in the kidney in support of separate physiological processes in spite of a closely linked evolutionary history.

Of the OATs found in the human genome, only OAT4 (*SLC22A11*) and URAT1 (*SLC22A12*) are predominantly expressed on the apical membrane of renal proximal tubule cells, which makes these transporters particularly relevant when considering renal reabsorption of small organic anions. It has been postulated that this apical pair of transporters, along with the basolateral OAT1 (*SLC22A6*) and OAT3 (*SLC22A8*) pair comprise a major route of anion reabsorption and excretion in the kidney[16]. OAT4 and URAT1 occur in tandem on human chromosome 11 and share the greatest level of amino acid identity among all of

the chromosomally paired OATs, a consequence of their recent and shared evolutionary history. While these two transporters share certain functional properties such as Na^+ independent transport and inhibition by traditional OAT inhibitors such as probenecid and bumetanide, the acute differences in substrate preference observed thus far suggest that their innate functional roles in the kidney have likely diverged substantially[3, 17, 18]. In particular, URAT1 possesses a strong preference for uric acid[3], the end product of purine catabolism in primates, with minimal to no interaction observed with steroid sulfate conjugates. In contrast, OAT4, while capable of transporting uric acid with low affinity, has shown a strong preference for sulfated steroid conjugates[18].Additionally, while the physiological impact of loss-of-function mutations in URAT1 are quite apparent, most often resulting in extreme hypouricemia[3, 19], no human disease associated with SNPs in OAT4 has been reported in the literature to this point, in spite of the higher frequency of nonsynonymous SNPs in OAT4found in several populations compared to URAT1[20, 21]. Taken together, these differences are indicative of an evolutionary history predicated on increasing specialization and substrate selectivity with divergent functional roles.

Using phylogenetic analysis, comparative genomics, and cell uptake studies, the current study clarifies the evolutionary history and functional specialization of these two transporters and the OAT family as a whole and better defines the increased specialization occurring during the evolution of the OAT family of transporters in mammals. Determination of the increasing functional specialization of OAT4 and URAT1, and in the context of the remaining members

of the other members of the OAT family, is significant as their high expression in the kidney provides a ready route of reabsorption that can significantly impact the renal elimination of drugs and toxins. Likewise, a more detailed evaluation of the evolution of and functional differences between these two transporters would undoubtedly provide insight into possible endogenous metabolite salvage pathways in the kidney as well as better inform the evolution of renal function in mammals.

Materials and Methods

Reagents

Radiolabeled [^{3}H]-estrone sulfate and [^{3}H]-dehydroepiandrosterone sulfate were purchased from Perkin-Elmer Life Sciences (Waltham, MA, USA). Radiolabeled [^{3}H]-adenine, [^{3}H]-adenosine, [^{3}H]-AMP, [^{3}H]-cAMP, [^{3}H]-guanine, [^{3}H]-guanosine, [^{3}H]-allopurinol, [^{3}H]-hypoxanthine, [^{3}H]-inosine, [^{3}H]-adefovir, and [^{14}C]-uric acid were purchased from Moravek (Brea, CA, USA). Radiolabeled [^{3}H]-ADP was purchased from American Radiolabeled Chemicals (St. Louis, MO, USA). All unlabeled chemicals were purchased from Sigma (St. Louis, MO, USA). All cell culture media and reagents were purchased from the University of California, San Francisco Cell Culture Facility (San Francisco, CA, USA).

Evolutionary and genomic analysis

All full-length mammalian and *D. melanogaster* SLC22 transporter protein sequences from completely sequenced genomes were downloaded from the Ensembl database (http://www.ensembl.org); incomplete sequences or those with unclear identity were omitted. Alignments of all validated mammalian organic anion transporters (*SLC22A6*, *SLC22A7*, *SLC22A8*, *SLC22A9*, *SLC22A10*, *SLC22A11*, *SLC22A12*, *SLC22A13*, *SLC22A20* and their orthologs) were performed using MUSCLE 3.6[22] and were manually adjusted as necessary. A total of 11 species (*H. sapiens, B. taurus, C. familiaris, E. caballus, P. troglodytes, M. mulatta, M. musculus, R. norvegicus, S. scrufus, M. domestica,* and *A. melanoleuca*) and 77 representative OAT protein sequences were used and an additional *D. melanogaster*SLC22-like sequence (CG3790) was used to root the phylograms. Evolutionary evaluation of OATs was performed using phylograms generated from two distinct methods: boot-strapped maximum likelihood using FastTree 2.1[23] and Bayesian inference using MrBayes 3.1[24]. The maximum likelihood phylogram used 1000 bootstrap replicates generated using SEQBOOT and a consensus tree was generated using CONSENSE, both part of the PHYLIP package[25]. The default FastTree settings were employed including those designed for more accuracy as detailed on the authors' website (http://www.microbesonline.org/fasttree/). The Bayesian inference phylogram was generated using mixed amino acid models with 4 independent runs using 4 chains with 1.5 million generations sampled every 1000 generations. After convergence, 25% of the samples were discarded as "burn-in." Phylograms

were visualized using Treeview 1.6.2[26]. Representations of multiple alignments were generated using the T_EXshade package[27]. Comparisons of related OATs and searches of species-specific genomes were performed using protein databases of NCBI (http://www.ncbi.nlm.nih.gov) and Ensembl (http://www.ensembl.org) using the BlastP method.

Measures of gene conservation based on the rate of non-synonymous (d_N) and synonymous (d_S) changes was performed using a maximum likelihood approach with a codon-based substitution model in PAML 4.4c[28]. The d_N/d_S ratio is a measure of selective actions on a protein, with $d_N/d_S > 1$ signifying positive selection, $d_N/d_S < 1$ negative selection, and $d_N/d_S = 1$ neutral selection based on the occurrence of synonymous and non-synonymous sites in the coding regions of related genes. The ratio was determined using the codeml package in PAML. Codon alignments used for this analysis were generated using the PAL2NAL server[29] based on protein alignments generated as described for phylogram generation.

Measures of amino acid similarity and identity were calculated using MatGat 2.0[30] using a BLOSUM62 matrix based on alignments using MUSCLE 3.6. Transmembrane regions were predicted using the PRODIV-TMHMM algorithm[31] as implemented on the TOPCONS server (http://topcons.cbr.su.se/index.php).

Real-time PCR expression profiling

Total RNA from 10 normal adult human tissues (whole brain, kidney, colon, small intestine, prostate, liver, uterus, placenta, testis, epididymis, and ovary) was

purchased from Clontech (Mountain View, CA, USA). Total RNA from normal epididymal tissue was purchased from Cytomyx (Lexington, MA, USA). cDNA was synthesized using Superscript® III (Invitrogen, Carlsbad, CA, USA) with oligo-dT primers following the manufacturer's standard protocol. Quantitative reverse-transcriptase PCR was performed using Taqman® chemistries with probes specific to each transporter purchased from Applied Biosystems (Foster City, CA, USA). Reactions were performed in 384 well plates in 10 µL total volume (2 µL diluted cDNA, 0.5 µL Taqman® probe, 5 µL Fast Universal PCR Master Mix, 2.5 µL sterile water) and quantified using a standard curve established using serial dilutions of cDNA containing expression vectors for OAT4 and URAT1. Each sample was measured in triplicate and was normalized to *GAPDH* levels, which were approximately equal in all samples used in this study. The results are expressed as the absolute number of copies of mRNA per microgram of total RNA.

Uptake studies

Stable HEK-293 cell lines expressing the reference forms of human OAT4 and URAT1 or transfected with pcDNA5/FRT alone (empty vector; EV) were developed as described elsewhere[20] and in a similar fashion to methods described previously[32]. Cells were maintained in a humidified 37° C incubator with 5% CO_2 in Dulbecco's-modified Eagle's medium (DMEM) H-21 supplemented with 10% fetal bovine serum, 100 U/mL penicillin, 100 µg/mL streptomycin, and 100 µg/mL hygromycin B. All uptake and inhibition studies were performed 24-36 hours after cell seeding using chloride-free uptake buffer

(125 mM sodium gluconate, 4.8 mM potassium gluconate, 1.2 mM K_2HPO_4, 1.2 mM $MgSO_4$, 1.3 mM calcium gluconate, and 25 mM HEPES/Tris; pH ≈ 7.4) at 37° C in 24 or 48 well poly-D-lysine coated cell culture plates (BD Biosciences, San Jose, CA, USA) for 2 minutes. Briefly, cells were initially washed with warm chloride-free uptake buffer for 5 minutes. The buffer was removed and replaced with uptake buffer containing either 20 nM [^{3}H]-estrone sulfate or [^{3}H]-DHEAS, 10 µM [^{14}C]-uric acid, 70 nM [^{3}H]-AMP, 50 nM [^{3}H]-ADP, or 40 nM of the radiolabeled purine-based compounds as indicated in the figures and figure legends. Following incubation with the radiolabeled test compounds, the cells were washed three times with ice-cold choline buffer (128 mM choline chloride, 4.73 mM KCl, 1.25 mM $MgSO_4$, 1.25 mM $CaCl_2$, and 5 mM HEPES/Tris; pH ≈ 7.4), the residual buffer was aspirated, and warm lysis buffer (0.1% SDS/0.1 N NaOH) was added to each well. The cells were incubated for a minimum of 45 minutes with shaking at room temperature prior to determination of the cellular uptake by liquid scintillation counting. Cellular uptake experiments using purine-based compounds was performed with inhibition of equilibrative nucleoside transporters (ENT) by co-incubation of the radiolabeled compound with 10 µM 6-S-[(4-nitrophenyl)methyl]-6-thioinosine (NBMPR), a selective ENT inhibitor.

Inhibition studies were performed similarly using either 20 nM radiolabeled estrone sulfate (OAT4) or 10 µM radiolabeled uric acid (URAT1) in the presence of 0.5 mM or 1.0 mM of unlabeled inhibitor for 5 minutes in 48 well poly-D-lysine coated cell culture plates (BD Biosciences); spironolactone and mifepristone inhibition was performed using 50 µM and 100 µM concentrations due to their

insolubility in uptake buffer at concentrations of 0.5 mM and above. Inhibition of URAT1 uptake of [^{3}H]-AMP and [^{3}H]-ADP was achieved by co-incubation with 500 µM of unlabeled uric acid.

Kinetic studies of AMP and ADP uptake by URAT1 were performed similarly using supplemental amounts of unlabeled compound in the uptake buffer to produce the final concentration of substrate as indicated in the respective figures. Kinetic parameters, specifically K_m and V_{max}, were determined using non-linear regression with Graphpad Prism 5.1 (Graphpad) after subtracting the observed uptake in the empty vector cell line at each concentration from the uptake in the URAT1 cell line. Curves were fit to the Michaelis-Menten equation $V = V_{max}[S]/(K_m + [S])$ where V is the rate of uptake, V_{max} is the maximal uptake rate of the substrate, K_m is the substrate concentration at half the V_{max}, and [S] is the substrate concentration.

All uptake levels were normalized to the total protein in each well as determined using a BCA protein assay kit (Pierce Biotechnology, Rockford, IL, USA) and all experiments were performed on three separate occasions. Experiments were performed in the linear range of uptake for both uric acid (URAT1) and estrone sulfate (OAT4) (data not shown). Statistically significant differences were evaluated using Graphpad Prism 5.1 (Graphpad, La Jolla, CA, USA) utilizing a one-way ANOVA followed by a Dunnett's post-hoc test with a false discovery rate of 0.05.

Results

Phylogenetic analysis of organic anion transporters in mammals

The evolutionary relationship between OAT4 and URAT1 has been surmised from their prominent sequence similarity and tandem chromosomal location[13], but the circumstances of their evolution remained indeterminate. The maximum likelihood phylogram based on a multiple sequence alignment of experimentally verified OATs is shown in Figure 5.1. An additional phylogram generated using Bayesian inference techniques in MrBayes produced nearly identical results and were largely in agreement with the predicted evolution of mammalian OATs, with the lone exception being the ordering of the OAT5 and OAT7 divergence. The phylogram results suggest that the unpaired OATs OAT10 (*SLC22A13*) and OAT2 (*SLC22A7*) appeared early in animal evolution with OAT10 predicted to be the most ancestral of the two. Based on the phylograms, two distinct lineages emerged thereafter with OAT6 (*SLC22A20*)and the OAT1 (*SLC22A6*) and OAT3 (*SLC22A8*) genomic pair forming one branch of the OAT family and OAT4 (*SLC22A11*), URAT1 (*SLC22A12*), OAT5 (*SLC22A10*), and OAT7 (*SLC22A9*) forming another distinct branch. OAT5 and OAT7 also appear to be a branch of the URAT1 lineage and are the most recently diverged set of OATs identified in this analysis. Many of the more recent OAT homologs appear to be specific to the placental mammals and have likely been under some selective pressure as they are not definitively identifiable in all mammalian genomes. Searches of public databases and comparisons of OATs using BlastP resulted in groupings of

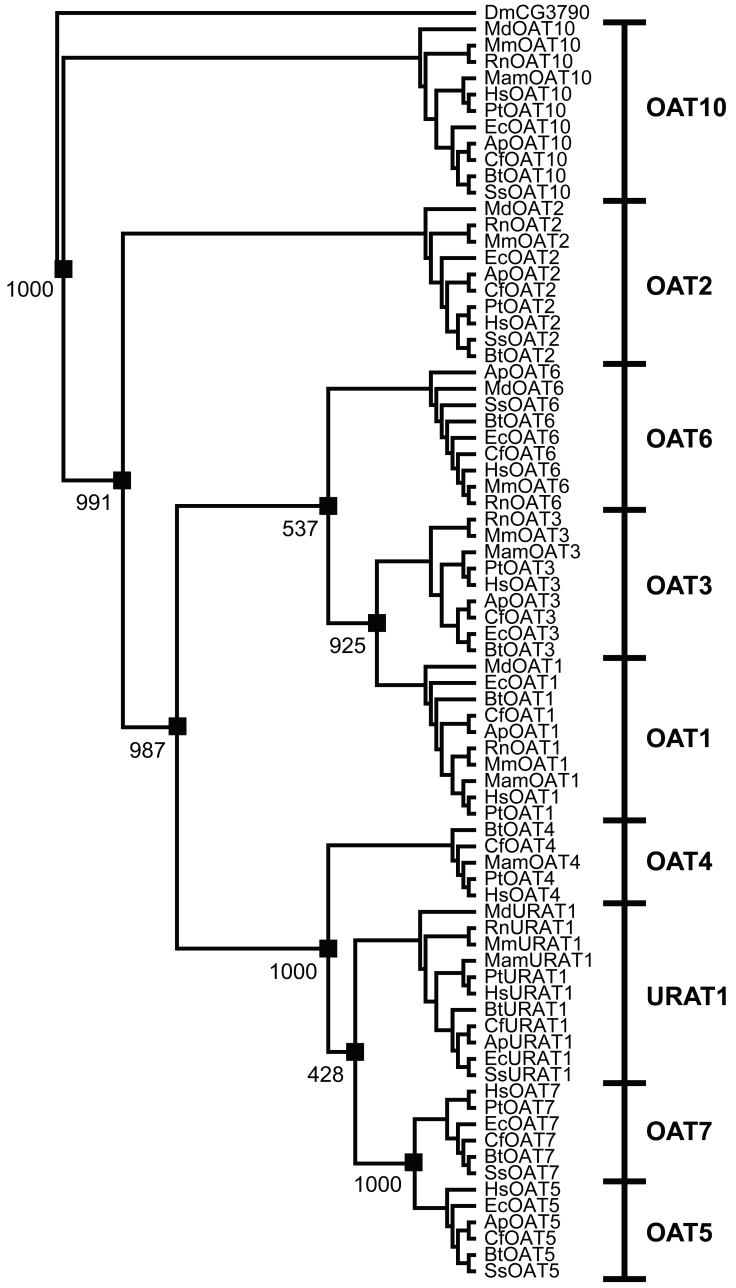

Figure 5.1: Evolutionary relationships between members of the organic anion transporter (OAT) family. Phylogram was generated using a multiple alignment of 77 full-length protein sequences from 11 completely sequenced mammalian genomes using maximum likelihood methods as implemented in FastTree. An additional OAT-like *D. melanogaster* ortholog was used as an outgroup. Black squares represent nodes of divergence between OAT members. Numbers adjacent to each node represent bootstrap values. Species abbreviations: Ap, *A. melanoleuca*; Bt, *B. taurus*; Cf, *C. familiaris*; Dm, *D. melanogaster*; Ec, *E. caballus*; Hs, *H. sapiens*; Mam, *M. mulatta*; Md, *M. domestica*; Mm, *M. musculus*; Pt, *P. troglodytes*; Rn, *R. norvegicus*; Ss, *S. scrofus*.

OATs into three major sets: an ancestral set comprised of unpaired OATs found in most vertebrate lineages (OAT10 and OAT2), a secondary expansion of OATs found in placental mammals and marsupials as well as some lower vertebrate species (OAT1, OAT3, and OAT6), and a tertiary group of OATs resulting from species-specific gene duplications found largely in placental mammals (OAT4, URAT1, OAT5, and OAT7). Of note, URAT1 orthologs or potential orthologs were identified in opossum and platypus genomes. This suggests that while the bulk of OAT expansion in this tertiary branch occurred around the divergence of eutherian and prototherian mammals approximately 220 million years ago, a number of specific selective pressures resulted in the retention of URAT1 and the presumed loss of OAT4. Furthermore, OAT4, predicted to be the ancestral OAT in this group, is absent from numerous mammalian genomes suggesting that its function is specific to the species that still have an intact version in their genome. Alternatively, incomplete genome assemblies or highly divergent sequences may result in inaccurate assessment of orthologous OAT sequences in these species using simple Blast-based techniques. These results are depicted in Figure 5.2.

Selective pressures on orthologs in the OAT family

Comparisons of the full-length amino acid sequences of primate OAT4 and URAT1, as shown in Figure 5.3, found that approximately 50% of the residues were completely conserved and 67% were similar between the two transporters. A number of areas of sequence divergence were observed in specific secondary structural elements however. Notably, the large extracellular loop domain

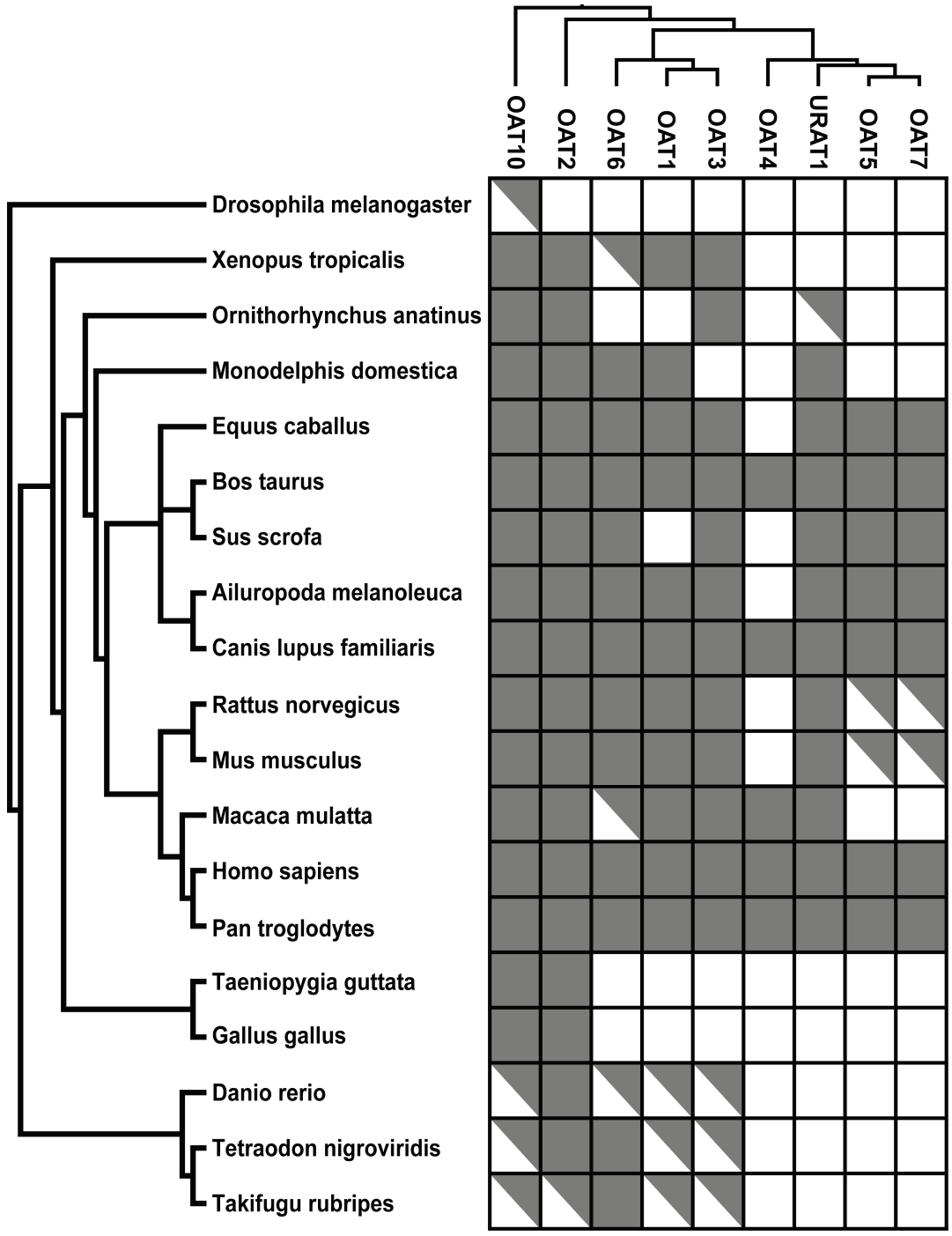

Figure 5.2: Species-specific OAT evolution. Presence of orthologous OATs in animal species was determined using protein databases in NCBI and Ensembl using the BlastP algorithm. The left dendogram depicts a species tree representative of the major vertebrate clades while the top dendogram is a reproduction of the maximum likelihood phylogram as shown in Figure 5.1. Gray boxes indicate presence of a definitive OAT ortholog, white boxes a distinct absence of an OAT ortholog, and the mixed boxes represent a potential, but inconclusive, ortholog.

between the first and second transmembrane helices, common to all SLC22 transporters, was highly conserved with 77% of the residues identical and 85% similar. This is in contrast to the sum loop region conserved residues which occurred at only 55% identical and 67% similar. Additionally, the predicted transmembrane domains (TMDs) throughout the proteins were noticeably less conserved with only 43% of residues completely conserved and only 56% displaying similarity. The lack of conservation in the TMDs was observed equally throughout all 12 regions with no more than 55% of the residues being conserved in any membrane-spanning helix. No significant differences were observed in specific species comparisons. These results are summarized in Table 5.1. In contrast, comparisons of these regions within orthologous OAT4 and URAT1 sequences found very high levels of sequence identity (greater than 90%) in all three regions among all four primate species examined, as indicated in Table 5.2.

Based on the d_N/d_S ratios calculated using the maximum likelihood methods implemented in PAML, a number of departures from the neutral model of evolution can be observed as indicated in Table 5.3. Specifically, when the human coding sequences were compared to the equivalent regions of canine orthologs the average d_N/d_S ratio of the OATs as a whole was 0.367. The d_N/d_S ratios of OAT1, OAT4, URAT1, and OAT6 all showed much stronger levels of purifying selection (d_N/d_S ratios of 0.079, 0.209, 0.169, and 0.114 respectively) compared to the entire OAT family. The very low ratio for OAT1 was particularly striking suggesting a conserved and important function of this transporter among

Table 5.1: Comparison of paralogous topological regions in primate OAT4 and URAT1

% Identity		OAT4/Oat4				% Similarity		OAT4/Oat4			
TMD		**Hs**	**Pt**	**Pp**	**Gg**	**TMD**		**Hs**	**Pt**	**Pp**	**Gg**
	Hs	41.3	41.3	40.7	41.3		**Hs**	56.3	56.3	56.1	56.3
URAT1/	**Pt**	41.3	41.3	40.7	41.3	**URAT1/**	**Pt**	56.3	56.3	56.1	56.3
Urat1	**Pp**	41.3	41.3	40.7	41.3	**Urat1**	**Pp**	56.3	56.3	56.1	56.3
	Gg	41.3	41.3	40.7	41.3		**Gg**	56.3	56.3	56.1	56.3
EC						**EC**					
	Hs	66.7	66.7	67.4	61.4		**Hs**	79.5	78.8	78.8	75.8
URAT1/	**Pt**	65.9	65.9	66.7	60.6	**URAT1/**	**Pt**	78.8	78.8	78.8	75.8
Urat1	**Pp**	66.7	66.7	67.4	61.4	**Urat1**	**Pp**	78.0	78.0	78.0	75.0
	Gg	65.9	65.9	66.7	61.4		**Gg**	78.8	78.8	78.8	75.8
IC						**IC**					
	Hs	49.4	50.0	47.2	49.4		**Hs**	66.9	66.9	65.3	66.9
URAT1/	**Pt**	48.9	49.4	46.6	48.9	**URAT1/**	**Pt**	66.9	66.9	65.3	66.9
Urat1	**Pp**	49.4	50.0	47.2	49.4	**Urat1**	**Pp**	67.4	67.4	65.9	67.4
	Gg	49.4	50.0	47.2	49.4		**Gg**	67.4	67.4	65.9	67.4
Total						**Total**					
	Hs	51.8	51.4	52.0	51.6		**Hs**	68.2	68.0	66.9	67.3
URAT1/	**Pt**	52.0	51.6	52.2	51.8	**URAT1/**	**Pt**	67.8	67.8	66.7	67.1
Urat1	**Pp**	51.3	50.9	51.4	51.1	**Urat1**	**Pp**	68.0	68.0	66.9	67.3
	Gg	50.5	50.2	50.7	50.5		**Gg**	68.0	68.0	66.9	67.3

Percent identity and similarity of OAT4 and URAT1 paralogs from *H. sapiens* (Hs), *P. troglodytes* (Pt), *P. pygmaeus* (Pp),and *G. gorilla* (Gg). TMD: transmembrane domain; EC: extracellular regions; IC: intracellular regions.

Table 5.2: Comparison of orthologous topological regions in primate OAT4 and URAT1

% Identity		OAT4/Oat4				% Identity		URAT1/Urat1			
TMD		**Hs**	**Pt**	**Pp**	**Gg**	**TMD**		**Hs**	**Pt**	**Pp**	**Gg**
	Hs	100					**Hs**	100			
OAT4/	**Pt**	100	100			**URAT1/**	**Pt**	99.6	100		
Oat4	**Pp**	98.8	98.8	100		**Urat1**	**Pp**	97.6	97.2	100	
	Gg	100	100	98.8	100		**Gg**	99.2	99.6	97.6	100
EC						**EC**					
	Hs	100					**Hs**	100			
OAT4/	**Pt**	99.2	100			**URAT1/**	**Pt**	98.5	100		
Oat4	**Pp**	97.6	97.6	100		**Urat1**	**Pp**	97.7	97.7	100	
	Gg	91.9	92.7	90.2	100		**Gg**	98.5	98.5	97.7	100
IC						**IC**					
	Hs	100					**Hs**	100			
OAT4/	**Pt**	99.4	100			**URAT1/**	**Pt**	98.8	100		
Oat4	**Pp**	94.3	93.7	100		**Urat1**	**Pp**	94.7	94.7	100	
	Gg	100	99.4	94.3	100		**Gg**	98.8	98.8	95.9	100
Total						**Total**					
	Hs	100					**Hs**	100			
OAT4/	**Pt**	99.6	100			**URAT1/**	**Pt**	99.1	100		
Oat4	**Pp**	97.3	97.1	100		**Urat1**	**Pp**	96.7	96.6	100	
	Gg	98.2	98.2	95.6	100		**Gg**	98.9	99.1	97.1	100

Percent identity of OAT4 and URAT1 orthologs from *H. sapiens* (Hs), *P. troglodytes* (Pt), *P. pygmaeus* (Pp),and *G. gorilla* (Gg). TMD: transmembrane domain; EC: extracellular regions; IC: intracellular regions.

mammals. Similarly, these ratios were also slightly lower than the overall ratios found in the renally expressed OAT subset and substantially lower than the hepatic subset. Likewise, these ratios were comparable to that observed in housekeeping genes[33], which are generally considered to be under strong purifying selection due to their critical functional roles. While the d_N/d_S ratios do indicate purifying selection at work, positive selection cannot be ruled out in this analysis, only that purifying selection is a larger factor.

When OAT4 and URAT1 are compared in more detail, as shown in Table 5.4, the d_N/d_S ratios show that URAT1 is generally subject to slightly greater negative selective pressures. When the ratios for specific topological domain were compared, the extent of divergence becomes more apparent; in particular, the d_N/d_S ratios of the transmembrane and extracellular domains of URAT1 are approximately two-fold lower than that of OAT4. The d_N values, indicative of the number of amino acid differences between the species in the region, was also exceedingly low in URAT1 transmembrane and extracellular domains. In contrast, the intracellular domain ratios of URAT1 and OAT4 were roughly equivalent at 0.375 and 0.326 respectively, which indicate only moderate and equivalent purifying selection.

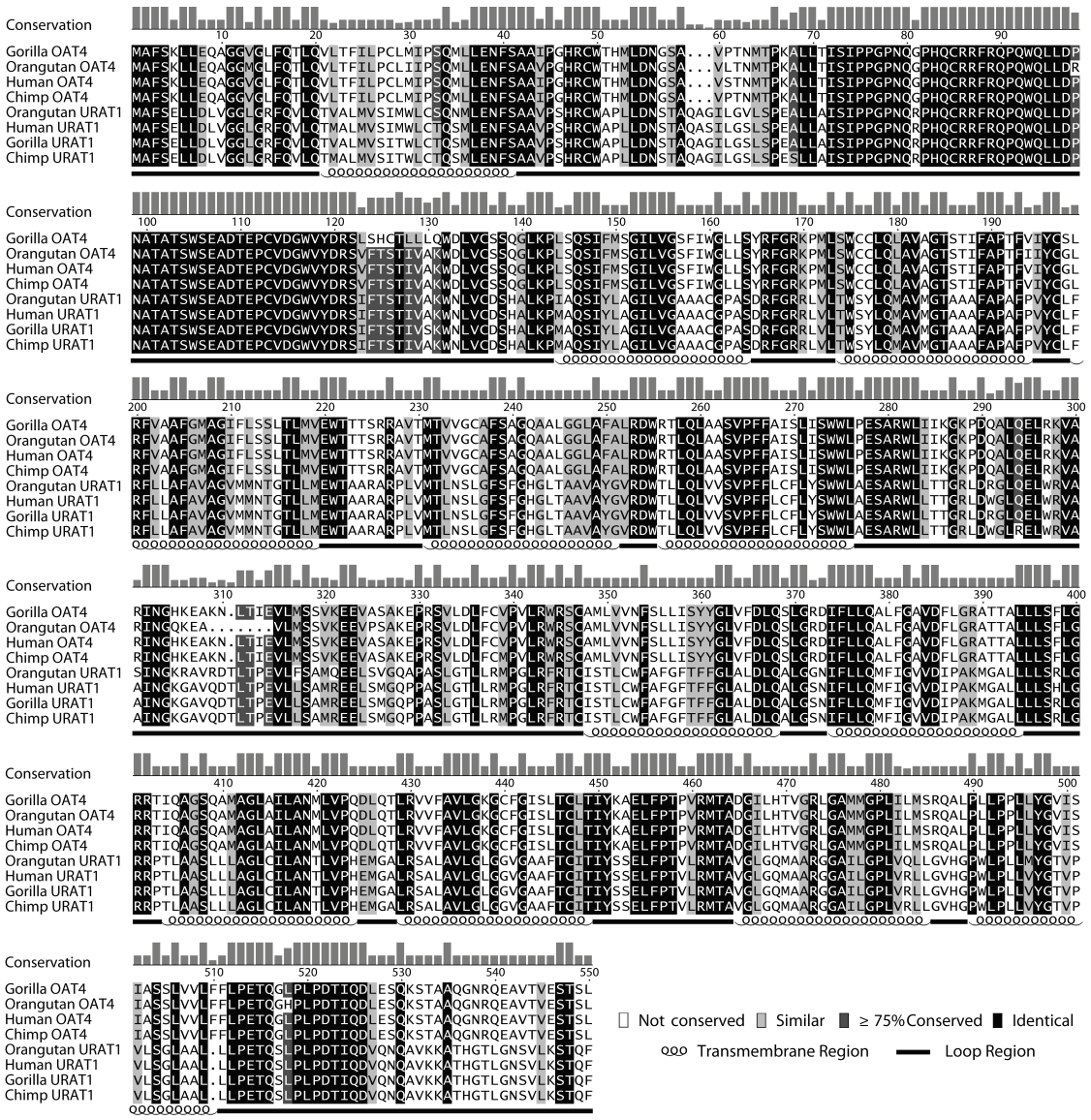

Figure 5.3: Conservation of primate OAT4 and URAT1. Multiple alignment of full-length primate OAT4 and URAT1 protein sequences with top bars indicating the level of conservation at a given position. Black shading indicates conservation of at least 75%, dark gray of conservation of at least 50%, light gray of a lack of conservation but the presence of chemically similar residues, while white shading indicates less than 50% conservation and no chemically similar residues. The amino acid position numbering and transmembrane domain predictions are reflective of OAT4.

Table 5.3: Conservation of OATs as measured by d_N/d_S ratios between human and canine orthologs

Gene	d_N	d_S	d_N/d_S
SLC22A6	0.036	0.457	0.079
SLC22A7	0.222	0.596	0.373
SLC22A8	0.151	0.456	0.331
SLC22A9	0.245	0.364	0.671
SLC22A10	0.228	0.334	0.681
SLC22A11	0.150	0.715	0.209
SLC22A12	0.095	0.564	0.169
SLC22A13	0.228	0.334	0.681
SLC22A20	0.069	0.603	0.114
OAT Avg.	0.158	0.492	0.367
Renal Avg.	0.132	0.505	0.294
Hepatic Avg.	0.231	0.432	0.575

OATs consist of *SLC22A1*, *SLC22A3*, *SLC22A11*, *SLC22A12*, and *SLC22A13;* hepatic OATs consist of *SLC22A7*, *SLC22A9*,and *SLC22A10*.

OAT4 and URAT1 gene expression in human tissues

Quantitative reverse transcriptase PCR (qRT-PCR) using commercially available RNA from normal, adult human tissues identified overlapping and distinct patterns of gene expression of OAT4 and URAT1 as shown in Figure 5.4. Specifically, and as reported previously[3, 34], both OAT4 and URAT1 exhibited high expression levels in the kidney, consistent with their documented functional roles. Whereas URAT1 expression was limited to the kidney and showed nearly undetectable levels in the other ten tissues examined, OAT4 expression was also high in the placenta and in the epididymis. While the expression of OAT4 in the

Table 5.4: Conservation of topological regions of OAT4 and URAT1 as measured by d_N/d_S ratios between human and canine orthologs

	SLC22A11	*SLC22A12*
TMD		
d_N	0.720	0.091
d_S	2.402	0.556
d_N/d_S	0.300	0.164
EC		
d_N	0.099	0.081
d_S	0.653	1.08
d_N/d_S	0.152	0.075
IC		
d_N	0.235	0.192
d_S	0.721	0.510
d_N/d_S	0.326	0.375
Total		
d_N	0.150	0.095
d_S	0.715	0.564
d_N/d_S	0.209	0.169

TMD: transmembrane domains; EC: extracellular loops; IC: intracellular loops.

placenta has been reported previously[17], expression in the epididymis has not been found prior to studies presented in this dissertation.

Substrate preferences in OAT4 and URAT1

Given the recognized preferences for steroid sulfates and purine-like compounds by OAT4 and URAT1 respectively, uptake of a number of these chemicals was undertaken to better detail potential substrate overlap between these two transporters. As shown in Figure 5.5A, OAT4 readily translocated both ES and

DHEAS with uptake between 8- and 18-fold more than in empty vector transfected cells, while URAT1 exhibited no uptake of either which is consistent with previous reports[3, 17]. In contrast, and as shown in Figure 5.5B, no uptake was observed for any of the 13 purine-like compounds tested in OAT4 transfected cells whereas URAT1 demonstrated high levels of uptake of uric acid and appreciable uptake of both AMP and ADP at approximately 3- and 2.5-fold respectively, both of which are newly discovered and novel substrates for URAT1 and previously not considered substrates for any other SLC22 transporter.

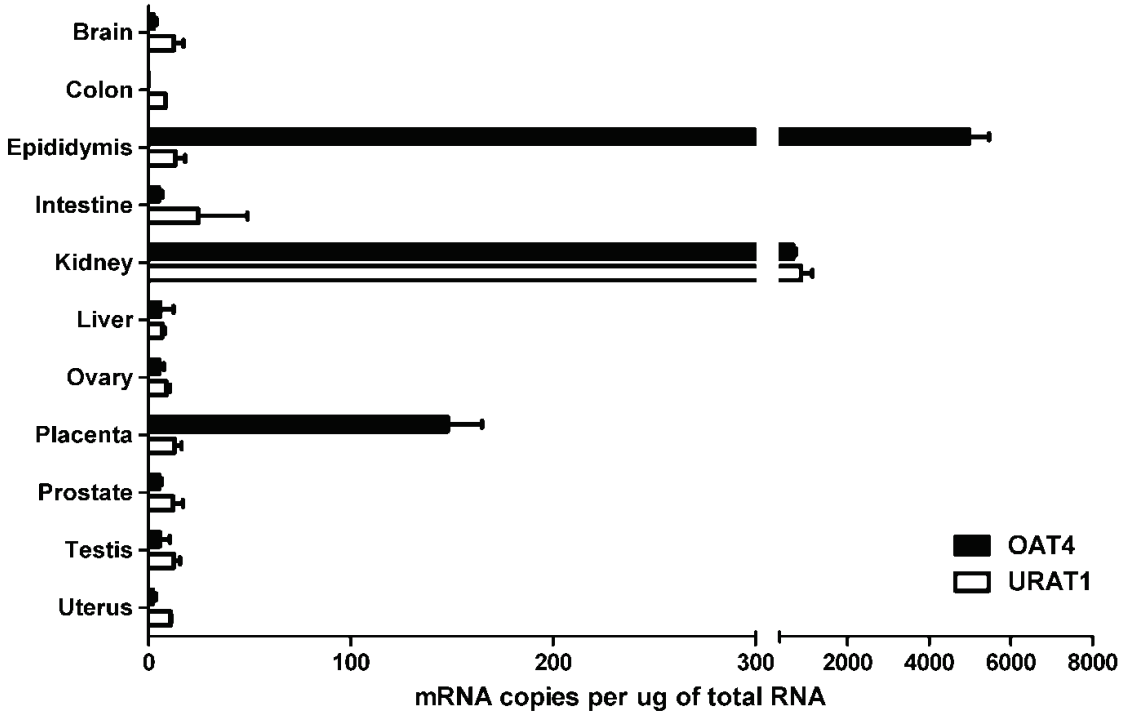

Figure 5.4: Expression levels of mRNA transcripts of *SLC22A11* and *SLC22A12* in healthy adult human tissues. mRNA expression levels of *SLC22A11* (OAT4) and *SLC22A12* (URAT1) in normal adult human tissues was determined using Taqman® assays specific to each transporter. Expression data were normalized to *GAPDH* expression and copy number was determined using a standard curve for each respective transporter. Each bar represents the mean ± SD of three independent measurements of single RNA samples.

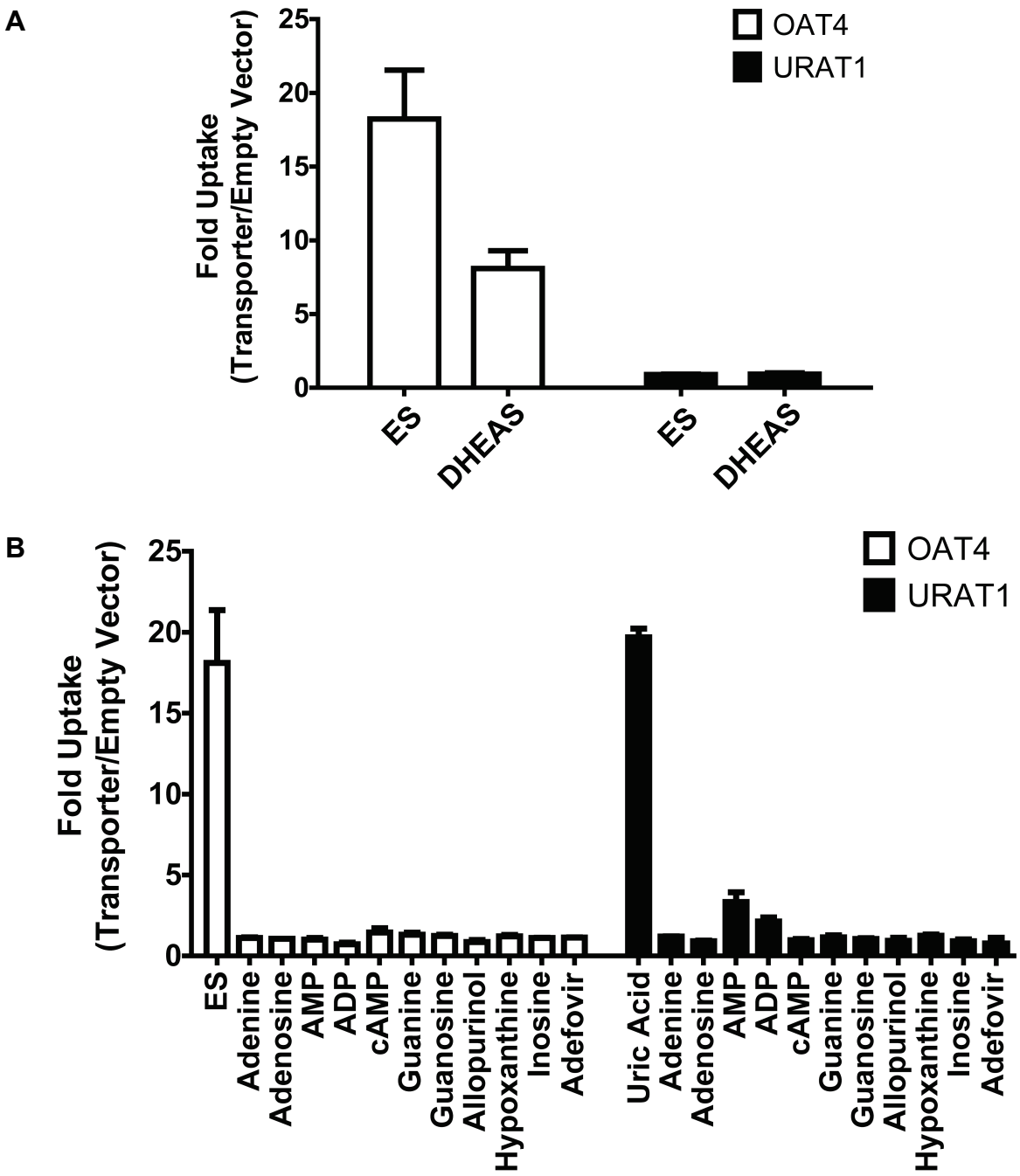

Figure 5.5: Substrate preferences of OAT4 and URAT1 using representative substrates. Uptake experiments were performed with stably transfeced 293-Flp-In® cells for 2 minutes at 37° C using 20 nM ^{3}H-estrone sulfate (ES) and ^{3}H-dehydroepiandrosterone (DHEAS), 25 μM ^{14}C-uric acid, or approximately 40 nM of the other tested radiolabeled substrates as indicated in the figure. All experiments were performed independently in triplicate and were normalized to total protein in each well as determined using a BCA assay. Values are expressed as the fold over empty vector transfected cells incubated concurrently with the respective substrates.

However, no other purine-like compounds showed any appreciable uptake via URAT1. Uptake of AMP and ADP by URAT1 was shown to be inhibitable by excess unlabeled uric acid as shown in Figure 5.6. In addition, uptake of AMP

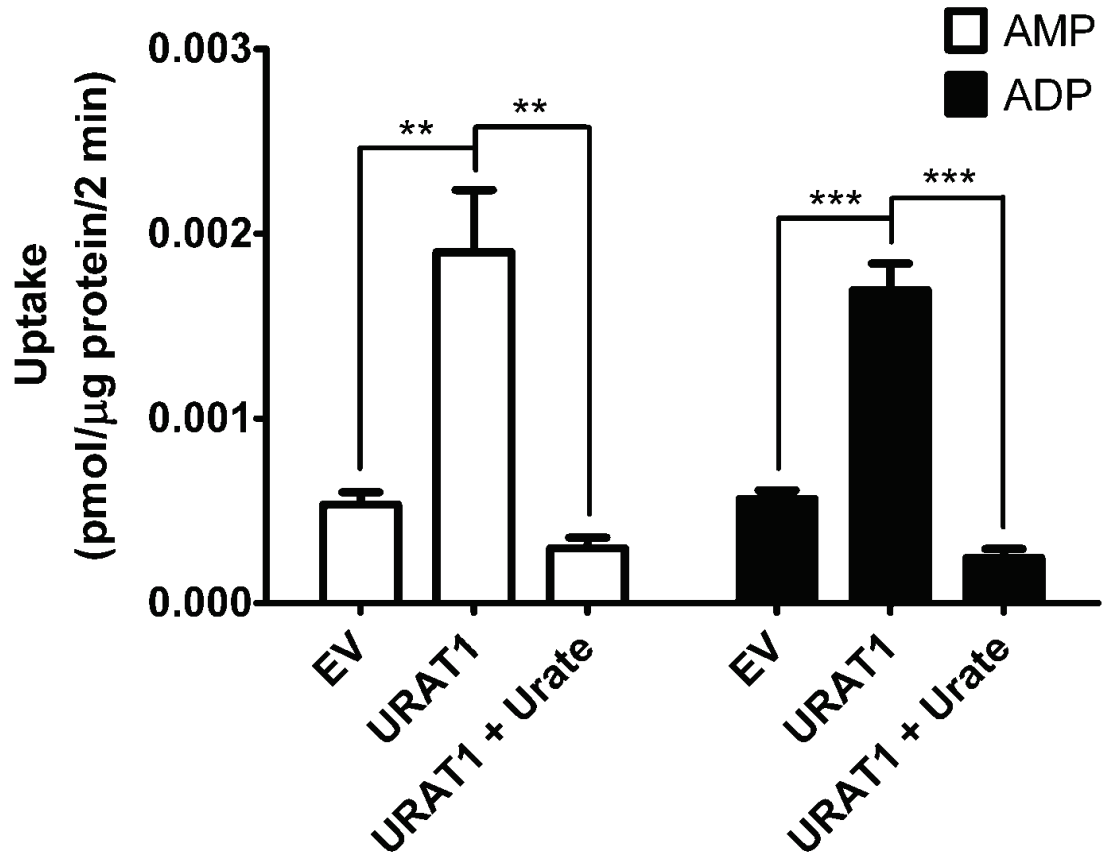

Figure 5.6: URAT1-mediated uptake of AMP and ADP. Uptake experiments were performed for 2 minutes at 37° C using 70 nM radiolabeled AMP and 50 nM radiolabeled ADP. All uptakes utilized stably transfected HEK-293 Flp-In cells. Uptake values were normalized to total protein per well and expressed as the total number of ρmol transported per µg of protein; each bar represents the mean ± SEM of three independent experiments. Uric acid (500µM) was used to inhibit AMP or ADP transport by URAT1. ** indicates p value ≤ 0.01; *** indicates p value ≤ 0.001 compared to URAT1 uptake as determined using a one-way ANOVA followed by a Dunnett's post-hoc test.

and ADP was saturable with K_m and V_{max} values of 14.6 ± 5.42 μM and 0.169 ± 0.0153 ρmol/μg protein/min for AMP and 2.94 ± 1.67 μM and 0.036 ± 0.00587 ρmol/μg protein/min for ADP as detailed in Figure 5.7A and 5.7B, making these two substrates kinetically distinct from transport of the model substrate uric acid, which has a K_m value for transport by URAT1 of approximately 300-400 μM[3].

Inhibition screening in OAT4 and URAT1

A larger inhibition screen of steroid sulfate- and purine-like metabolites and drugs was undertaken to better define the chemical features that elicit interaction with OAT4 and/or URAT1. Inhibition studies using various steroid sulfates and purine-based compounds, as well as previously noted OAT inhibitors and structurally similar compounds, identified broad chemical preferences and revealed subtle overlapping and specific interactions within these three groups. As expected, and illustrated in Figure 5.8, uptake of estrone sulfate (3.11×10^{-4} ρmol/μg protein/min average uptake in reference vs. 3.04×10^{-5} ρmol/μg protein/min average uptake in empty vector) was completely abolished by co-incubation with other steroid sulfates including estrone sulfate (ES), dehydroepiandrosterone sulfate (DHEAS), and pregnenolone sulfate (PS) while estradiol-3-sulfate resulted in only 40-60% inhibition. Likewise, inhibition by the canonical OAT inhibitors diclofenac, losartan, and indomethacin was also virtually complete, while salicylate and phenytoin produced inhibition near 50%. Co-incubation with morin, a natural flavanol, and enoximone, a phosphodiesterase inhibitor, also resulted in near complete loss of estrone sulfate uptake by OAT4. In contrast, inhibition of OAT4-mediated estrone sulfate

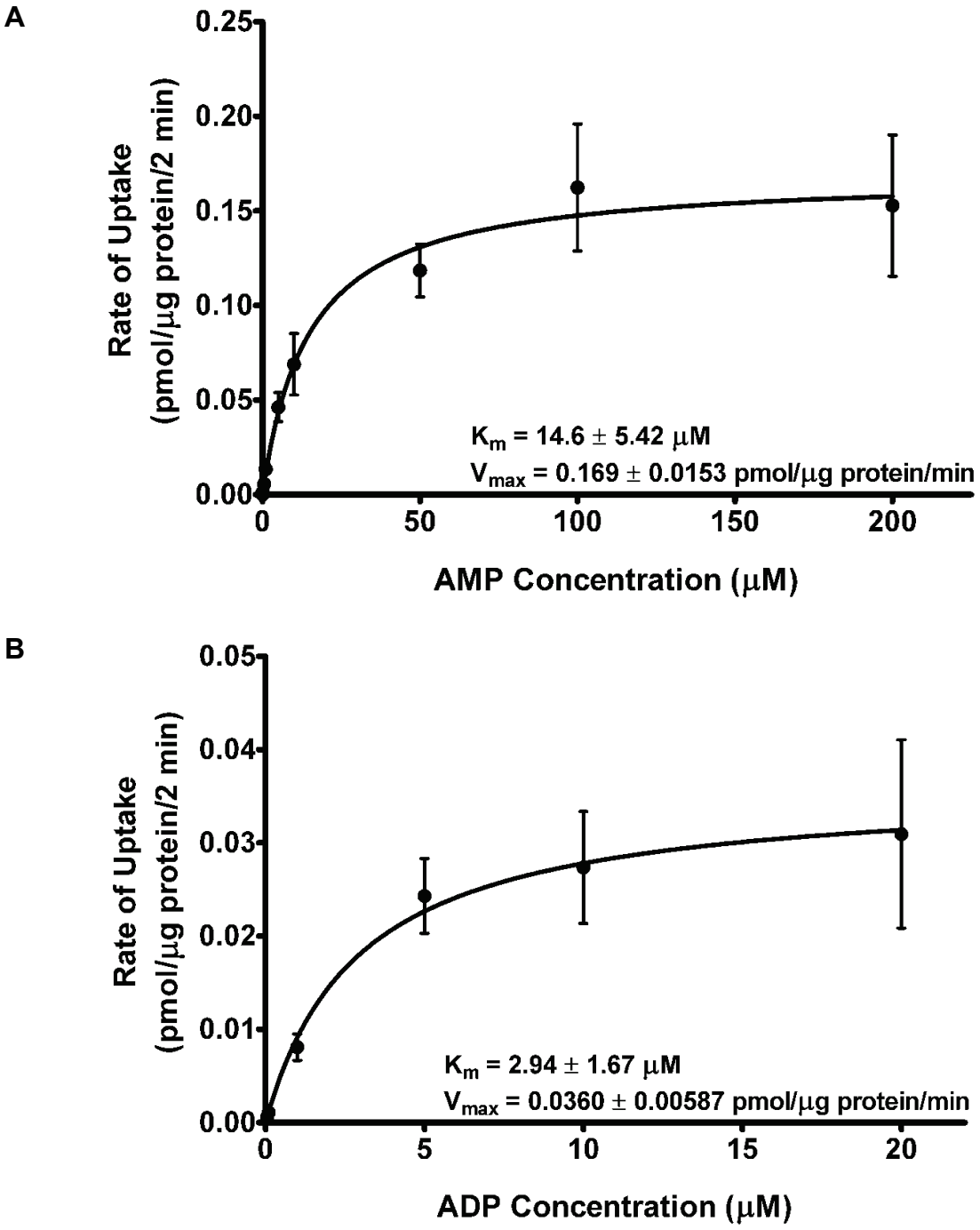

Figure 5.7: Concentration dependent uptake of AMP and ADP by URAT1. Experiments were performed for 2 minutes at 37° C using A) 100 nM radiolabeled AMP and unlabeled AMP for the remainder or B) 100 nM radiolabeled ADP and unlabeled ADP for the remainder as indicated in the figure. Uptake values were normalized to total protein and adjusted for the uptake of AMP or ADP in empty vector transfected cells. Curves were generated using non-linear regression with automatic removal of outliers in Graphpad Prism 5.1.

uptake showed minimal effect by co-incubation with purine-like chemicals with maximum inhibition (approximately 30-40%) by the adenine derivatives xanthine, theobromine, theophylline, and uric acid.

As shown in Figure 5.9, inhibition of uric acid uptake by URAT1 (1.09×10^{-1} ρmol/μg protein/min average uptake in reference vs. 6.21×10^{-3} ρmol/μg protein/min average uptake in empty vector) was not appreciably affected by co-incubation of any steroid sulfates with the exception of PS which inhibited uric acid uptake approximately 50% whereas greater than 50% inhibition occurred with co-incubation of uric acid, xanthine, theophylline, hypoxanthine, and theobromine. Similar to OAT4, URAT1-mediated uptake of uric acid was inhibited completely by diclofenac, indomethacin, and losartan, and morin. In contrast to OAT4, very little inhibition was observed during co-incubation with steroid sulfates or similar synthetic steroid derivatives; PS exhibited the greatest degree of inhibition at roughly 50% with DHEAS at 30-40%. Enoximone also had no effect on uric acid uptake by URAT1, in stark contrast to the complete loss of transport activity when co-incubated with radiolabeled estrone sulfate in OAT4-transfected cells.

Discussion

Organic anion transporters perform a wide variety of functions in the mammalian kidney, facilitating both the reabsorption and excretion of innumerable

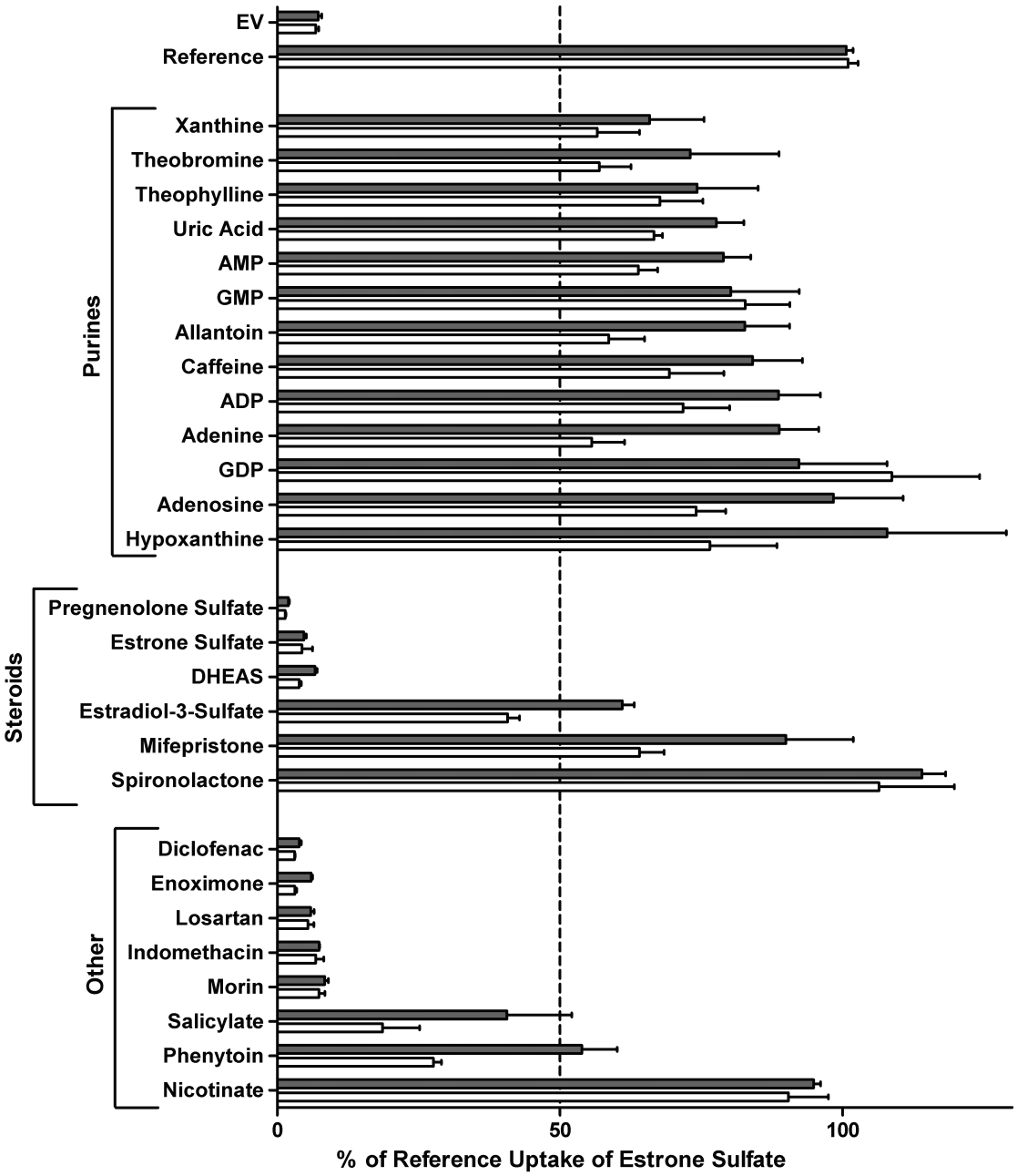

Figure 5.8: Inhibition of OAT4 uptake of estrone sulfate by purines, steroid sulfates and derivatives, and selected OAT inhibitors. Inhibition experiments were performed for 5 minutes at 37° C using 20 nM radiolabeled estrone sulfate and 0.5 mM (grey bars) and 1 mM (white bars) of unlabeled inhibitor (50 and 100 μM of spironolactone and mifepristone) dissolved in water or DMSO. All uptakes used stably transfected HEK-293 Flp-In® cells. Uptake values were normalized to total protein and expressed as a percentage of OAT4 reference uric acid uptake and each bar represents the mean ± SEM of three independent experiments.

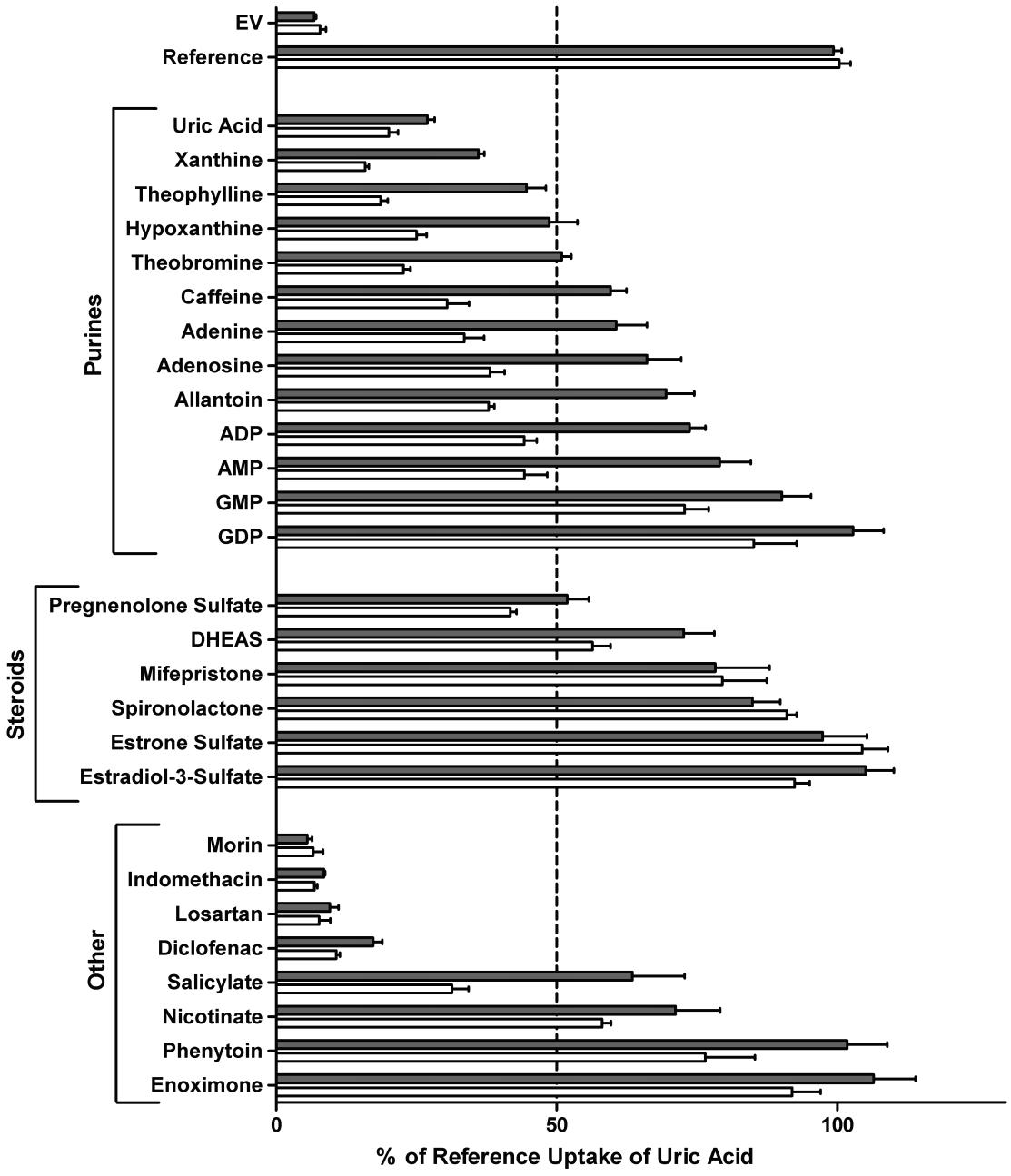

Figure 5.9: Inhibition of URAT1 uptake of uric acid by purines, steroid sulfates and derivatives, and selected OAT inhibitors. Inhibition experiments were performed for 5 minutes at 37° C using 10 µM radiolabeled uric acid and 0.5 mM (grey bars) and 1 mM (white bars) of unlabeled inhibitor dissolved in water or DMSO. All uptakes used stably transfected HEK-293 Flp-In cells. Uptake values were normalized to total protein and expressed as a percentage of URAT1 reference uric acid uptake and each bar represents the mean ± SEM of three independent experiments.

xenobiotics and endogenous metabolites. While precise structure-activity relationships for these transporters are still ill-defined, a central feature within this family are sub-groups of OATs that evolved from gene duplication events that display overlapping, yet distinct, functional properties. The recent cloning and characterization of a number of new members of the OAT family have allowed for the opportunity to investigate the ongoing adaptability and specialization that has occurred in this gene family during the evolution of mammals. Comparison of the paired OATs, OAT4 and URAT1, is indicative of this phenomenon and acts as a primary example of the increasing functional specialization that is occurring in this gene family.

OAT4 and URAT1 are expressed on the renal apical membrane and are believed to have evolved from a common ancestor. Like other pairs of OATs examined thus far, these transporters share a high level of amino acid identity and occur in tandem on human chromosome 11 with approximately 20kb separating the coding regions of each of these genes. In spite of their close proximity on the genome and the evidence supporting their evolution from a gene duplication event, OAT4 and URAT1 possess exceptionally divergent functional characteristics as detailed previously. Based on the prior work of Wu et al[12], it has been established that the OATs are undergoing substantial gene duplication in mammals, with numerous species-specific serial duplication occurring at the point of metatherian and eutherian speciation. However, the impact of these duplications on overall OAT function was not ascertained, in large part due to the incomplete functional characterization of the majority of these OAT orthologs and

paralogs. Phylogenetic analysis of the OAT family suggests that OAT-like proteins were present in early invertebrate animals such as *D. melanogaster*, but that subsequent speciation and gene divergence resulted in the presence of numerous additional OATs in the mammalian lineage. OAT4 and URAT1 both appear in their present forms after the divergence of mammals from other animals including fish, birds, and amphibians. Previous work has speculated that OAT4 expression in the placenta provides a unique mechanism for the regulation of steroid sulfates and in turn steroid activity[35], which is known to be of critical importance in normal fetal development in mammals[36] and can influence sex ratios in other non-placental amniotes[37]. The emergence of OAT4 in placental mammals supports this role, however, OAT4 is absent from a number of mammalian species suggestive of either redundant or more recently evolved mechanisms that have supplanted OAT4 function in these species or a specific functional benefit in the species conferred by the retention of a functional OAT4. In contrast, URAT1 is found in a larger number of mammalian genomes, including in marsupials and potentially in monotremes. While not definitive, the broader presence of URAT1 in mammals suggests that its role is more ubiquitous and potentially more critical than that of OAT4. Recent investigations have found that loss of URAT1 function results in hypouricemia in humans which in turn leaves people more susceptible to exercise-induced renal failure[38] and neurological diseases[39]. The true impact of URAT1 in non-primate species, where uric acid is further metabolized to allantoin, is unclear but does leave the possibility that other important functions of URAT1 do exist, providing a selective

advantage to URAT1 retention in species without a clear benefit or need for high levels of uric acid transport. Mice null for Rst1, the ortholog of human URAT1, did not present with any gross abnormalities aside from impaired uric acid reabsorption in the kidney although the known redundancy provided by GLUT9 (*SLC2A9*) uric acid transport in the kidney may obfuscate any detrimental impact from the loss of uric acid reabsorption by URAT1[10]. Recent clinical and animal model studies have shown that loss-of-function mutations in GLUT9 result in hyperuricemia, the opposite effect of impaired URAT1 uric acid reabsorption, suggesting that while these two transporters may both strongly influence uric acid levels, they do so using alternate means and with differing physiological consequences[40, 41]. Thus the role of URAT1 may not solely be the transport of uric acid, as indicated by the presence of alternate methods of uric acid uptake in spite of presence in most mammalian genomes.

While OAT1, OAT3, and OAT4 have all been shown to transport uric acid at modest levels, URAT1 does so with exceedingly high rates of transport, which is a specific feature within SLC transporters known to be expressed on the apical membrane of the renal proximal tubule and in SLC22 transporters as a whole. Thus the function of URAT1 may be in response to an increased need for purine reabsorption from the urine for metabolic or, as reasoned by Maxwell et al., for reasons related to oxidative stress[42] that could not be accomplished with OATs that existed at that stage of evolution, predicating the evolution of the novel functions of URAT1.Examination of the major classes of compounds transported by OAT4 and URAT1, primarily purines and steroid sulfates, also identified

divergent and somewhat specialized functions. In particular, URAT1-mediated uric acid uptake was inhibited appreciably by most purine-based molecules. Likewise, URAT1 was also capable of transporting AMP and ADP which was inhibitable by excess uric acid. While other transporters, namely OAT2 and the concentrative (SLC28) and equilibrative nucleoside (SLC29) transporters, are known to transport a wide variety of nucleic acid-based compounds, uptake of AMP and ADP has not been demonstrated. The only SLC transporter previously reported to transport AMP and ADP with any noticeable affinity is *SLC25A42*, a member of the mitochondrial uptake transporter family[43] and while the level of transport of AMP and ADP surpasses that of URAT1, its expression is limited to the inner mitochondrial membrane thereby precluding its involvement in renal reabsorption processes. The affinity of these two metabolites for URAT1 was also up to 100 fold greater than that of uric acid, implicating a class of molecules, rather than solely uric acid, as the major substrates of URAT1. As the levels of AMP and ADP in the blood are approximately 10 and 160 μM respectively, whereas their concentration in urine is almost undetectable, the expected reabsorptive action of URAT1 may contribute to the reclamation pathway for these purine nucleotides, in addition to the well-documented reabsorption of uric acid.

OAT4 also demonstrates distinct substrate specificity in comparison to URAT1. In particular, only a slight inhibition of OAT4 by purine-like molecules was observed. OAT4 seems to prefer steroid sulfates as indicated by its high uptake of estrone sulfate and a strong inhibitory effect of coincubation with all steroid

sulfates examined. Further, the transporter interacts with a wide variety of chemically unique compounds such as phenytoin, and enoximone (Figure 5.8). These compounds possess similar 5-member nitrogen substituted ring structures as uric acid but also include large heterogeneous lipophilic groups. Together, these results indicate that OAT4 is capable of interacting with a wider range of compounds, including those with larger and more lipophilic regions, and that while base interactions are shared between these two transporters, their mechanisms of substrate restriction have diverged considerably, at least in the context of this common structural framework.

Sequence comparisons of OAT4 and URAT1 identified potential regions responsible for the differential substrate and inhibitor preferences. In particular, multiple alignments of primate OAT4 and URAT1 identified high levels of conservation between the two transporters in the loop regions while the transmembrane domains were largely unconserved as a whole. In particular, the extracellular regions demonstrated a high level of amino acid identity. This is in distinct contrast to the high level of conservation of all of these regions between orthologous sequences. While individual changes in these regions cannot be excluded as causative factors in the differences in substrate preference, it is also possible that a set of changes resulting in the comparatively unconserved transmembrane regions could be responsible for the divergent substrate class preferences observed between OAT4 and URAT1. Previous evidence for this occurrence has been found with point mutations in rat Oat3. Specifically, replacement of a lysine at position 370 with alanine and an arginine at position

454 with aspartate resulted in the ablation of anion transport capacity and the new ability to transport cationic substrates[44]. Both of these residues occurred in C-terminal transmembrane regions, indicating that these regions can have strong influences on both transport efficiency and substrate selectivity. While the lack of conservation in these regions may result in a change in functional capacity, the regional differences between OAT4 and URAT1 may also be inconsequential due to the preponderance of changes in residues that are not important for transport function. However, evaluation of these regions using d_N/d_S ratios, calculated using the human and canine orthologs, found that while purifying selection was present in all regions, a nearly 2-fold greater level of purifying selection was observed in URAT1 in both the extracellular and transmembrane regions compared to OAT4. This is suggestive of specific amino acids in URAT1 present in these regions that are preserved throughout evolution and strongly suggests a conserved function. In contrast, the intracellular loop regions in OAT4 and URAT1 have similar ratios indicating that changes in these regions are not likely to have elicited the change in substrate preference observed in these two transporters. The selective pressures on the transmembrane and extracellular regions of URAT1 may be due to the requisite physiological functions it is now responsible for, namely the reabsorption of uric acid, after other selective pressures caused the initial divergence and functional specialization between the two genes.

While increased specialization can manifest itself through divergent functional attributes, altered regulation of transporters could also result in differential

functions. In particular, OAT10 is found in a number of tissues aside from the site of its highest expression in the kidney including the brain, heart, small intestine, and colon at roughly equivalent levels[45], suggestive of a common function in these tissues. Similarly, OAT2, while considered to be a liver-specific OAT, is in fact expressed at relatively high levels in a number of non-hepatic tissues such as kidney, pancreas, and testis[46]. However, as the evolution of the OAT family progresses, more specific expression is observed. When the expression patterns of OAT4 and URAT1 were examined using qRT-PCR, it was found that OAT4, the more ancestral of the two, was expressed in wider range of tissues, with particularly high expression in the epididymis. This is of note as the kidney and the epididymis are derived from the same embryonic tissue, the mesonephros[47]. While purely observational at this stage, this would seem to indicate both that OAT4 is indeed ancestral and that its method of gene regulation is less finely controlled compared to URAT1. In fact, as URAT1 is expressed at an appreciable level only in the kidney, without any noticeable levels in the epididymis, would seem to indicate that its regulatory mechanisms have also evolved to accommodate a more specific functional role, one that is unnecessary in the male reproductive tract but important in the kidney. Similar observations of functional specialization have been observed in other transporter families such as the glucose transporters (SLC2), which display unique functional properties and are expressed in a tissue-specific manner while retaining a substantial level of sequence identity[48]. Likewise, OCTN2 (*SLC22A5*) displays a similar pattern of restricted expression and highly specialized function. In

particular, high levels of OCTN2 expression are largely limited to the kidney and placenta, two tissues with critical roles in maintaining appropriate physiological levels of carnitine[49]; while OCTN2 is known to transport other small molecules, much like URAT1, its uptake of carnitine is substantial and has significant repercussions in the form of primary carnitine deficiency.

In the kidney, redundancy and specificity of function results in both overlapping mechanisms for transporting a variety of small molecules and those that transport very explicit compounds in a tightly controlled manner. This paradigm has previously been suggested to be a hallmark of renal development in mammals[50] but the question remains: did the expansion of OATs in mammals occur by chance gene duplication events and result in redundant function or were there selective pressures that caused duplicated genes to evolve towards a specific, non-redundant function in the kidney? Examination of OAT4 and URAT1 in the present study revealed that within primates and other mammals, distinct selective processes are at work leading to divergent functional properties between these two transporters, which can also be observed in other members of the OAT family. The uptake of purine derivatives, primarily uric acid but also others such as AMP and ADP, would appear to be a specific reclamation pathway unique to URAT1 that has evolved concomitantly with the evolution of placental mammals and is strongly indicative of OAT evolution steered towards more specialization of function rather than the creation of redundant and broad transport mechanisms. Likewise, the recent expansion of OAT genes may be in response to the need for more specific transport mechanisms for definite

substrates rather than redundant mechanisms for more promiscuous functions. By addressing the potential differences in the genetics and function of OAT4 and URAT1, the results presented herein provide an increased understanding of not only how these two transporters contribute to reabsorption of a variety of diverse solutes in the urine but also how pairs of transporters can evolve distinct roles in the kidney in spite of their recent divergence and overall genetic similarities.

References

1. Klaassen CD, Lu H. Xenobiotic transporters: ascribing function from gene knockout and mutation studies. *Toxicol Sci* 2008; **101**(2)**:** 186-196.

2. Lahjouji K, Mitchell GA, Qureshi IA. Carnitine transport by organic cation transporters and systemic carnitine deficiency. *Mol Genet Metab* 2001; **73**(4)**:** 287-297.

3. Enomoto A, Kimura H, Chairoungdua A, Shigeta Y, Jutabha P, Cha SH*, et al*. Molecular identification of a renal urate anion exchanger that regulates blood urate levels. *Nature* 2002; **417**(6887)**:** 447-452.

4. You G, Lee WS, Barros EJ, Kanai Y, Huo TL, Khawaja S*, et al*. Molecular characteristics of Na(+)-coupled glucose transporters in adult and embryonic rat kidney. *J Biol Chem* 1995; **270**(49)**:** 29365-29371.

5. Gopal E, Fei YJ, Sugawara M, Miyauchi S, Zhuang L, Martin P*, et al*. Expression of slc5a8 in kidney and its role in Na(+)-coupled transport of lactate. *J Biol Chem* 2004; **279**(43)**:** 44522-44532.

6. Dawson PA, Beck L, Markovich D. Hyposulfatemia, growth retardation, reduced fertility, and seizures in mice lacking a functional NaSi-1 gene. *Proc Natl Acad Sci U S A* 2003; **100**(23)**:** 13704-13709.

7. Beck L, Karaplis AC, Amizuka N, Hewson AS, Ozawa H, Tenenhouse HS. Targeted inactivation of Npt2 in mice leads to severe renal phosphate wasting, hypercalciuria, and skeletal abnormalities. *Proc Natl Acad Sci U S A* 1998; **95**(9)**:** 5372-5377.

8. Matsuo H, Chiba T, Nagamori S, Nakayama A, Domoto H, Phetdee K*, et al*. Mutations in glucose transporter 9 gene SLC2A9 cause renal hypouricemia. *Am J Hum Genet* 2008; **83**(6)**:** 744-751.

9. Calado J, Soto K, Clemente C, Correia P, Rueff J. Novel compound heterozygous mutations in SLC5A2 are responsible for autosomal recessive renal glucosuria. *Hum Genet* 2004; **114**(3)**:** 314-316.

10. Eraly SA, Vallon V, Rieg T, Gangoiti JA, Wikoff WR, Siuzdak G*, et al*. Multiple organic anion transporters contribute to net renal excretion of uric acid. *Physiol Genomics* 2008; **33**(2)**:** 180-192.

11. Hediger MA, Rhoads DB. Molecular physiology of sodium-glucose cotransporters. *Physiol Rev* 1994; **74**(4)**:** 993-1026.

12. Wu W, Baker ME, Eraly SA, Bush KT, Nigam SK. Analysis of a large cluster of SLC22 transporter genes, including novel USTs, reveals species-specific amplification of subsets of family members. *Physiol Genomics* 2009; **38**(2)**:** 116-124.

13. Eraly SA, Hamilton BA, Nigam SK. Organic anion and cation transporters occur in pairs of similar and similarly expressed genes. *Biochem Biophys Res Commun* 2003; **300**(2)**:** 333-342.

14. Kaler G, Truong DM, Khandelwal A, Nagle M, Eraly SA, Swaan PW*, et al*. Structural variation governs substrate specificity for organic anion transporter (OAT) homologs. Potential remote sensing by OAT family members. *J Biol Chem* 2007; **282**(33)**:** 23841-23853.

15. Vallon V, Rieg T, Ahn SY, Wu W, Eraly SA, Nigam SK. Overlapping in vitro and in vivo specificities of the organic anion transporters OAT1 and OAT3 for loop and thiazide diuretics. *Am J Physiol Renal Physiol* 2008; **294**(4)**:** F867-873.

16. Eraly SA, Bush KT, Sampogna RV, Bhatnagar V, Nigam SK. The molecular pharmacology of organic anion transporters: from DNA to FDA? *Mol Pharmacol* 2004; **65**(3)**:** 479-487.

17. Cha SH, Sekine T, Kusuhara H, Yu E, Kim JY, Kim DK*, et al*. Molecular cloning and characterization of multispecific organic anion transporter 4 expressed in the placenta. *J Biol Chem* 2000; **275**(6)**:** 4507-4512.

18. Hagos Y, Stein D, Ugele B, Burckhardt G, Bahn A. Human renal organic anion transporter 4 operates as an asymmetric urate transporter. *J Am Soc Nephrol* 2007; **18**(2)**:** 430-439.

19. Ichida K, Hosoyamada M, Hisatome I, Enomoto A, Hikita M, Endou H*, et al*. Clinical and molecular analysis of patients with renal hypouricemia in Japan-influence of URAT1 gene on urinary urate excretion. *J Am Soc Nephrol* 2004; **15**(1)**:** 164-173.

20. Shima JE, Komori T, Taylor TR, Stryke D, Kawamoto M, Johns SJ*, et al*. Genetic variants of human organic anion transporter 4 demonstrate altered transport of endogenous substrates. *Am J Physiol Renal Physiol* 2010; **299**(4)**:** F767-775.

21. Xu G, Bhatnagar V, Wen G, Hamilton BA, Eraly SA, Nigam SK. Analyses of coding region polymorphisms in apical and basolateral human organic anion transporter (OAT) genes [OAT1 (NKT), OAT2, OAT3, OAT4, URAT (RST)]. *Kidney Int* 2005; **68**(4)**:** 1491-1499.

22. Edgar RC. MUSCLE: multiple sequence alignment with high accuracy and high throughput. *Nucleic Acids Res* 2004; **32**(5)**:** 1792-1797.

23. Price MN, Dehal PS, Arkin AP. FastTree 2--approximately maximum-likelihood trees for large alignments. *PLoS One* 2010; **5**(3)**:** e9490.

24. Ronquist F, Huelsenbeck JP. MrBayes 3: Bayesian phylogenetic inference under mixed models. *Bioinformatics* 2003; **19**(12)**:** 1572-1574.

25. Felsenstein J (2010). In: *PHYLIP (Phylogeny Interface Package)*. Self Published: University of Washington.

26. Page RD. TreeView: an application to display phylogenetic trees on personal computers. *Comput Appl Biosci* 1996; **12**(4)**:** 357-358.

27. Beitz E. TEXshade: shading and labeling of multiple sequence alignments using LATEX2 epsilon. *Bioinformatics* 2000; **16**(2)**:** 135-139.

28. Yang Z. PAML 4: phylogenetic analysis by maximum likelihood. *Mol Biol Evol* 2007; **24**(8)**:** 1586-1591.

29. Suyama M, Torrents D, Bork P. PAL2NAL: robust conversion of protein sequence alignments into the corresponding codon alignments. *Nucleic Acids Res* 2006; **34**(Web Server issue)**:** W609-612.

30. Campanella JJ, Bitincka L, Smalley J. MatGAT: an application that generates similarity/identity matrices using protein or DNA sequences. *BMC Bioinformatics* 2003; **4:** 29.

31. Viklund H, Elofsson A. Best alpha-helical transmembrane protein topology predictions are achieved using hidden Markov models and evolutionary information. *Protein Sci* 2004; **13**(7)**:** 1908-1917.

32. Urban TJ, Yang C, Lagpacan LL, Brown C, Castro RA, Taylor TR*, et al*. Functional effects of protein sequence polymorphisms in the organic cation/ergothioneine transporter OCTN1 (SLC22A4). *Pharmacogenet Genomics* 2007; **17**(9)**:** 773-782.

33. Wang Y, Gu X. Functional divergence in the caspase gene family and altered functional constraints: statistical analysis and prediction. *Genetics* 2001; **158**(3)**:** 1311-1320.

34. Ekaratanawong S, Anzai N, Jutabha P, Miyazaki H, Noshiro R, Takeda M*, et al*. Human organic anion transporter 4 is a renal apical organic anion/dicarboxylate exchanger in the proximal tubules. *J Pharmacol Sci* 2004; **94**(3)**:** 297-304.

35. Ugele B, St-Pierre MV, Pihusch M, Bahn A, Hantschmann P. Characterization and identification of steroid sulfate transporters of human placenta. *Am J Physiol Endocrinol Metab* 2003; **284**(2)**:** E390-398.

36. Taeusch HW, Ballard RA, Gleason CA, Avery ME. *Avery's diseases of the newborn*, 8th edn. W.B. Saunders: Philadelphia, Pa., 2005, xxi, 1633 p.pp.

37. Paitz RT, Bowden RM. Biological activity of oestradiol sulphate in an oviparous amniote: implications for maternal steroid effects. *Proc Biol Sci* 2010.

38. Tanaka M, Itoh K, Matsushita K, Wakita N, Adachi M, Nonoguchi H*, et al*. Two male siblings with hereditary renal hypouricemia and exercise-induced ARF. *Am J Kidney Dis* 2003; **42**(6)**:** 1287-1292.

39. Weisskopf MG, O'Reilly E, Chen H, Schwarzschild MA, Ascherio A. Plasma urate and risk of Parkinson's disease. *Am J Epidemiol* 2007; **166**(5)**:** 561-567.

40. Preitner F, Bonny O, Laverriere A, Rotman S, Firsov D, Da Costa A*, et al*. Glut9 is a major regulator of urate homeostasis and its genetic inactivation induces hyperuricosuria and urate nephropathy. *Proc Natl Acad Sci U S A* 2009; **106**(36)**:** 15501-15506.

41. Bannasch D, Safra N, Young A, Karmi N, Schaible RS, Ling GV. Mutations in the SLC2A9 gene cause hyperuricosuria and hyperuricemia in the dog. *PLoS Genet* 2008; **4**(11)**:** e1000246.

42. Maxwell SR, Thomason H, Sandler D, Leguen C, Baxter MA, Thorpe GH*, et al*. Antioxidant status in patients with uncomplicated insulin-dependent and non-insulin-dependent diabetes mellitus. *Eur J Clin Invest* 1997; **27**(6)**:** 484-490.

43. Fiermonte G, Paradies E, Todisco S, Marobbio CM, Palmieri F. A novel member of solute carrier family 25 (SLC25A42) is a transporter of coenzyme A and adenosine 3',5'-diphosphate in human mitochondria. *J Biol Chem* 2009; **284**(27)**:** 18152-18159.

44. Feng B, Dresser MJ, Shu Y, Johns SJ, Giacomini KM. Arginine 454 and lysine 370 are essential for the anion specificity of the organic anion transporter, rOAT3. *Biochemistry* 2001; **40**(18)**:** 5511-5520.

45. Bahn A, Hagos Y, Reuter S, Balen D, Brzica H, Krick W*, et al*. Identification of a new urate and high affinity nicotinate transporter, hOAT10 (SLC22A13). *J Biol Chem* 2008; **283**(24)**:** 16332-16341.

46. Cropp CD, Komori T, Shima JE, Urban TJ, Yee SW, More SS*, et al*. Organic anion transporter 2 (SLC22A7) is a facilitative transporter of cGMP. *Mol Pharmacol* 2008; **73**(4)**:** 1151-1158.

47. Dudek RW, Fix JD. *Embryology*, 2nd ed edn. Williams & Wilkins: Baltimore, 1998, xiii, 293 p.pp.

48. Uldry M, Thorens B. The SLC2 family of facilitated hexose and polyol transporters. *Pflugers Arch* 2004; **447**(5)**:** 480-489.

49. Wu X, Huang W, Prasad PD, Seth P, Rajan DP, Leibach FH*, et al*. Functional characteristics and tissue distribution pattern of organic cation transporter 2 (OCTN2), an organic cation/carnitine transporter. *J Pharmacol Exp Ther* 1999; **290**(3)**:** 1482-1492.

50. Sweet DH, Bush KT, Nigam SK. The organic anion transporter family: from physiology to ontogeny and the clinic. *Am J Physiol Renal Physiol* 2001; **281**(2)**:** F197-205.

Chapter 6

Generation and Validation of a Transgenic Mouse Model Expressing Human Organic Cation Transporter 1 in the Liver

Introduction

The development of effective pharmaceuticals is dependent upon an understanding of the pharmacokinetic properties of candidate small molecules in order to select lead compounds with optimal absorption, distribution and elimination properties. While studies to characterize these properties in human subjects are ultimately requisite for all new drugs, experiments using animal models provide invaluable preliminary results needed to gauge the pharmacokinetic properties of these drugs as well as allowing for more complex pharmacological experiments to be performed that would be impractical or unethical in human subjects.

With the advent of gene targeting and transgenic strategies, better animal models have been created to simulate the impact of important pharmacologically relevant genes on drug disposition and pharmacokinetics. Currently these models are largely relegated to the loss of function variety wherein an orthologous mouse gene has been knocked out, allowing for a comparative investigation between mice lacking a particular gene and its wild-type counterpart. While knockout models do provide immensely valuable information, by design they are not inherently useful when studying genes that may exhibit different characteristics between mammalian species, especially between mouse

and human. In particular, distinct differences in the molecular and physiological properties of orthologous genes related to drug metabolism and transport have been noted between rodents and humans[1-3]. Thus the creation of humanized mouse models for drug metabolizing enzymes and transporters is of particular importance when considering the relevancy of pre-clinical data in mouse models that are intended to inform the potential effects, beneficial and deleterious, of pharmaceuticals in human subjects. In the quest to produce a model more reflective of human pharmacokinetic properties, humanized mouse models are becoming the ideal model for pre-clinical investigations of the efficacy and toxicity of new drugs. A number of humanized mouse models have been developed to better characterize the impact of a variety of pharmacologically relevant genes including a multitude of cytochrome P450 enzymes (CYPs) such as CYP3A4[4] and CYP2D6[5] and xenobiotic receptors including AHR[6], PXR[7], and CAR[8] (both reviewed by Gonzalez, et al.[9]). However, humanized mouse models designed to study the impact of human versions of membrane transporters in pharmacological and pharmacokinetic studies are lacking in breadth and availability with models currently for only the folate carrier *SLC19A1*[10], *ABCA1*[11], OATP1B1[12], ENT1[13], OCTN2[14], and the vitamin C transporter *SLC23A2*[15]. Thus, there is a clear need for additional such models considering the emerging importance of many xenobiotic transporters in the absorption and elimination of a multitude of drugs and their role in a growing number of physiologic processes.

To provide a better model for the function and impact of the xenobiotic transporter organic cation transporter 1 (OCT1; *SLC22A1*), a humanized mouse

model was generated that expresses OCT1 at a high level in the liver, its primary site of expression in humans. OCT1 is a noteworthy transporter of xenobiotics due to its high expression in the liver, a major site of drug metabolism and a target tissue in its own right, and the numerous documented interactions between it and clinically relevant cationic small molecule drugs, including chemotherapeutic and anti-diabetic agents. In particular, OCT1 has been found to be a significant contributor to the pharmacokinetics of the biguanide anti-diabetic drug metformin[16, 17] and impacts its efficacy in the treatment of diabetes[18, 19]. Similarly, OCT1 has been implicated in the action of the platinum-based chemotherepeutics oxaliplatin and picoplatin[20, 21] and the neurotoxic effects of MPTP exposure[22]. Recent unpublished studies (Chen, L; personal communication) have also revealed further functional differences between human OCT1 and mouse Oct1 in the transport of endogenous neurotransmitters, suggesting that a humanized mouse model for OCT1 may in fact prove beneficial in the understanding of the pharmacological and physiological role of OCT1 in the context of human beings. Further, mouse Oct1 has a distinct pattern of expression in comparison to the human ortholog; expression levels in the mouse liver are similar to that found in human liver while substantial expression is also found in the mouse kidney whereas negligible expression is observed in the human kidney. Thus a rodent model that more closely reflects the expression patterns of OCT1 in humans would be far more useful in probing pharmacokinetic and pharmacodynamic effects influenced by OCT1 in humans. Ultimately, the use of a mouse model for OCT1 with functional and expression

features more comparable to those encountered in humans could greatly benefit the understanding of the pharmacokinetics of drugs such as metformin when studies require the flexibility of animal models. Likewise, a humanized mouse model for OCT1 could provide an invaluable platform to effectively translate physiological studies of OCT1 from rodent models to humans.

Materials and Methods

Creation of the Transgenic Mouse Line

The construct controlling the desired expression profile of the hOCT1 transgene was based on the vector initially designed and utilized by Pinkert, et al.[23], which employed the then recently identified promoter elements controlling the specific and abundant expression of albumin normally found in the mouse liver. These elements, specifically a single enhancer region and the proximal promoter, were identified functionally via restriction enzyme-mediated promoter mapping. To create the pAlb-hOCT1 transgene construct (human OCT1 expression controlled by the mouse albumin promoter and enhancer), a 2.2kb enhancer element located approximately 10kb upstream of the transcription start site and the 400bp mouse albumin proximal promoter were inserted upstream of a human OCT1 cDNA in the expression vector pcDNA3.1(+)-hygro (Invitrogen, Carlsbad, CA, USA). The full-length human OCT1 cDNA used for this construct was cloned and functionally characterized previously[24]. The enhancer and promoter sequences were PCR-amplified from a BAC vector containing the entire mouse

Table 6.1: Primer sequences for transgene construction

Primer Name	Primer Sequence	Product Size
Mouse albumin enhancer	F: 5'-gatcggtaccATACCCGAAGATGATCTGTTCCTTTCTT-3' R: 5'-gatcggatccTGTGACAGTCTTACGGCATGAGAAG-3'	2200bp
Mouse albumin promoter	F: 5'-cgatatttaaatTTGGGATGAACAACCTATGCAATTC-3' R: 5'-cgatgcggccgcGGGTTGATAGGAAAGGTGATCTGTG-3'	403bp
SacI mutagenesis	F: 5'-GAAAGAACCAGCTGGAGCTCTAGGGGGTATC-3' R: 5'-CTTTCTTGGTCGACCTCGAGATCCCCCATAG-3'	N/A

Lowercase bases indicate introduced restriction enzyme sites used for cloning purposes.

Table 6.2: Primer sequences for transgene detection and genotyping

Primer Name	Primer Sequence	Product Size
Transgenic hOCT1	F: 5'-CTCCAGCTTGGGATCCACTAGTCC-3' R: 5'-CCGAGCCAACAAATTCTGTGATTAG-3'	1711bp
Endogenous mOCT1	F: 5'-CGCTTGAGTGGTTCTCTTCTGAGAC-3' R: 5'-ACAGGAGAACGACAGCCATCTTGTA-3'	1135bp
Transgene Southern Probe	F: 5'-TGCTCAAATGGGAGACAAAGAG-3' R: 5'-TGGTTCCAGTCCACTTCATAGC-3'	607bp

Albumin coding and 5' intergenic/promoter sequence (Clone # RP23-301A23; CHORI, Oakland, CA, USA) using primers detailed in Table 6.1. A SacI restriction enzyme site was introduced downstream of the bovine growth hormone (bGH) polyadenylation sequence in the pcDNA3.1(+)-hygro vector in order to effectively excise the transgene while including the polyadenylation sequence. This was accomplished using site-directed mutagenesis with the primers listed in Table 6.1. The introduction of the mutation allowed for the efficient excision of the transgene using a single enzyme (SacI). The entire transgene vector sequence was approximately 9.75kb in length and was confirmed by direct sequencing. A schematic diagram of the final pAlb-hOCT1 vector is presented in Figure 6.1.

The transgene fragment was excised from the vector by overnight digestion using the restriction enzymes SacI, KpnI, and PmlI at 37°C which produced a transgene fragment approximately 4.5kb in length. The use of these enzymes liberated the transgene from the remaining vector backbone and further reduced the size of the vector backbone fragments to effectively separate them from the transgene during the subsequent purification steps. The 4.5kb digestion product was gel purified using a QIAquick® Gel Extraction Kit (Qiagen, Valencia, CA, USA) with endotoxin-free water. The concentration of the transgene fragment was determined spectrophotometrically and its identity verified using an analytical restriction enzyme digest prior to use in the generation of transgenic

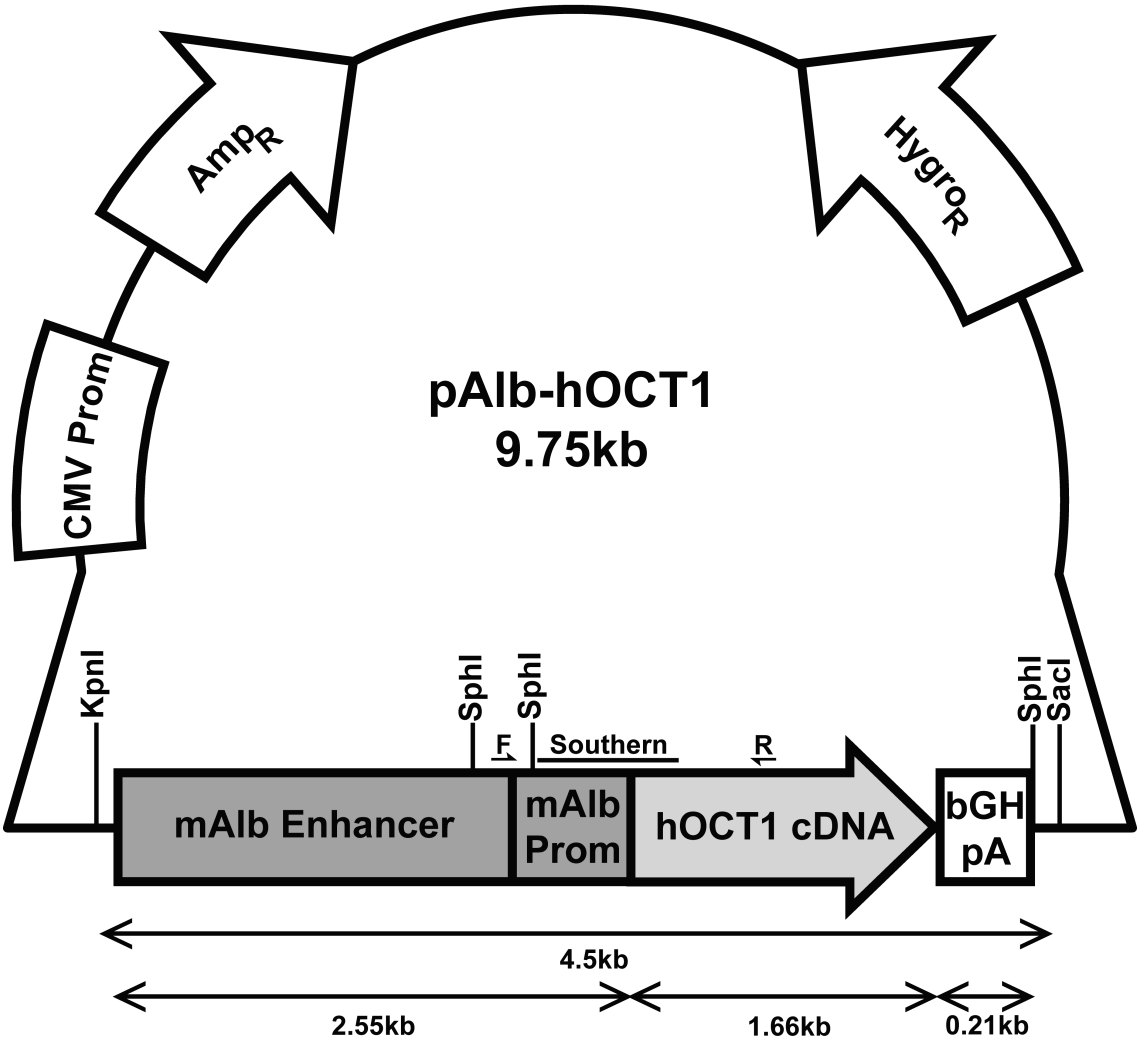

Figure 6.1: Schematic representation of the pAlb-hOCT1 transgene construct. mAlb Enhancer and mAlb Prom represent the mouse albumin enhancer and proximal promoter regions respectively. KpnI, SphI, and SacI indicate the relative positions of the respective restriction enzyme sites. F indicates the forward primer location while R indicates the reverse primer location for the genotyping PCR. "Southern" indicates the approximate location and size of the probe used for Southern blot analyses to detect the transgene. bGH pA represents the bovine growth hormone polyadenylation sequence, CMV Prom represents a CMV constitutive promoter element, Amp_R indicates an ampicillin resistance cassette, and $Hygro_R$ indicates a hygromycin resistance cassette, all of which were derived from the pcDNA 3.1(+)-hygro vector (Invitrogen).

animals. The 4.5kb gel-purified transgene fragment was used in pronuclear microinjection procedures to introduce human OCT1 cDNA construct into fertilized oocytes from FVB/N mice which were subsequently implanted into pseudopregnant female mice. These procedures were performed by the UCSF Comprehensive Cancer Center Transgenic Core Facility. All work performed with mice was approved by the UCSF Institutional Animal Care and Use Committee and followed standard procedures governing the handling and care of vertebrate animals.

Chimeric transgenic founder animals were screened using Southern blotting with genomic DNA isolated from tail segments with a Wizard® Genomic DNA purification kit (Promega, Madison, WI, USA) following the manufacturer's default protocol. Briefly, 10 µg of genomic DNA was digested with an excess of NotI overnight at 37°C and electrophoretically separated on a 0.7% agarose gel running at 40V in 1X TAE buffer. Copy number standards were treated similarly and used to gauge the approximate number of transgene copies in the founder animals. The DNA was transferred to an Immobilon-Ny+® nylon membrane (Millipore, Billerica, MA, USA) using standard Southern blotting and transfer procedures. The resulting membrane was probed using a biotinylated DNA probe specific to the transgene sequence. The probe was labeled using PCR with primers detailed in Table 6.2. The final reaction conditions to synthesize the probe were as follows: 1X iProof High Fidelity PCR buffer (Bio-Rad, Hercules, CA, USA), 2.75 mM $MgCl_2$, 200 µM dNTP mixture (200 µM of dATP, dGTP, and dTTP, and 50 µM of dCTP plus 150 µM of biotin-11-dCTP [Perkin Elmer Life

Sciences, Waltham, MA, USA]), 250 nM of each primer, 0.05 U/μL iProof DNA polymerase (Bio-Rad), and approximately 50 ng of pAlb-OCT1 vector as template. The reactions were run using an Applied Biosystems 9700 thermal cycler (Foster City, CA, USA) utilizing the following cycling conditions: 98°C for 30 seconds, 98°C for 10 seconds, 58°C for 20 seconds, and 72°C for 1 minute for a total of 40 cycles, followed by a 72°C hold for 10 minutes. The location of the Southern probe in relation to the transgene construct is shown in Figure 6.1. The membrane was UV cross-linked with a Stratalinker 1800 (Stratagene, Santa Clara, CA, USA) using the default settings and was pre-hybridized at 42°C for 1 hour in formamide hybridization buffer (KPL, Gaithersburg, MD, USA) supplemented with 200 ng/mL denatured, fragmented salmon sperm DNA. Following pre-hybridization, the membrane was hybridized with 50 ng of heat denatured probe and 200 ng/mL denatured, fragmented salmon sperm DNA in formamide hybridization buffer overnight at 45°C. The membrane was subsequently washed and detection of the probe achieved using an alkaline phosphatase-linked chemiluminescent detection system (KPL) following the manufacturer's default procedures. High stringency washes were performed at approximately 64°C with 0.1X SSPE/0.1% SDS buffer. Development of the Southern blot followed the manufacturer's standard protocol. Subsequent Southern blotting of confirmed transgenic animals followed the same procedures with the exception that all DNA samples were digested with SphI overnight at 37°C. Upon detection of positive founder mice, they were crossed to a mouse OCT1 knockout line in the FVB/N background previously developed by Shu, et

al.[19]. These lines were genotyped using primers for the Neo cassette as described elsewhere[19] and were propagated as mouse OCT1-null lines in addition to being positive for human OCT1. Mice were backcrossed at least two generations and the stability of transgene inheritance was established using these Southern blotting procedures described previously prior to any further characterization of the lines. However, further backcrosses are necessary in order to adequately characterize the mouse model and ensure that the transgene is stable and that it elicits the desired phenotype.

Genotyping of Transgenic Mice

Genomic DNA was extracted from tail sections from each mouse using the Wizard® Genomic DNA purification kit (Promega) following the manufacturer's standard protocol. DNA concentrations were determined spectrophotometrically and diluted in Tris-EDTA buffer as necessary for PCR. PCR genotyping for the transgene and the endogenous mouse *Slc22a1* gene was performed in duplex reactions in a 50 µL volume using a *Taq* PCR Core kit (Qiagen) under the following conditions: 1X *Taq* PCR buffer, 3.5 mM $MgCl_2$, 0.6 mg/mL bovine serum albumin (BSA), 200 µM dNTP mixture (consisting of equal concentrations of dATP, dCTP, dGTP, and dTTP), 150 nM of each primer, 0.1 U/µL *Taq* polymerase, and approximately 100-500 ng of genomic DNA as a template. The reactions were run using an Applied Biosystems 9700 thermal cycler utilizing the following cycling conditions: 94°C for 3 minutes, 94°C for 30 seconds, 68°C for 20 seconds, and 72°C for 1 minute for a total of 40 cycles, followed by a 72°C

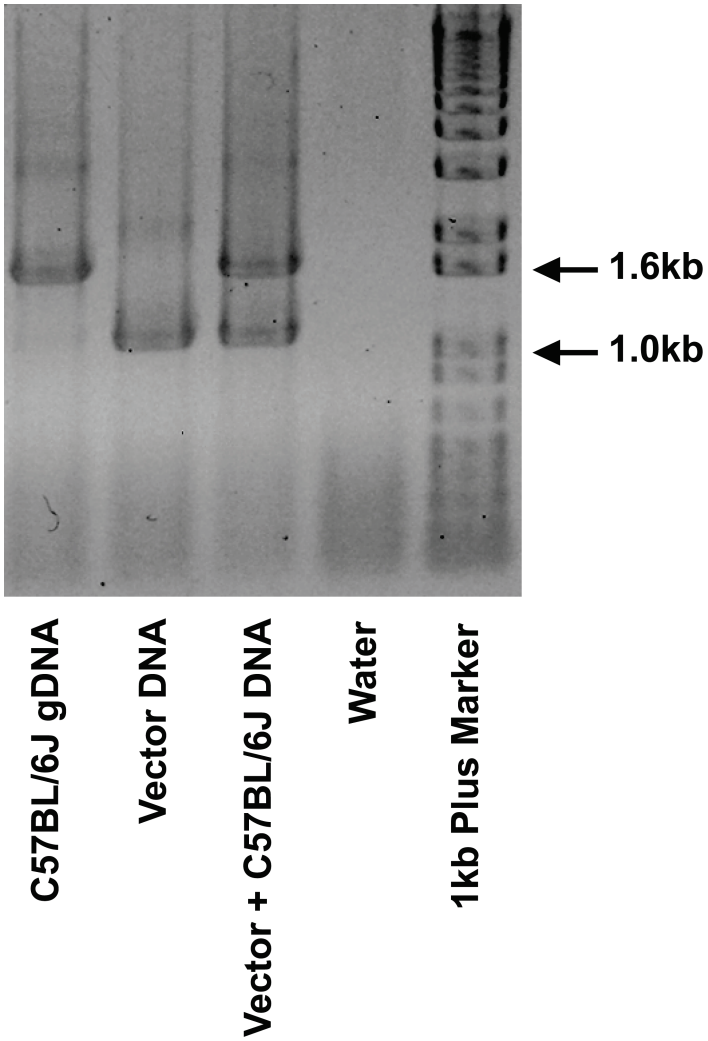

Figure 6.2: PCR controls for genotyping hOCT1 transgenic mice. Bands were amplified from the endogenous mouse *Slc22a1* gene (approximately 1.7kb) and the human OCT1 transgene (approximately 1.1kb) and were resolved on a 1.0% agarose gel and stained with ethidium bromide. Reactions used either 1 ρg of pAlb-OCT1 vector, 500 ng of genomic DNA from C57BL/6J mice, or both as template with duplex primer mixes as described in the Materials and Methods section.

hold for 10 minutes. The forward and reverse primers used for transgene genotyping are shown in Figure 6.1 as “F” and “R” respectively and the details of the primers are shown in Table 6.2. The resulting amplicons were visualized on a 1% agarose gel stained with ethidium bromide. Figure 6.2 shows the expected

PCR genotyping bands. Genotyping for the presence of the *Neo* cassette (indicative of the presence of the null allele in the OCT1 knockout mouse line) was performed using primers and methods referenced previously.

RNA Isolation and Quantitative RT-PCR

Tissue samples from mouse brain, colon, heart, kidney, liver, lung, skeletal muscle, small intestine, spleen, and gonads (testis and ovary) were collected from 8-10 week old animals. Tissues were immediately placed in cold TRIzol reagent (Invitrogen) and purified using the standard RNA purification protocol. RNA concentration and quality was assessed using the presence of intact 28S and 18S ribosomal RNA bands and the ratio of absorbance at 260 nm and 280 nm. Total RNA from human brain, colon, kidney, liver, small intestine, and testis was purchased from Clontech (Mountain View, CA, USA). cDNA was synthesized from 1 µg of RNA from each sample using a SuperScript III® reverse transcriptase kit (Invitrogen) with oligo-dT primers following the manufacturer's default procedure. The samples were diluted 1:5 in sterile water and used for quantitative reverse-transcriptase PCR (qRT-PCR). qRT-PCR utilized Taqman® primers and probes (Applied Biosystems, Foster City, CA, USA) specific to human *SLC22A1*; qRT-PCR was also performed using a primer and probe set specific to mouse *Slc22a1* to verify the genotyping results. Measurements of mRNA levels were performed using 10 µL reaction volumes in a 384-well plate format with 2 µL of diluted cDNA and 0.5 µL of the gene-specific probe and primer reagent per well. A standard curve using the pAlb-hOCT1 vector was developed and all absolute levels of human *SLC22A1* mRNA were normalized to

the resulting curve. The number of copies detected in each sample were normalized to corresponding mouse *Gapdh* levels and were run in triplicate wells on each plate. The results are expressed as the absolute number of copies of human *SLC22A1* mRNA per microgram of total RNA.

Results

Generation of Humanized Transgenic OCT1 Mice

Pronuclear microinjection procedures produced 55 potential transgenic founder animals expected to express human OCT1 under the control of the mouse albumin promoter. Initial Southern blot screening, as shown in Figure 6.3, identified nine mice potentially expressing the transgene which was verified using PCR genotyping; the genotype of two of the founder mice was indeterminant resulting in approximately 17% of the mice presenting with positive transgene integration in the genome. No transgene signal was detected in the Southern blot in DNA from mice with negative PCR results (Figure 6.3) or in wild-type mouse DNA in PCR genotyping (data not shown). The founder mice displayed noticeable variability in the transgene copy number ranging from less than 2 to possibly 50 or more copies in a hemizygous genome, although some of this variability may be due to multiple transgene integration sites in the genome. All of the founder animals appeared normal with no obvious differences compared to wild-type animals in behavior, weight, or overall appearance. However, one of the animals died prematurely at approximately 7 weeks of age, three

demonstrated a lack of fertility and were unsuccessfully propagated after repeated attempts at crossing with animals from the Oct1 knockout background,

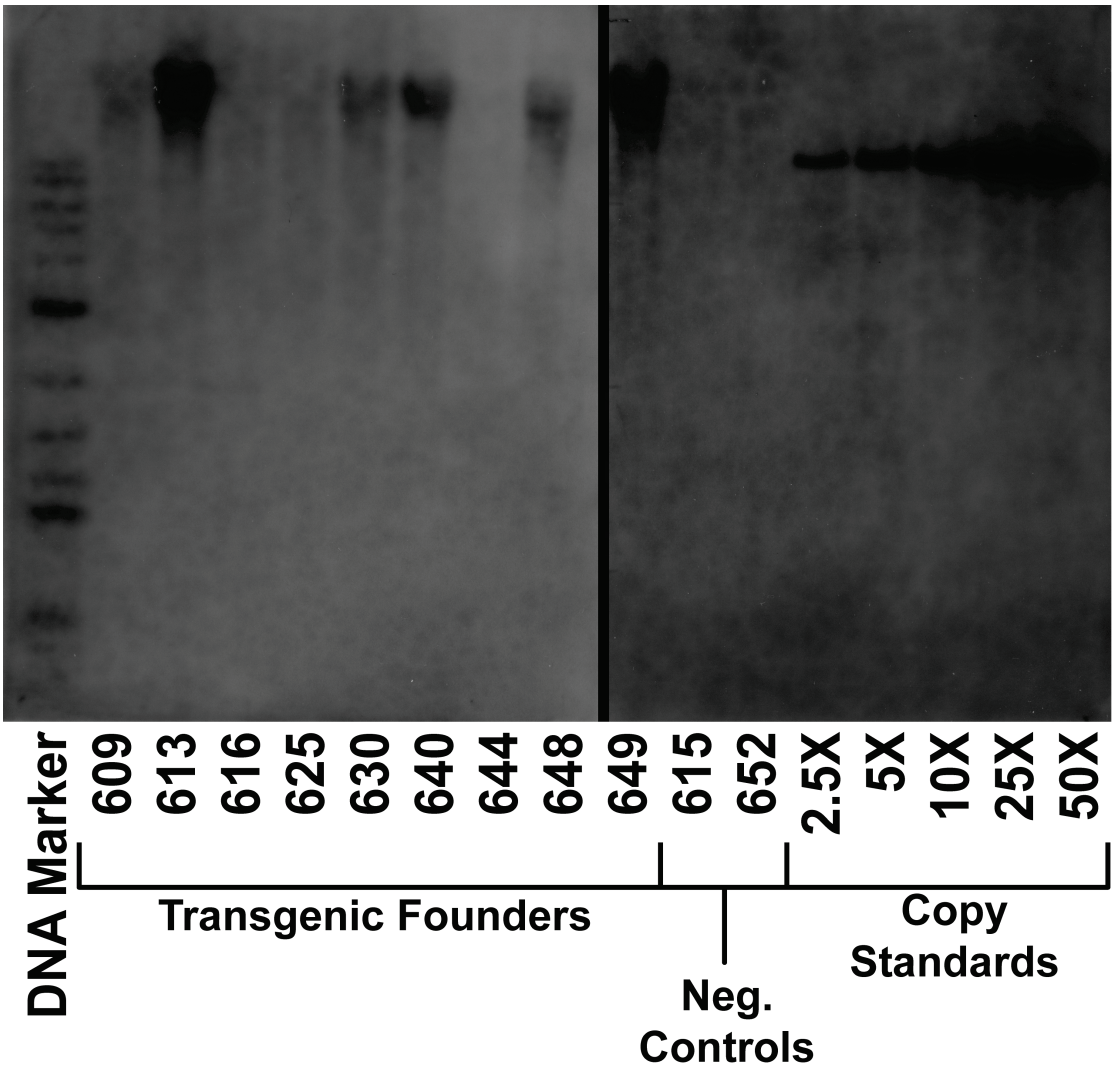

Figure 6.3: Screening of OCT1 transgenic founder mice using Southern blotting. A membrane with 10 µg of genomic DNA from each founder animal was digested with NotI and probed for the OCT1 transgene. Numbers indicate the ID of the transgenic founder animal. Copy standards were included to estimate the number of copies inserted into the genome of each animal.

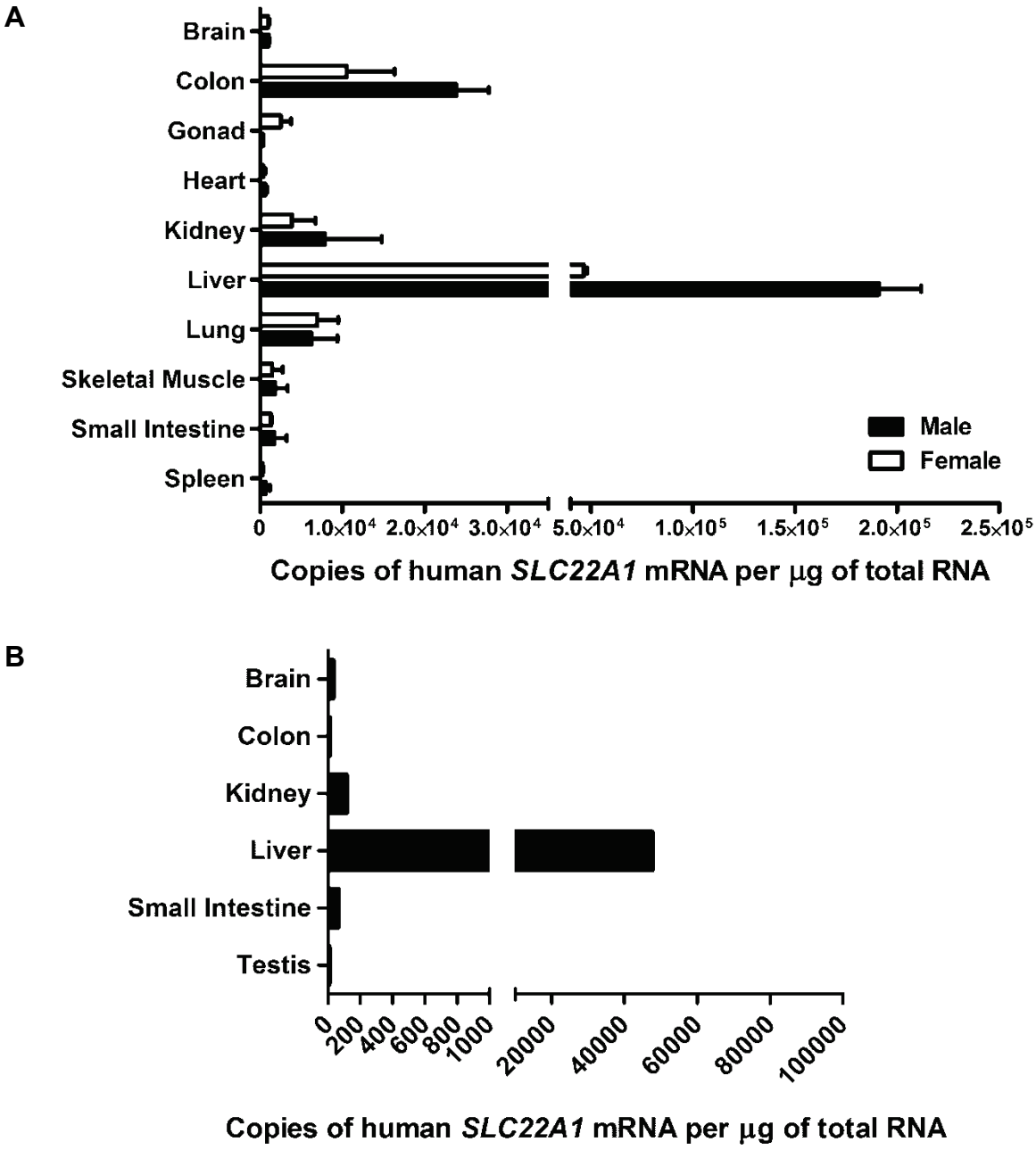

Figure 6.4: Expression of the human OCT1 transgene mRNA in male and female mouse tissues and *SLC22A1* in reference human tissues. A) mRNA expression of levels of human *SLC22A1* mRNA in mouse tissues from male and female F3 and F4 generation mice. Each bar is representative of the mean ± SD from two individual mice of each sex. The "Gonad" tissue is male or female specific and refers to either the testis or ovary respectively. B) mRNA expression of levels of human *SLC22A1* mRNA in select human tissues. Each bar represents the mean from a single sample. qRT-PCR was performed using a Taqman® probe specific to human *SLC22A1* and normalized to *GAPDH* expression levels. A standard curve using intact pAlb-hOCT1 was used to determine copy number.

and an additional animal demonstrated a lack of germ-line transmission of the transgene with no subsequent progeny testing positive for the transgene. Examination of transgene expression in tissues collected from F2 generation mice from each of the four remaining transgenic lines demonstrated a lack of elevated and/or specific liver expression of the transgene in all but one line (#609; data not shown). Out of 53 initial founder animals successfully genotyped, only this single line produced the requisite high expression of OCT1 in the liver and comparatively low expression in other tissues for a final rate of success of transgenic development at less than 2%. However, this line appeared to possess the necessary phenotype and was further propagated and examined as the desired humanized OCT1 mouse model. This line was subsequently crossed with the Oct1 knockout line in the FVB/N background created previously[19], to produce and propagate a fully humanized mouse model for human OCT1 lacking any endogenous expression of the mouse ortholog for OCT1.

Characterization of the Humanized Transgenic OCT1 Mouse Model

Once identified as a viable humanized model for OCT1, the line was examined for any gross morphological or anatomical phenotypes; no readily apparent abnormalities were observed and the mice appeared morphologically normal with no change in fecundity, behavior, or life span compared to other wild-type FVB/N mice. Likewise, no obvious differences were identified in internal organ size, condition, or orientation. At this early stage, the potential physiological or biochemical differences between this line and wild-type FVB/N mice were not

examined although determination of these differences would be both informative and necessary in the complete characterization of this mouse model.

Upon verification of elevated expression of the OCT1 transgene in the liver of the humanized mouse line, transgene expression was evaluated in ten tissues from male and female mice from the F3 and F4 generation. As shown in Figure 6.4A, expression of the transgene was remarkably high in the livers from both male and female mice with expression levels between 50,000 and 200,000 copies per microgram of total RNA. This is in comparison to the normal expression of OCT1 in the human liver which is approximately 40,000 to 50,000 copies per microgram of total RNA as depicted in Figure 6.4B. Transgene expression in other tissues was also elevated, specifically in the colon, with slightly lower levels in the kidney and lung. Thus while the humanized OCT1 transgenic mouse line expresses human OCT1 between 1.2 and 4-fold higher than in normal human livers, it also spuriously expresses the transgene in other tissues that do not normally express OCT1. In these other tissues the expression levels of OCT1 are between 50-fold higher (kidney) and several thousand-fold higher (colon) than the normal expression levels found in human tissues but are still substantially lower than the expression levels in both mouse and human liver.

Comparison of transgene expression in the livers of male and female mice identified potential sex-specific expression patterns with OCT1 expression in the male liver approximately double that observed in the female liver (Figure 6.4A). Due to the random nature of transgene integration, however, the zygosity of this line remains indeterminate. Similarly, the chromosomal location of the transgene

also needs to be determined as does the determination of possible multiple integration sites of the transgene. The requisite experiments to make these determinations were undertaken but currently have not been completed. Thus, while all of the mice examined in this study were positive for the transgene as determined through PCR genotyping, it was unknown whether they were hemizygous or homozygous for the transgene due to the unidentified chromosomal location. While the expression of the OCT1 transgene in three of the four highest expressing tissues was 50% or less in females compared to males, this may have been the result of a difference in zygosity rather than a true effect of sex on expression of the transgene. Likewise, the unknown zygosity of these mice suggests that the average expression levels of the transgene achieved in Figure 6.4A may actually increase once homozygosity of the transgene is achieved.

Discussion

Much of the knowledge of the pharmacokinetics and pharmacological effectiveness of nearly all drugs currently on the market was initially produced using experiments in animals with the intent to simulate the human genetic and physiological circumstances in which these drugs would eventually be used. Various rodent species are the most common animal models in pre-clinical drug evaluation, and while they are not a perfect substitute for a living human subject, they do allow for straightforward genetic manipulation which enables a greater

degree of freedom in the experimental characterization of the efficacy, side effects, and pharmacokinetic properties of drugs. In particular, knockout models for specific mouse orthologs of human disease or pharmacologically relevant genes have provided immense amounts of information about the impact of these genes on the efficacy and toxicity of specific drugs and other xenobiotics. As an alternative yet complementary approach to knockout models, humanized transgenic mouse models provide the ability to assess the function of the human form of a gene in an intact, easy to manipulate physiological system.

The recent creation of knockout models for OCT1[19, 25] have produced a greater understanding of its impact on the accumulation of organic cations in the liver[25] and the efficacy of drugs that modulate hepatic function such as metformin[19, 26]. These studies have validated the importance of OCT1 in liver-mediated drug disposition but have not allowed for the ability to assess the role of human OCT1 in these same controlled *in vivo* experimental conditions. Comparison of the orthologous sequences of OCT1 in rodents and humans indicates that while highly conserved overall (approximately 78% amino acid identity between orthologous mouse and human sequences), there are distinct functional attributes present in each isoform. In particular, and detailed in Table 6.3, a number of substrates and inhibitors of rodent and human OCT1 interact with dramatically different affinities. Specifically, important drugs such as metformin and endogenous small molecules such as choline and corticosterone all show dramatically different affinities between species with the rodent orthologs possessing a generally greater affinity for these cations with up to a 400-fold

difference in affinity in the case of choline. In addition, Dresser, et al. demonstrated that human OCT1 does not interact as strongly with n-tetraalkylammonium (nTAA) species compared to the rodent orthologs whereas human OCT1 had a significantly higher turnover rate of larger nTAA species compared to rodent OCT1 orthologs[1]. Thus while the overlap of substrates is significant, there exists substantial functional differences between rodent and human OCT1 which not only preclude direct comparisons in many cases, but also create difficulties in the interpretation of pre-clinical data from rodent species using OCT1 substrates and inhibitors. The creation of a humanized OCT1 mouse model will allow for further investigation by potentially eliminating cryptic differences in xenobiotic interaction between mouse and human OCT1 and in any endogenous roles that may differ between these two species.

Table 6.3: Disparate transport/inhibition constants between hOCT1 and rodent Oct1 orthologs

Compound	Human OCT1	Rodent Oct1	Ref
TMA	12,400	2040[a]	1
n-Methylnicotinamide	7,700	384[b]	27, 28
Metformin	**1,470**	**377**[b]	17, 29
Corticosterone	7	160[b]	27, 28
Choline	16,700	**42**[a]	30, 31
Vecuronium	120	4.3[b]	28, 32

Values are in μM and represent either K_i or K_m determinations; bold indicates K_m values. a: mouse Oct1 b: rat Oct1.

In spite of the use of a previously published and well-documented set of promoter elements designed to drive both high expression levels and liver-specific expression patterns, the pAlb-hOCT1 construct achieved only one of these features when integrated into the mouse genome. At the onset, only nine of the 55 initial founder animals were positive for the transgene and after characterization of these nine humanized OCT1 mouse lines by qRT-PCR, only a single line displayed the requisite high transgene expression in the liver. However, the expression of the transgene in this line was abundant with levels similar and even surpassing that found in the normal human liver. This expression level, albeit only observed in mRNA at this stage, should provide more than adequate amounts of OCT1 in hepatocytes and be sufficient for inquiries into OCT1 function. Contrary to the desired high hepatic expression of the OCT1 transgene, significant expression of the transgene was observed in a number of other tissues. While not expected or especially advantageous for the model, this issue has been encountered previously when using the promoter elements in this construct. Specifically, the initial use of these promoter elements resulted in a number of lines with some expression of the transgene in the kidney[23]. Similarly, later mouse models derived using a similar vector construct produced founder animals with an appreciable expression of the transgene in the testis in addition to the liver[33]. However, this issue appears to have been overcome previously by screening large numbers of founder animals and identifying lines with only expression in the liver. In spite of the large number of initial OCT1 transgenic founder animals, only a single line demonstrated the

requisite high expression of human OCT1 in the liver, in part due to large number of founder lines displaying infertility or a lack of germ line transmission of the transgene. While the presence of OCT1 in other mouse tissues does not necessarily make the model any less useful in the study of liver-based phenotypes and functions, it does introduce an additional factor when interpreting the data derived from experiments using this model. However, the impact of the spurious transgenic OCT1 expression on these experiments remains to be determined; mice normally express Oct1 in the kidney which, in combination with the humanized OCT1 mouse model, may allow for better cross-species comparisons of OCT1 function.

The exact cause of transgene expression outside of the liver is unclear; the random nature of transgene integration into the genome could allow for the presence of the transgene adjacent to promoter elements driving ubiquitous expression which may modulate the high level of expression driven by the albumin enhancer element. Alternatively, the mouse albumin promoter elements used in the pAlb-hOCT1 construct may not function optimally with the OCT1 cDNA and bGH polyadenylation sequence when lacking intronic or insulator sequences. A number of studies have shown that incorporation of an intron or the use of insulator sequences increases transgene expression and can aid in the specificity of transgene expression[34, 35] but these were not routinely used in many of the previous studies attempting to drive specific expression in the liver of mice. Likewise, in the initial characterization of these elements, 15 positive transgenic founder mice were screened in order to identify only a few mice

possessing the desired phenotype[23] suggesting that it is not the most efficient vector design when attempting to achieve highly abundant liver-specific expression. Many humanized transgenic mouse models attempt to use a BAC or YAC vector to introduce the complete promoter and exon-intron structure of a gene to avoid issues with fragmented and altered promoter elements. However, this strategy is also not without issues as illustrated by the inexact tissue expression pattern observed in the CYP3A4 humanized mouse model which lacked expression in the liver, a tissue it is normally expressed in at a high level[4]. Use of a BAC in the creation of the humanized OCT1 mouse model was impractical due to the lack of BAC vectors containing both the entire coding region of *SLC22A1* and sufficient promoter sequence while also excluding additional genes or gene fragments (including those of the homologous genes *SLC22A2* and *SLC22A3*) which may inadvertently introduce a phenotype not related to the gene of interest.

No prior studies have identified sex-specific expression patterns of albumin in humans or rodents, suggesting that the observed differences in expression of the transgene are due to 1) unrecognized factors related to the random nature of transgene insertion, such as adjacent sex-dependent transcriptional elements, 2) post-transcriptional regulation of the OCT1 mRNA that differs between male and female mice, or 3) unequal zygosity between the male and female mice used in the study. The non-specific transgene expression observed in the tissue panel could be explained by positional effects in the chromosomal site of integration, it could be argued that the most likely cause of the observed sex-dependent

differences in expression are due to indeterminate zygosity as it would be unlikely that expression would be reduced by approximately 50% in multiple distinct tissues subject to different regulatory mechanisms of gene transcription. This being the case, once full homozygosity of the transgene is achieved, expression of the transgene should remain high and in fact, is likely to rise on average although the sex-specific differences in expression may disappear or at least be attenuated.

While the use of humanized mouse models to study the effects of drugs and toxins is not the perfect solution for assuring relevancy in the conversion of *in vivo* animal data to human beings, their use does minimize the primary confounding factor: functional differences between human genes and their model animal orthologs. This humanized OCT1 mouse model does not entirely recapitulate the endogenous expression pattern of OCT1 in human tissues, but the expression attained in mouse tissues does provide for an excellent model of high expression in the liver with comparatively lower level of expression in other tissues. Similarly, in spite of the presence of a high level of human OCT1 in the mouse liver, limitations still exist in that it is only one gene out of thousands present in the mouse genome that can potentially impact pharmacokinetic and pharmacodynamic measurements and data produced using the humanized OCT1 mouse model are unlikely to be directly transferable or quantitative in nature when comparisons are made between mice and humans. However, in spite of these limitations, use of this model will undoubtedly aid in characterizing candidate and existing drugs that may interact with OCT1 and in the

characterization of the rapidly expanding innate physiological role of OCT1 using the humanized mouse model as a surrogate for human subjects.

References

1. Dresser MJ, Gray AT, Giacomini KM. Kinetic and selectivity differences between rodent, rabbit, and human organic cation transporters (OCT1). *J Pharmacol Exp Ther* 2000; **292**(3)**:** 1146-1152.

2. Martignoni M, Groothuis GM, de Kanter R. Species differences between mouse, rat, dog, monkey and human CYP-mediated drug metabolism, inhibition and induction. *Expert Opin Drug Metab Toxicol* 2006; **2**(6)**:** 875-894.

3. Stride BD, Grant CE, Loe DW, Hipfner DR, Cole SP, Deeley RG. Pharmacological characterization of the murine and human orthologs of multidrug-resistance protein in transfected human embryonic kidney cells. *Mol Pharmacol* 1997; **52**(3)**:** 344-353.

4. Granvil CP, Yu AM, Elizondo G, Akiyama TE, Cheung C, Feigenbaum L*, et al*. Expression of the human CYP3A4 gene in the small intestine of transgenic mice: in vitro metabolism and pharmacokinetics of midazolam. *Drug Metab Dispos* 2003; **31**(5)**:** 548-558.

5. Corchero J, Granvil CP, Akiyama TE, Hayhurst GP, Pimprale S, Feigenbaum L*, et al*. The CYP2D6 humanized mouse: effect of the human CYP2D6 transgene and HNF4alpha on the disposition of debrisoquine in the mouse. *Mol Pharmacol* 2001; **60**(6)**:** 1260-1267.

6. Moriguchi T, Motohashi H, Hosoya T, Nakajima O, Takahashi S, Ohsako S*, et al*. Distinct response to dioxin in an arylhydrocarbon receptor (AHR)-humanized mouse. *Proc Natl Acad Sci U S A* 2003; **100**(10)**:** 5652-5657.

7. Xie W, Barwick JL, Downes M, Blumberg B, Simon CM, Nelson MC*, et al*. Humanized xenobiotic response in mice expressing nuclear receptor SXR. *Nature* 2000; **406**(6794)**:** 435-439.

8. Zhang J, Huang W, Chua SS, Wei P, Moore DD. Modulation of acetaminophen-induced hepatotoxicity by the xenobiotic receptor CAR. *Science* 2002; **298**(5592)**:** 422-424.

9. Gonzalez FJ, Yu AM. Cytochrome P450 and xenobiotic receptor humanized mice. *Annu Rev Pharmacol Toxicol* 2006; **46:** 41-64.

10. Patterson D, Graham C, Cherian C, Matherly LH. A humanized mouse model for the reduced folate carrier. *Mol Genet Metab* 2008; **93**(2)**:** 95-103.

11. Coutinho JM, Singaraja RR, Kang M, Arenillas DJ, Bertram LN, Bissada N*, et al*. Complete functional rescue of the ABCA1-/- mouse by human BAC transgenesis. *J Lipid Res* 2005; **46**(6)**:** 1113-1123.

12. van de Steeg E, van der Kruijssen CM, Wagenaar E, Burggraaff JE, Mesman E, Kenworthy KE*, et al*. Methotrexate pharmacokinetics in transgenic mice with liver-specific expression of human organic anion-transporting polypeptide 1B1 (SLCO1B1). *Drug Metab Dispos* 2009; **37**(2)**:** 277-281.

13. Parkinson FE, Xiong W, Zamzow CR, Chestley T, Mizuno T, Duckworth ML. Transgenic expression of human equilibrative nucleoside transporter 1 in mouse neurons. *J Neurochem* 2009; **109**(2)**:** 562-572.

14. Zhu Y, Jong MC, Frazer KA, Gong E, Krauss RM, Cheng JF*, et al*. Genomic interval engineering of mice identifies a novel modulator of triglyceride production. *Proc Natl Acad Sci U S A* 2000; **97**(3)**:** 1137-1142.

15. Fan X, Reneker LW, Obrenovich ME, Strauch C, Cheng R, Jarvis SM*, et al*. Vitamin C mediates chemical aging of lens crystallins by the Maillard reaction in a humanized mouse model. *Proc Natl Acad Sci U S A* 2006; **103**(45)**:** 16912-16917.

16. Shu Y, Brown C, Castro RA, Shi RJ, Lin ET, Owen RP*, et al*. Effect of genetic variation in the organic cation transporter 1, OCT1, on metformin pharmacokinetics. *Clin Pharmacol Ther* 2008; **83**(2)**:** 273-280.

17. Wang DS, Jonker JW, Kato Y, Kusuhara H, Schinkel AH, Sugiyama Y. Involvement of organic cation transporter 1 in hepatic and intestinal distribution of metformin. *J Pharmacol Exp Ther* 2002; **302**(2)**:** 510-515.

18. Becker ML, Visser LE, van Schaik RH, Hofman A, Uitterlinden AG, Stricker BH. Genetic variation in the organic cation transporter 1 is associated with metformin response in patients with diabetes mellitus. *Pharmacogenomics J* 2009; **9**(4)**:** 242-247.

19. Shu Y, Sheardown SA, Brown C, Owen RP, Zhang S, Castro RA*, et al*. Effect of genetic variation in the organic cation transporter 1 (OCT1) on metformin action. *J Clin Invest* 2007; **117**(5)**:** 1422-1431.

20. More SS, Li S, Yee SW, Chen L, Xu Z, Jablons DM*, et al*. Organic cation transporters modulate the uptake and cytotoxicity of picoplatin, a third-generation platinum analogue. *Mol Cancer Ther* 2010; **9**(4)**:** 1058-1069.

21. Zhang S, Lovejoy KS, Shima JE, Lagpacan LL, Shu Y, Lapuk A*, et al*. Organic cation transporters are determinants of oxaliplatin cytotoxicity. *Cancer Res* 2006; **66**(17)**:** 8847-8857.

22. Giacomini KM, Huang SM, Tweedie DJ, Benet LZ, Brouwer KL, Chu X*, et al*. Membrane transporters in drug development. *Nat Rev Drug Discov* 2010; **9**(3)**:** 215-236.

23. Pinkert CA, Ornitz DM, Brinster RL, Palmiter RD. An albumin enhancer located 10 kb upstream functions along with its promoter to direct efficient, liver-specific expression in transgenic mice. *Genes Dev* 1987; **1**(3)**:** 268-276.

24. Shu Y, Leabman MK, Feng B, Mangravite LM, Huang CC, Stryke D*, et al*. Evolutionary conservation predicts function of variants of the human organic cation transporter, OCT1. *Proc Natl Acad Sci U S A* 2003; **100**(10)**:** 5902-5907.

25. Jonker JW, Wagenaar E, Mol CA, Buitelaar M, Koepsell H, Smit JW*, et al*. Reduced hepatic uptake and intestinal excretion of organic cations in mice with a targeted disruption of the organic cation transporter 1 (Oct1 [Slc22a1]) gene. *Mol Cell Biol* 2001; **21**(16)**:** 5471-5477.

26. Hundal RS, Krssak M, Dufour S, Laurent D, Lebon V, Chandramouli V*, et al*. Mechanism by which metformin reduces glucose production in type 2 diabetes. *Diabetes* 2000; **49**(12)**:** 2063-2069.

27. Koepsell H, Gorboulev V, Arndt P. Molecular pharmacology of organic cation transporters in kidney. *J Membr Biol* 1999; **167**(2)**:** 103-117.

28. Zhang L, Brett CM, Giacomini KM. Role of organic cation transporters in drug absorption and elimination. *Annu Rev Pharmacol Toxicol* 1998; **38:** 431-460.

29. Kimura N, Masuda S, Tanihara Y, Ueo H, Okuda M, Katsura T*, et al*. Metformin is a superior substrate for renal organic cation transporter OCT2 rather than hepatic OCT1. *Drug Metab Pharmacokinet* 2005; **20**(5)**:** 379-386.

30. Koepsell H, Lips K, Volk C. Polyspecific organic cation transporters: structure, function, physiological roles, and biopharmaceutical implications. *Pharm Res* 2007; **24**(7)**:** 1227-1251.

31. Sinclair CJ, Chi KD, Subramanian V, Ward KL, Green RM. Functional expression of a high affinity mammalian hepatic choline/organic cation transporter. *J Lipid Res* 2000; **41**(11)**:** 1841-1848.

32. Zhang L, Dresser MJ, Gray AT, Yost SC, Terashita S, Giacomini KM. Cloning and functional expression of a human liver organic cation transporter. *Mol Pharmacol* 1997; **51**(6)**:** 913-921.

33. Zhang Y, Huang SZ, Wang S, Zeng YT. Development of an HSV-tk transgenic mouse model for study of liver damage. *FEBS J* 2005; **272**(9)**:** 2207-2215.

34. Choi T, Huang M, Gorman C, Jaenisch R. A generic intron increases gene expression in transgenic mice. *Mol Cell Biol* 1991; **11**(6)**:** 3070-3074.

35. Potts W, Tucker D, Wood H, Martin C. Chicken beta-globin 5'HS4 insulators function to reduce variability in transgenic founder mice. *Biochem Biophys Res Commun* 2000; **273**(3)**:** 1015-1018.

Chapter 7

Summary and Future Considerations

Membrane transporters have shown ever-increasing importance in a number of processes relevant to human health and physiology. In particular, members of the Solute Carrier (SLC) 22 family of transporters, colloquially known as xenobiotic transporters, have been thoroughly implicated in the uptake of drugs, toxins, and other synthetic and endogenous chemicals into the hepatic and renal compartments, and subsequent reabsorptive and excretory processes therein[1, 2].

Recently, however, numerous studies have illuminated a variety of specific and unique effects on basal physiologic processes dependent upon or strongly influenced by members of the SLC22 family[3-5]. These discoveries hint at a greater role of this family of transporters other than incidentally providing entry and exit mechanisms for various drugs and endogenous small molecules. While these transporters continue to understandably garner extensive interest in the drug development field, considerable interest is being shifted towards the inherent and oftentimes obscured endogenous roles of transporters previously known primarily for uptake of clinically relevant drugs. As an added layer of complexity, extensive genetic variability in these transporters has been uncovered, providing discrete evidence for the genetic basis of differential drug response[6]. While the impact of these genetic variants have largely been limited to studies of a pharmacogenetic nature, these same variants could also equally impact physiological processes and provide explanations for differences in basic

bodily functions in the general populace or prove to be a contributing factor in complex disorders and diseases with obfuscated and complex underlying causes.

The studies presented within this dissertation were undertaken with the intent of investigating the more basal functional roles and genetic features of members of the organic anion transporter (OAT) and organic cation transporter (OCT) families (both being subsets of the broader SLC22 family) with the supposition that while drug disposition and xenobiotic handling are important facets of these proteins, there are likely to be other presently undocumented and potentially significant functions unrelated to their predominantly ascribed role of small molecule drug transport.

Summary of Dissertation Research

While the major barrier and metabolically active tissues, namely the liver, kidney, brain, and placenta, are known to express a multitude of SLC22 transporters, the expression of and physiological implications in other tissues has not been examined with anywhere near as much interest or depth. This poses unique opportunities for the discovery of basal transporter functions separate from the comparatively well-characterized implications in drug efficacy and toxicity. Using an expression screen for SLC22 transporter expression in the major male and female reproductive tract tissues, *SLC22A11* (OAT4) was found to be present in the epididymis and absent from any other reproductive tissues examined. OAT4

expression in the epididymis was an intriguing occurrence as this tissue comprises a significant portion of the male reproductive tract and is largely responsible for the maturation, concentration, and storage of spermatozoa after their production in the testes. Furthermore, OAT4 was previously only identified in the kidney and placenta[7], where it was speculated to be involved in steroid sulfate homeostasis between the fetal and maternal compartments[8], implicating it in steroid signaling which is an important facet of all reproductive tissues. In light of this finding, the work comprising Chapter 2 was undertaken to investigate the role of OAT4 in the epididymis and examine the potential underlying consequences in male fertility. Further characterization of OAT4 expression found levels comparable to that observed in the kidney and identified OAT4 as the sole OAT expressed in the epididymis, suggestive of a specific and potentially critical role in establishing or maintaining a microenvironment suitable for the maturation of spermatozoa. Additional immunohistochemistry studies established OAT4 expression primarily on the apical membrane of the principal cells of the caput epididymis, with the highest expression in the efferent ductules, a region well-established to have substantial reabsorptive properties[9]. However, the question remained as to whether the uptake of a particular small molecule in the epididymal fluid by OAT4 could impact male fertility. Using metabolomic techniques, samples of bovine testicular lysate and human plasma were incubated with OAT4 and empty vector stably transfected cell lines to identify potential endogenous substrates present in the epididymal microenvironment and eventually ascertain if these substrates could have an impact on epididymal

function, sperm survival and/or maturation, and thus impact male fertility. A number of potential substrates were identified however, only estrone sulfate, a previously known substrate of OAT4, was confirmed. Based on these results, it is plausible that estrone sulfate is the primary metabolite substrate for OAT4 in the epididymal microenvironment and its transport and conversion to active estrogens in the epididymal epithelium could significantly impact epididymal function. Previous studies have identified active estrogen signaling pathways in the epididymis and loss of estrogen receptors leads to infertility in knockout mice[10]. Thus, while no novel substrates were identified in these experiments, the potential impact of OAT4 on epididymal function and male reproductive capacity may be akin to its speculated role in the placenta; however the full impact of OAT4 in the epididymis remains unclear and worthy of future investigations.

Given the high expression of OAT4 in the epididymis, placenta, and kidney and the potential to provide critical transport mechanisms for a variety of endogenous substrates in these tissues, nine non-synonymous variants of OAT4 were characterized experimentally to evaluate their potential impact on OAT4 function. As detailed in Chapter 3, genetic variants found in healthy human subjects from multiple ethnic groups were evaluated using uptake of three endogenous substrates: estrone sulfate, ochratoxin A, and uric acid. Of the nine variants examined, three resulted in a complete loss-of-function phenotype with all three substrates tested (L29P, R48Stop, and H469R). These three variants occurred at a very low allele frequency, with the exception of R48Stop which was identified at a slightly higher frequency of approximately 2.3% in Caucasians. Subsequent

mechanistic investigation of these variants found the likely explanation for the loss of function was a drastic reduction in the amount of protein on the plasma membrane, suggestive of membrane trafficking issues arising from the presence of these altered amino acid residues or in the case of the R48Stop variant, a severely truncated or non-existent protein. Interestingly, the remaining variants with allele frequencies greater than 1% (R121C, V155G, and V155M), while not showing any change in substrate uptake, did show differences in the kinetic properties of estrone sulfate uptake, with generally lower V_{max} values and approximately equivalent K_m values. The presence of these nonfunctional variants suggest that an appreciable number of individuals could have reduced, or absent, OAT4 function while the higher frequency variants characterized herein indicate that other variants may impact OAT4 function in a more subtle manner.

In addition to *SLC22A11*, five non-synonymous genetic variants in healthy individuals were also discovered in its closely related paralog *SLC22A12* (URAT1) and were characterized in the work comprising Chapter 4. In contrast to OAT4, coding variants in URAT1 have previously been recognized as significant factors in uric acid homeostasis, with a number of rare mutations resulting in the severe loss of uric acid reabsorption in the kidney, the primary site of URAT1 expression, and the development of hypouricemia. The variants identified in this chapter were relatively rare with only the G65W and T542LysfsX13 variants found in multiple individuals. The rarity of these variants, and the overall extreme conservation of coding regions of URAT1, was

juxtaposed by the large number of observed haplotypes found in all four ethnic groups examined, suggestive of a high degree of selection occurring in this gene, presumably to conserve uric acid reabsorption. These variants resulted in little overall change in uric acid uptake, with only the T542LysfX13 indel displaying a statistically significant reduction in uric acid uptake. In contrast, all of the variants were kinetically altered with substantial reductions in both V_{max} and K_m values for uric acid uptake indicating that while the net uptake of uric acid remains an efficient process overall, there are subtle differences in protein function when these variants are present. Subsequent investigation into the mechanism of these functionally reduced variants identified a distinct reduction in protein on the plasma membrane with the T542LysfX13 variant present at less than 50% of the reference protein in spite of comparable mRNA levels. Previous work from a number of groups has identified a number of rare variants directly responsible for hypouricemia, most often resulting from a single point-mutation that results in a complete loss of uric acid reabsorption in the kidney and result in hypouricemia[4, 11, 12]. In this case, however, protein- and function-altering variants were found in DNA from presumably healthy individuals. While people with these variants are unlikely to present with hypouricemia, the altered function produced by these variants could influence the degree of renal uric acid reabsorption and thus predisposition to certain uric acid-modulated diseases such as metabolic syndrome and multiple sclerosis[13, 14], as well as the response to commonly used uricosuric drugs known to interact directly with URAT1.

In spite of their close evolutionary history, OAT4 and URAT1 possess unique functional characteristics and genomic features. While functionally comparable and similar in many ways to other members of the OAT family, these two transporters in particular exhibit features of divergent evolution and functional specialization. As detailed in Chapter 5, phylogenetic analysis found that OAT4 is the ancestral OAT from which URAT1, as well as OAT5 and OAT7, evolved suggesting that OAT4 also possesses the ancestral functional properties and genomic features of this branch of the OATs. This is further substantiated by an amino acid identity of approximately 50% between these two transporters and a high level of conservation between both orthologous and paralogous proteins. Examination of the patterns of conservation, both within and between species, suggests that amino acid differences that occur in the transmembrane regions are likely to elicit many of these functional differences. However, in spite of these high level of conservation, OAT4 and URAT1 display distinctive patterns of tissue distribution and substrate preferences. Specifically, while OAT4 has been detected in the kidney, placenta, and epididymis with low-level expression in a number of additional tissues, expression of URAT1 is largely restricted to the kidney. In consideration of the predicted evolutionary features of these proteins, the restriction of URAT1 tissue expression is significant and indicative of its substantial role in the kidney in the reabsorption of uric acid. Furthermore, it could be speculated that expression of these OATs was initially broad but as the role of URAT1 became more specialized, so did its expression pattern. Similar to the increasing specificity of gene expression observed with URAT1, when these

two substrate classes were examined further, OAT4 was confirmed to interact with a variety of steroid-sulfate conjugates as well as a wider range of small molecule inhibitors, including losartan, salicylate, and enoximone, whereas URAT1 demonstrated noticeable interactions with a wide range of purine-like compounds but with narrower range of interactions with the same subset of known and unknown small molecule inhibitors, somewhat predicated on size as exemplified by the lack of an observable interaction with enoximone. This functional divergence is further emphasized by the discovery that URAT1 is an effective transporter for both AMP and ADP while OAT4 displayed no interaction with either compound, further substantiating the specific functional capacity of URAT1 that has evolved separately from OAT4 and is not limited solely or incidentally to uric acid. Taken together, these finding suggest that while a product of the same common ancestral gene and in spite of a high level of amino acid identity, these two OATs have diverged substantially, with unique roles in specific tissues. The conservation and functional evolution of these transporters hints at conserved and specialized physiological roles, however, the full extent of these differences remains to be seen as does the full scope of the potential impact on the physiological capacity of tissues expressing OAT4 and/or URAT1.

While the creation of *in vivo* models for altered OAT4 and URAT1 function would be an ideal and logical continuation of the preceding studies of OAT4 and URAT1, limitations in potential rodent models, namely the lack of an identifiable ortholog (OAT4) and the increased complexity and redundancy in uric acid disposition (URAT1)[15], precluded their creation and utilization for studies aiming

to uncover novel basal physiological functions of these transporters. However, recent studies of OCT1 (*SLC22A1*), another member of the SLC22 transporter family, have found significant effects on the excretion of cationic small molecules[16] as well as the development of fatty liver disease[17]. Knockout models for the orthologous *SLC22A1* gene in mice have been well characterized and have provided substantial insights into the impact of OCT1 on mammalian physiology and disease predisposition and treatment. However, translating the altered physiological responses from rodent to primate species has proven difficult due to the inherent differences between these species and due to the slight but significant functional differences observed in between the mouse and human OCT1 proteins. Considering these circumstances, the work in Chapter 6 describes the efforts invested in the creation of a transgenic mouse model that expresses the human OCT1 in the mouse liver. Transgenic mouse lines anticipated to express OCT1 in a liver-specific fashion were created by injecting the OCT1 transgene, comprised of the mouse albumin gene proximal promoter and distal enhancer regions, as described by Pinkert, et al[18], the human OCT1 full-length cDNA, and a bovine growth hormone poly-adenylation sequence. The majority of the resultant lines displayed varying OCT1 expression levels, with most lacking any appreciable expression in any tissue examined. However, a single line was found to express human OCT1 at an extremely high level, approximately 1.2 to 4-fold higher than in normal human liver, and was subsequently backcrossed into an Oct1 knockout mouse line to create the final humanized OCT1 transgenic mouse model. This transgenic line also expressed

OCT1 at elevated levels in other tissues, primarily the colon, kidney and lung, but at substantially lower levels than in the liver. In spite of this spurious tissue expression, the levels detected in the liver should allow for more accurate assessments of the impact of OCT1 in human physiology and disease while maintaining the ability to conduct these investigations in an intact mammalian model organism.

Future Considerations

Since the completion of the first draft of the human genome more than ten years ago, avenues of scientific inquiry have expanded dramatically with increasing emphasis being given to both the construction of and the variability in the human genome. The discoveries made possible through advances in sequencing throughput and computational power have unveiled innumerable associations between genotype and phenotype far beyond what was attainable using traditional, largely Mendelian approaches, and in fact has created entirely new scientific disciplines devoted to uncovering these associations. A substantial portion of funding and research interest has specifically been vested into work related to the variability of the human genome and has resulted in a greater understanding as to how minute changes in DNA can result in the plethora of physical traits observed in vertebrate animals[19-21] while also illuminating many of the factors behind the development of multitudinous diseases[22-24]. While the promises of a “genomic revolution” in medical care professed by the initial

genomics pioneers have yet to be fully realized, considerable efforts are currently being made to develop and implement facets of the field of personalized medicine, wherein the course of medical treatment is determined by a person's individual physiological makeup, driven largely by their own unique DNA.

Two major components are key to the implementation of truly genomics-based medicine: 1) the identification and characterization of variants in numerous human populations and 2) the methodologies and infrastructure to accurately and completely interpret the impact of these variants in an individual. The former was initially limited by the inability to produce high-quality sequence data cheaply and quickly; sequencing the first draft composite human genome was done at a cost of nearly $3 billion and took 10 years to complete. Advances in both scalability and the science of DNA sequencing since then has resulting in an explosion of personal genomics data with estimates of thousands of genomes being sequenced yearly. These advances have also resulted in the creation of immense data resources such as HapMap[25] and the 1000 Genomes Project[26] which are now maturing and providing an incredibly detailed map of human genetic variation in numerous ethnically diverse populations. However, the precise impact of these variants, especially outside of an *in vitro* laboratory-based setting, lags far behind the pace of their discovery. Ultimately, this is the paradox of the current genomics age – the relative ease in identifying variable regions of DNA contrasted with the difficulty in determining the impact of these variants. Numerous small-scale efforts have been undertaken to illuminate the effects of naturally occurring genetic variants and these have met with some

success, as evidenced by increasing number of well-studied and clinically validated pharmacogenetic variants recognized by the FDA. Efforts such as those presented in this dissertation provide and additional, incremental step toward a greater understanding of how simple nucleotide polymorphisms in xenobiotic transporters in the SLC22A family can impact basal physiological processes in the kidney or epididymis as well as potentially lead to the discovery of clinically-relevant pharmacogenetic relationships, an important facet of personalized medicine. However, a more concerted and ultimately broader scale approach will be needed in order to make full use of the data currently being generated. This most certainly is an oversimplification of a daunting task considering a recent study that found ~442,000 previously unreported variants, including ~3,000 nonsense or frameshift variants (with a high likelihood of negatively impacting the function of a protein) occurring in the average genome[27], but will be necessary if we are to effectively transition from the discovery to the application phase of personalized medicine.

Recently dubbed the "interpretome"[28], providing complete variant interpretation to researchers, clinicians, and patients in a timely and easily interpretable manner is potentially the last true technical hurdle in moving genomic data to the clinic where it can directly impact medical treatment. In conjunction with the limited availability of effect data for variants, the other major issue currently facing movement of this data to the clinic is the scope of the conditions where both variant and phenotype information are available. Nearly 20,000 entries currently exist in the Online Mendelian Inheritance in Man (OMIM) database that relate a

particular variant to a disease condition, however, these variants by and large are exceedingly rare and generally result in severe phenotypes where relatively little medical intervention is currently possible. While the focus on Mendelian disorders is understandable and has produced some substantial results, in particular the identification of new causative variants that result in Miller's syndrome[29] and Kabuki syndrome[1] to name a few, the majority of patients that could benefit from personalized medicine will not be suffering from these rare disorders. Thus while this information is important to those suffering from these rare and debilitating diseases, and can have important implications in genetic counseling of carriers, wider use of this information in the clinic would be achieved through the determination of the impact of more frequently occurring variants and those that arise in genes known to be involved in more common maladies, such as diabetes, cardiovascular disease, asthma, and cancer. Effective utilization of this data will therefore require a more thorough attempt at identifying genes and variants that influence the development of complex disorders and phenotypes. But taking these more common, and in some cases non-Mendelian, variants to this level of predictive power also requires many other considerations, namely accounting for more subtle interactions between multiple variants in multiple genes, compound heterozygosity, gene-environment interactions, and the mode of inheritance, in addition to the complexities of pharmaceutical interactions in the body.

Pharmacogenetics in particular is well situated to identify and characterize potentially harmful variants and then apply this knowledge to a clinical setting

where it can immediately impact patients. Currently, more than 100 drugs have pharmacogenetics information included in their labels, informing clinicians and patients alike of how a variant allele can impact the use of this particular drug[30]. Pharmacogenetics studies have transformed the usage of a number of drugs, namely the anti-coagulant warfarin[31] and the anti-neoplastic agents irinotecan, azathioprine, and 6-mercaptopurine[32], allowing these drugs to be used more safely and more effectively than previously possible. Instances of beneficial applications of pharmacogenetics data are sure to increase as more research is performed to determine the factors relevant to drug response and the pace of targeted therapy development increases as well.

Additionally, the comparatively small number of genes involved in drug disposition, largely limited to drug targets (predominantly consisting of ion channels, G-protein receptors, nuclear receptors, and kinases), membrane transporters, and cytochrome P450 enzymes, allows for a more thorough and focused approach to relating a variant to a drug response phenotype; pharmacogenetics benefits from this "narrower" view of the genome and as a result is able to avoid the pitfalls of complex diseases where oftentimes the causative genetic factors are multitudinous and obscured. These efforts have proven fruitful with variants identified in 1150 genes and interactions found with more than 370 clinically relevant drugs as described in the Pharmacogenetics Knowledge Base (PharmGKB)[33]. Further activity aimed at the interpretation of impactful pharmacogenetic variants would undoubtedly aid in the movement of the sequencing data to the clinic as its application to pharmaceutics is

immediately actionable and can both prevent adverse drug events and optimize medication usage, aiding in both the treatment of severe diseases and in the overall safety and efficacy of medications in general use.

With the precipitous drop in cost for whole genome sequencing and the converging interests from both industry and the public to provide in-depth genetic information for patients, the next big leap in the utilization of genomic data will undoubtedly be in the realm of interpretation. This will likely encompass a leap forward in our understanding of complex diseases, increased ability to evaluate variant effect in a high-throughput fashion, and a substantial improvement in the computational and engineering side to aid in our ability to generate, capture, store, and transmit vast stores of genetic data. In short, while incredible achievements are being made in personalized medicine, the application of genomic sequencing data to patient care will unquestionably require many more advancements in scale and accuracy of variant identification in addition to an increased emphasis on determining and/or predicting adverse effects resulting from variants in a patient's DNA, in the form of disease or drug response.

References

1. Giacomini KM, Huang SM, Tweedie DJ, Benet LZ, Brouwer KL, Chu X*, et al*. Membrane transporters in drug development. *Nat Rev Drug Discov* 2010; **9**(3)**:** 215-236.

2. Koepsell H, Endou H. The SLC22 drug transporter family. *Pflugers Arch* 2004; **447**(5)**:** 666-676.

3. Wang Y, Ye J, Ganapathy V, Longo N. Mutations in the organic cation/carnitine transporter OCTN2 in primary carnitine deficiency. *Proc Natl Acad Sci U S A* 1999; **96**(5)**:** 2356-2360.

4. Enomoto A, Kimura H, Chairoungdua A, Shigeta Y, Jutabha P, Cha SH*, et al*. Molecular identification of a renal urate anion exchanger that regulates blood urate levels. *Nature* 2002; **417**(6887)**:** 447-452.

5. Vallon V, Eraly SA, Wikoff WR, Rieg T, Kaler G, Truong DM*, et al*. Organic anion transporter 3 contributes to the regulation of blood pressure. *J Am Soc Nephrol* 2008; **19**(9)**:** 1732-1740.

6. Zair ZM, Eloranta JJ, Stieger B, Kullak-Ublick GA. Pharmacogenetics of OATP (SLC21/SLCO), OAT and OCT (SLC22) and PEPT (SLC15) transporters in the intestine, liver and kidney. *Pharmacogenomics* 2008; **9**(5)**:** 597-624.

7. Enomoto A, Takeda M, Shimoda M, Narikawa S, Kobayashi Y, Yamamoto T*, et al*. Interaction of human organic anion transporters 2 and 4 with organic anion transport inhibitors. *J Pharmacol Exp Ther* 2002; **301**(3)**:** 797-802.

8. Ugele B, St-Pierre MV, Pihusch M, Bahn A, Hantschmann P. Characterization and identification of steroid sulfate transporters of human placenta. *Am J Physiol Endocrinol Metab* 2003; **284**(2)**:** E390-398.

9. Hermo L, Robaire B. Epididymal cell types and their functions. In: Robaire B, Hinton BT (eds). *The Epididymis: From Molecules to Clinical Practice*. Kluwer Academic/Plenum Publishers: New York, 2002, pp 81-102.

10. Hess RA, Zhou Q, Nie R, Oliveira C, Cho H, Nakaia M*, et al*. Estrogens and epididymal function. *Reprod Fertil Dev* 2001; **13**(4)**:** 273-283.

11. Iwai N, Mino Y, Hosoyamada M, Tago N, Kokubo Y, Endou H. A high prevalence of renal hypouricemia caused by inactive SLC22A12 in Japanese. *Kidney Int* 2004; **66**(3)**:** 935-944.

12. Komatsuda A, Iwamoto K, Wakui H, Sawada K, Yamaguchi A. Analysis of mutations in the urate transporter 1 (URAT1) gene of Japanese patients with hypouricemia in northern Japan and review of the literature. *Ren Fail* 2006; **28**(3)**:** 223-227.

13. Nakagawa T, Hu H, Zharikov S, Tuttle KR, Short RA, Glushakova O*, et al*. A causal role for uric acid in fructose-induced metabolic syndrome. *Am J Physiol Renal Physiol* 2006; **290**(3)**:** F625-631.

14. Toncev G, Milicic B, Toncev S, Samardzic G. Serum uric acid levels in multiple sclerosis patients correlate with activity of disease and blood-brain barrier dysfunction. *Eur J Neurol* 2002; **9**(3)**:** 221-226.

15. Eraly SA, Vallon V, Rieg T, Gangoiti JA, Wikoff WR, Siuzdak G*, et al*. Multiple organic anion transporters contribute to net renal excretion of uric acid. *Physiol Genomics* 2008; **33**(2)**:** 180-192.

16. Jonker JW, Wagenaar E, Mol CA, Buitelaar M, Koepsell H, Smit JW*, et al*. Reduced hepatic uptake and intestinal excretion of organic cations in mice with a targeted disruption of the organic cation transporter 1 (Oct1 [Slc22a1]) gene. *Mol Cell Biol* 2001; **21**(16)**:** 5471-5477.

17. Chen L, Giacomini KM (2010). Unpublished work. University of California, San Francisco: San Francisco.

18. Pinkert CA, Ornitz DM, Brinster RL, Palmiter RD. An albumin enhancer located 10 kb upstream functions along with its promoter to direct efficient, liver-specific expression in transgenic mice. *Genes Dev* 1987; **1**(3)**:** 268-276.

19. Yoshiura K, Kinoshita A, Ishida T, Ninokata A, Ishikawa T, Kaname T*, et al*. A SNP in the ABCC11 gene is the determinant of human earwax type. *Nat Genet* 2006; **38**(3)**:** 324-330.

20. Sutter NB, Bustamante CD, Chase K, Gray MM, Zhao K, Zhu L*, et al*. A single IGF1 allele is a major determinant of small size in dogs. *Science* 2007; **316**(5821)**:** 112-115.

21. Lamason RL, Mohideen MA, Mest JR, Wong AC, Norton HL, Aros MC*, et al*. SLC24A5, a putative cation exchanger, affects pigmentation in zebrafish and humans. *Science* 2005; **310**(5755)**:** 1782-1786.

22. King MC, Marks JH, Mandell JB. Breast and ovarian cancer risks due to inherited mutations in BRCA1 and BRCA2. *Science* 2003; **302**(5645)**:** 643-646.

23. Bobadilla JL, Macek M, Jr., Fine JP, Farrell PM. Cystic fibrosis: a worldwide analysis of CFTR mutations--correlation with incidence data and application to screening. *Hum Mutat* 2002; **19**(6)**:** 575-606.

24. Losekoot M, Haarloo C, Ruivenkamp C, White SJ, Breuning MH, Peters DJ. Analysis of missense variants in the PKHD1-gene in patients with autosomal recessive polycystic kidney disease (ARPKD). *Hum Genet* 2005; **118**(2)**:** 185-206.

25. Frazer KA, Ballinger DG, Cox DR, Hinds DA, Stuve LL, Gibbs RA*, et al*. A second generation human haplotype map of over 3.1 million SNPs. *Nature* 2007; **449**(7164)**:** 851-861.

26. Felsenstein J (2010). In: *PHYLIP (Phylogeny Interface Package)*. Self Published: University of Washington.

27. Pelak K, Shianna KV, Ge D, Maia JM, Zhu M, Smith JP*, et al*. The characterization of twenty sequenced human genomes. *PLoS Genet* 2010; **6**(9).

28. Karczewski K, Tatonett N, Tirrell R, Zimmerman N (2011). Interpretome: Palo Alto.

29. Ng SB, Buckingham KJ, Lee C, Bigham AW, Tabor HK, Dent KM*, et al*. Exome sequencing identifies the cause of a mendelian disorder. *Nature genetics* 2010; **42**(1)**:** 30-35.

30. FDA (2011). Table of Pharmacogenomic Biomarkers in Drug Labels. FDA.

31. Schwarz UI, Ritchie MD, Bradford Y, Li C, Dudek SM, Frye-Anderson A*, et al*. Genetic determinants of response to warfarin during initial anticoagulation. *N Engl J Med* 2008; **358**(10)**:** 999-1008.

32. Maitland ML, Vasisht K, Ratain MJ. TPMT, UGT1A1 and DPYD: genotyping to ensure safer cancer therapy? *Trends Pharmacol Sci* 2006; **27**(8)**:** 432-437.

33. Klein TE, Chang JT, Cho MK, Easton KL, Fergerson R, Hewett M*, et al*. Integrating genotype and phenotype information: an overview of the PharmGKB project. Pharmacogenetics Research Network and Knowledge Base. *Pharmacogenomics J* 2001; **1**(3)**:** 167-170.

Publishing Agreement

It is the policy of the University to encourage the distribution of all theses, dissertations, and manuscripts. Copies of all UCSF theses, dissertations, and manuscripts will be routed to the library via the Graduate Division. The library will make all theses, dissertations, and manuscripts accessible to the public and will preserve these to the best of their abilities, in perpetuity.

Please sign the following statement:

I hereby grant permission to the Graduate Division of the University of California, San Francisco to release copies of my thesis, dissertation, or manuscript to the Campus Library to provide access and preservation, in whole or in part, in perpetuity.

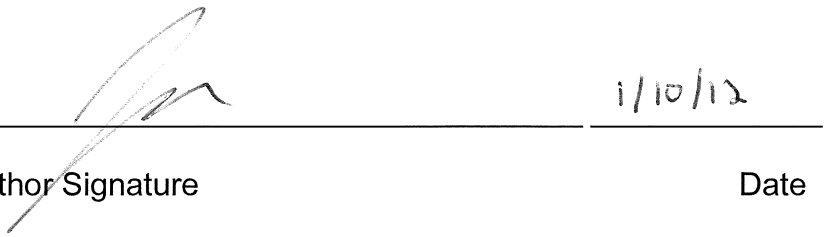

1/10/12

Author Signature Date